1999

Sedimentary structures and facies in the Helena and Wallace formations: Middle Proterzoic belt supergroup Montana

D. Jay Johnson
The University of Montana

INFORMATION TO USERS

This manuscript has been reproduced from the microfilm master. UMI films the text directly from the original or copy submitted. Thus, some thesis and dissertation copies are in typewriter face, while others may be from any type of computer printer.

The quality of this reproduction is dependent upon the quality of the copy submitted. Broken or indistinct print, colored or poor quality illustrations and photographs, print bleedthrough, substandard margins, and improper alignment can adversely affect reproduction.

In the unlikely event that the author did not send UMI a complete manuscript and there are missing pages, these will be noted. Also, if unauthorized copyright material had to be removed, a note will indicate the deletion.

Oversize materials (e.g., maps, drawings, charts) are reproduced by sectioning the original, beginning at the upper left-hand corner and continuing from left to right in equal sections with small overlaps. Each original is also photographed in one exposure and is included in reduced form at the back of the book.

Photographs included in the original manuscript have been reproduced xerographically in this copy. Higher quality 6" x 9" black and white photographic prints are available for any photographs or illustrations appearing in this copy for an additional charge. Contact UMI directly to order.

UMI®

Bell & Howell Information and Learning
300 North Zeeb Road, Ann Arbor, MI 48106-1346 USA
800-521-0600
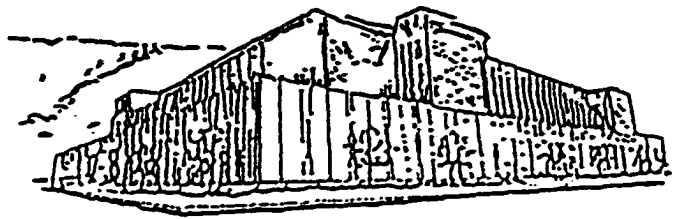
Permission is granted by the author to reproduce this material in its entirety, provided that this material is used for scholarly purposes and is properly cited in published works and reports.

** *Please check "Yes" or "No" and provide signature* **

Yes, I grant permission   _D. Jet_

No, I do not grant permission   _____

Author's Signature _____

Date _____4/26/99_____

Any copying for commercial purposes or financial gain may be undertaken only with the author's explicit consent.

SEDIMENTARY STRUCTURES AND FACIES
IN THE HELENA AND WALLACE FORMATIONS
MIDDLE PROTERZOIC, BELT SUPERGROUP, MONTANA

By

D. Jay Johnson

M. Sc., Michigan Technological University

presented in partial fulfillment of the requirements

for the degree of

Doctor of Philosophy

The University of Montana

1999

Approved by:

_____
Chairman, Board of Examiners

_____
Dean, Graduate School

$\underline{\quad 4\text{-}28\text{-}99 \quad}$
Date

i

UMI Number: 9940362

Copyright 1999 by
Johnson, D. Jay

UMI Microform 9940362
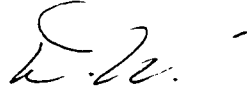Copyright 1999, by UMI Company. All rights reserved.

UMI

300 North Zeeb Road
Ann Arbor, MI 48103

Sedimentary structures and facies in the Helena and Wallace formations, Middle Proterozoic, Belt Supergroup, Montana.

Director: Donald Winston II

The Helena and Wallace formations contain four facies. Each facies preserves a characteristic suite of beds or graded beds that display a narrow range of sandstone-mudstone ratios and thicknesses. The sandstone facies, facies A, consists of 5 to 15 cm thick graded beds, containing more than 65 percent, and commonly over 90 percent sandstone. The 50/50 sandstone-mudstone facies, facies B, displays 2 to 15 cm thick graded beds containing between 35 percent to 65 percent sandstone. The laminated mudstone facies, facies C, consists of thin graded beds, ranging from about 1 mm to about 2 cm thick, that contain less than 35 percent sandstone. The thickly graded bedded mudstone facies, facies D, displays 5 to 20 cm thick graded beds, containing less than 35 percent sandstone.

The primary current laminae and the shapes and spacing of the bedforms in graded beds show that deposition in the Helena and Wallace formations took place in two very different sedimentary environments. Facies A, sandstone facies, and facies D, thickly graded bedded mudstone facies, were deposited in a wave dominated environment. Facies A contains abundant sedimentary structures recording deposition from high velocity oscillatory and combined currents. Symmetric bedforms record deposition under large Airy waves, offshore of the storm surf zone. Planar laminae and quasi-planar laminae indicate deposition within the storm surf zone. Airy wave equations suggest the sandstone facies formed in water between 4 and 50 m deep. Suspended sediment loads suggest deposition in water between 30 and 50 m deep.

Trochoidal ripples in mud rich graded beds comprising the facies D record low velocity, purely oscillatory currents. Suspended sediment loads suggest deposition in water ranging from 60 to 240 m deep. Low velocity oscillatory current bedforms and thicknesses of graded beds indicate facies D deposition occurred in deep water, offshore of the sandstone facies.

Rare planar laminae in the graded beds in facies B, the 50/50 sandstone-mudstone facies, and rare low angle cross-laminae in facies C, the laminated mudstone facies, record deposition from either a unidirectional or combined current. But, the origin of this current is controversial. Suspended sediment loads suggest deposition occurred in water between 10 and 50 m deep in facies B, and in water between 2.4 and 48 m deep in facies C.

The data lead to the following conclusions: (1) Facies D deposition occurred in a deep, wave-dominated shelf environment. (2) Facies A deposition occurred in a shallow, wave-dominated shelf environment. (3) Facies B deposition probably occurred in a mud rich, deep subtidal environment, and (4) Facies C deposition probably occurred in a shallow subtidal to deep intertidal environment.

TABLE OF CONTENTS

vi

LIST OF TABLES

viii

ix

INTRODUCTION

This dissertation reports the techniques and results of a study of the sedimentary rocks comprising the Middle Proterozoic Helena and Wallace formations of the Belt Supergroup, western Montana and northern Idaho, Figure I.1. This study differs from previous studies in four ways.

First, the data represent a different approach to describing the strata comprising the Helena and Wallace formations.

Second, the data represent far more detailed descriptions of the bedforms and current laminae within the strata. Improved descriptions of stratification, bedforms and current laminae permit far more detailed hydraulic interpretations than those undertaken before.

Third, this dissertation describes a suite of revised and expanded hydrodynamic models that describe erosion, transportation, deposition and compaction of fine grained sediment. These expanded hydrodynamic models permit far more detailed interpretations of the currents that transported and deposited the sediments in the Helena and Wallace formations.

Fourth, I base the depositional environment interpretations only on the hydrodynamic interpretations of the strata and the primary sedimentary structures within the graded beds, unconstrained by the stratigraphic framework. Adshead (1963), Price (1964), O'Connor (1967), Horodyski (1976, 1983), Eby (1977) and Grotzinger (1986) placed the Helena and Wallace formations in a marine environment. Walcott (1914), Grotzinger (1981) Winston et al. (1984) Winston (1986 b, 1989,1993) and Winston and Link (1993) placed the Helena and Wallace formations in a lake environment.

1

Figure 1. 1.

> • = *measured sections: CC - Cedar Creek; HC - Howard Creek; HH - Hungry Horse; LD Libby Dam; MF - Morrell Falls; OG - Oregon Gulch; RH - Ravalli Hill; RM - Red Mountain; RP - Rogers Pass; SLP - Storm Lake Pass; WVR - Weeksvill Road.*

> ❑ = *cities: EG - East Glacier; H - Helena; K- Kimberly; L - Libby; M - Missoula; N - Newport; S - Salmon; W- Wallace.*

These interpretations were based on the composition, texture, sedimentary structures, depositional processes and stratigraphy of the rocks of interest as compared to those in a suite of accepted ideal depositional facies models (Anderton, 1985; Walker, 1992). Anderton (1985) believes that the ideal facies models do not capture all the variability in ancient depositional systems. For instance, Walcott (1914) interpreted deposition of the Helena Formation in a lake environment because, in 1914, the only known modern examples of stromatolites came from lakes. It wasn't until Black (1933) found stromatolites growing on the tide flats in the Bahamas that stromatolites were recognized in modern marine environments.

In this dissertation I try to side step potential problems like this by interpreting only the hydrodynamics of the currents that deposited the sediment in the Helena and Wallace formations. The hydrodynamic interpretations document the type of transporting current, current velocities, suspended sediment loads, frequency and intensity of depositional events and the relative water depth of deposition. Taken together these imply specific depositional environments. Previous studies did not address these considerations in detail.

ACKNOWLEDGEMENTS

genetic link between sandstone layer and the mudstone layer. This dissertation would not have been possible without these insights.

I am greatly indebted to D. Alt, N. Hinman and G. Thompson in the Geology Department and D. Potts of the School of Forestry for serving on my committee and providing valuable discussions and critical reviews of the organization and content of this dissertation. I also thank M. Hendrix for providing a detailed critique of the dissertation and J. Moore and J. Sears for their support and valuable discussions of my ideas.

PREVIOUS STUDIES

Many of researchers have described the mineralogy, sedimentary structures, molar-tooth structures, stratigraphy and the biogenetic remains in the formations that comprise the formations of the middle Belt carbonate. However, I will review only the major studies that provide detailed mineral descriptions, stratigraphic descriptions or interpreted the depositional environments of the Helena, Wallace or Siyeh formations.

STRATIGRAPHY. The Middle Proterozoic Belt Supergroup (Childers, 1963; Harrison, 1972) of western Montana, northern Idaho and eastern Washington, is laterally equivalent to the Middle Proterozoic Purcell Supergroup of southwestern Alberta and southeastern British Columbia. The Belt Supergroup is divided into the informal lower Belt group, the Ravalli Group, the informal middle Belt carbonate and the Missoula Group (Harrison, 1972). This dissertation deals with the informal middle Belt carbonate (Harrison, 1972) that encompasses the carbonate bearing rocks in the middle of the Belt Supergroup.

The middle Belt carbonate consists of the more-or-less equivalent Helena, Wallace, Siyeh and Kitchener formations. The interval was originally called the Piegan Group (Fenton and Fenton, 1937) but Harrison (1972) synonymized the Siyeh Formation with the Helena Formation dropped the Piegan Group

Figure 1.2. Original nomenclature and stratigraphy of the Belt and Purcell supergroups. Stippled intervals show relationships among the Helena, Wallace, Siyeh and Kitchner formations as originally defined.

and the Siyeh Formations. However, I use the terms where other authors used them in previous studies. Figure I.2 shows stratigraphic relationships among the Helena, Wallace, Siyeh and Kitchener formations as they were originally defined.

Walcott (1899), working in the eastern Belt, named the Helena Limestone for exposures of carbonate-bearing rocks near Helena, and Ransome (1905), working in the western Belt, named the carbonate bearing rocks the Wallace Formation for exposures in the Coeur d'Alene mining district. Willis (1902) named the carbonate-rich interval in Glacier National Park the Siyeh Formation, for exposures on Mount Siyeh. Daly (1905) named the carbonate-bearing rocks in the Purcell Supergroup the Kitchener formation for exposures near Kitchener, British Colombia.

Childers (1963) defined and extracted the Snowslip Formation from the upper part of Willis' (1902) Siyeh Formation, and placed the newly defined Snowslip Formation and the redefined and Shepard Formation into the Missoula Group (Clapp and Deiss, 1931). Lemoine (1979) and Lemoine and Winston (1986) showed that the Snowslip and Shepard formations are laterally equivalent to informal units 3, 4 and 5 (Harrison and Jobin, 1963) of the Wallace Formation as originally defined in Ransome (1905). Figure I.3 shows the currently accepted middle Belt carbonate nomenclature and lithostratigraphic correlations.

DEPOSITIONAL ENVIRONMENTS. Previous students of the Helena and Wallace formations suggested deposition occurred in either a lake environment (Walcott, 1914; Peterson, 1971; Grotzinger, 1981; Winston et al., 1984; Winston, 1986 b, 1989, 1991, 1993; Winston and Link, 1993) or in a marine environment (Price, 1964; Eby, 1977; Horodyski, 1976, 1983; Grotzinger, 1986). These authors reached their conclusions by comparing the composition, bedding styles, stratigraphy, biologic remains and sedimentary structures in the middle Belt carbonate to those in found in established lake or tidal depositional environment models. A notable exception is of O'Connor (1967) who also included the depositional processes.
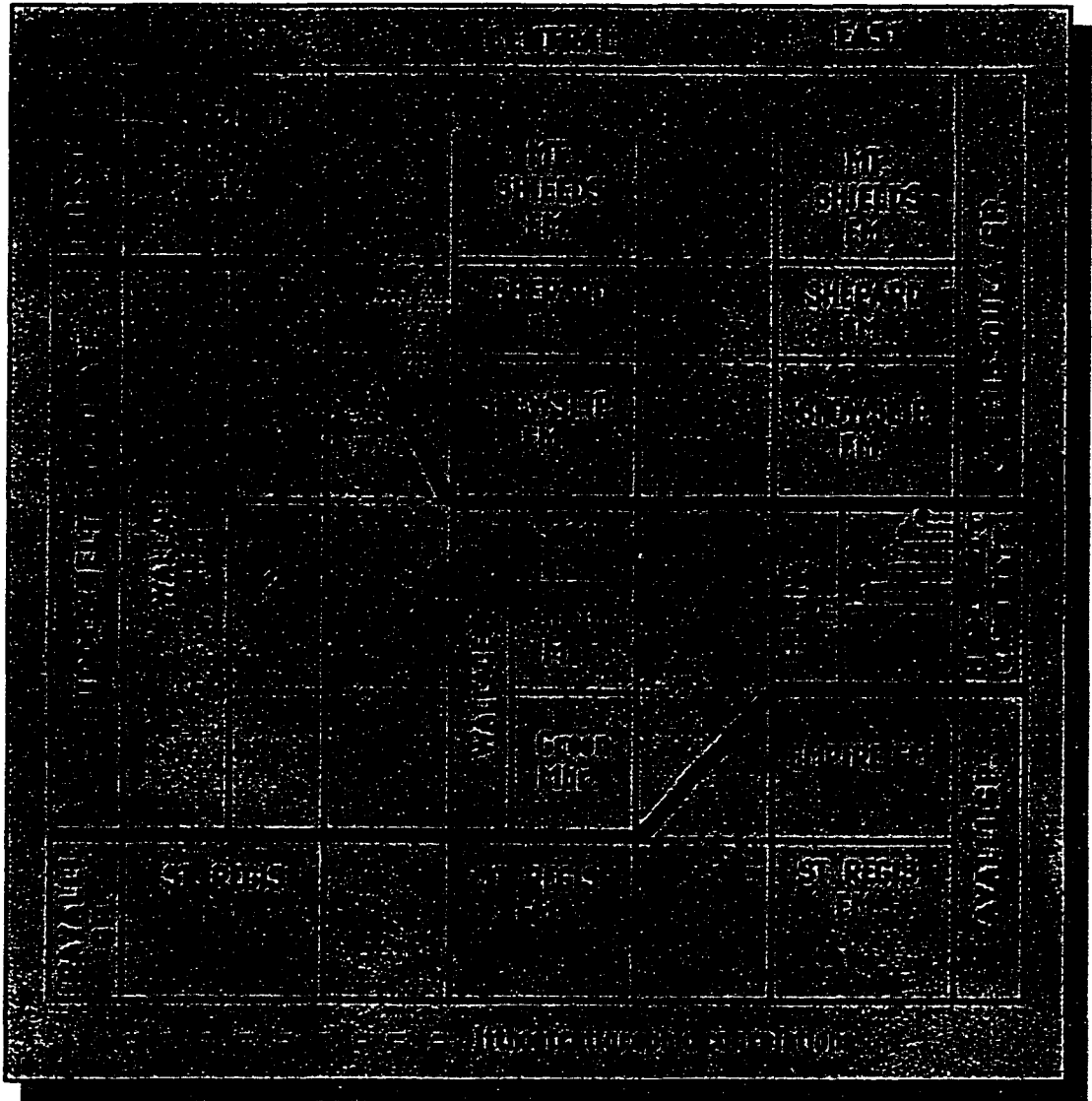
Figure I.3. Currently accepted stratigraphy and lithostratigraphic correlations of the middle
Belt carbonate and adjacent formations.

Sources: West - Harrison and Jobin (1963);
Central - Lemoine and Winston (1986) and Grotzinger (1986);
East - Winston and Link (1993) and Winston (1993).

MINERALOLOGY. The mineral composition of the Helena and Wallace formations makes naming the rocks difficult. Most all of the Helena and Wallace formations contain mixtures of both siliciclastic and carbonate minerals (Adshead, 1963; O'Connor, 1967; Horodyski, 1976 a; Eby, 1977). Furthermore, x-ray studies of the rocks in the Belt Supergroup (Reynolds, 1963; Maxwell and Hower, 1967; Maxwell, 1973) show that they have undergone either high rank diagenesis or low grade metamorphism.

Carbonate verses siliciclastic rocks Many previous workers called most of the rocks in the Helena and Wallace formations limestone, dolostone or dolomite in order to emphasize their different mineralogy from other formations in the Belt Supergroup (Horodyski, 1976 a). However, most rocks in the Helena and Wallace formations contain between 50 to 70 percent siliciclastic minerals (Adshead, 1963; Horodyski, 1976 a; Harrison and Grimes, 1970). Notable exceptions include oolitic limestone beds, stromatolite beds, and molar-tooth ribbon intraclast conglomerate beds (Adshead, 1963; Horodyski, 1976 a; Harrison and Grimes, 1970), but these lithologies comprise a relatively minor part of the formations.

Thin sections of Helena and Wallace sediments show the carbonate occurs in the form of 3 to 35 μm diameter, euhedral to subhedral calcite and dolomite grains (Adshead, 1963; Eby, 1977). Adshead (1963, p. 90) concluded that all of the calcite and dolomite in the Siyeh [Helena] Formation ". . . is of authigenic rather than clastic origin, having resulted from early cementation of the still-wet detrital framework during diagenesis". Adshead (1963) also suggested that the dolomite formed by dolomitization of authigenic calcite.

Metamorphic verses sedimentary rocks Helena and Wallace formations consist of very well indurated sedimentary rocks. Harrison and Campbell (1963), Harrison and Grimes (1970) Harrison (1972) and Harrison (1993, personal communication) argue that metamorphic rock terms quartzite, siltite and argillite should be used for rocks in the Belt Supergroup. However, the rocks in the Helena and Wallace

formations contain a wealth of primary and secondary sedimentary structures and, in most places, exhibit no metamorphic textures or visible metamorphic minerals. This is not true near Proterozoic mafic sills and Cretaceous felsic intrusions, where the rocks contain contact metamorphic textures and minerals.

Totten and Blatt (1993, p. 899) suggest that diagenesis grades into metamorphism where illite recrystallizes to muscovite, and quartz increases in size. Lemoine (1979, p. 38) found illite, chlorite and detrital muscovite in an x-ray and optical study of the argillaceous laminae in the Snowslip and Shepard formations, but no authigenic muscovite, near Thompson Falls, Montana. Maxwell and Hower (1967) found that 2M polymorph of illite comprised between 54 and 75 percent of the illite in the Wallace formation near Lake Pend Oreille, Idaho. Reynolds (1963) found that the illite in the Siyeh Formation [Helena] in Glacier National Park contains between 11 and 26 percent 2M polymorph. Maxwell (1973, p. 135) concluded "The layer silicate mineralogy of the Belt rocks (dioctahedral mica + chlorite) is indicative of either late stage diagenesis or early greenschist facies".

I use sedimentary rock terms conglomerate, sandstone, siltstone, mudstone and claystone to describe different rock textures because: (1) The rocks were originally sedimentary rocks; (2) The goal is to interpret the rock's sedimentary origins; and (3) At most locations, metamorphic minerals and textures in no way obscure the sedimentary textures and structures.

ORGANIZATION

I present the methods of study and the approach to describing stratification in Chapter II. The data in the form of detailed descriptions of the bedforms, current laminae, graded beds, ungraded beds and facies are given in Chapter III. I present up-to-date models for the erosion, transport, deposition and compaction of fine suspension load material in Chapter IV. Chapters V, VI, and VII cover the hydraulic interpretation of the bedforms and current laminae, graded bed interpretations and facies interpretations respectively.

The identification of the sedimentary environments is the ultimate goal of the hydraulic interpretations, and these are presented in Chapter VIII. In the final chapter I discuss the strengths and weaknesses of the tidal environment interpretations and the problems with the storm dominated shelf-tidal environment interpretation. Appendix I presents a modified bed phase diagram for oscillatory and combined unidirectional and oscillatory currents.

METHODS

This study is based on two methods: (1) Detailed descriptions of bedding and current produced bedforms and laminae on vertical exposures, sabed rock samples, and thin-sections; and (2) Hydrodynamic interpretation of the bedding, current produced bedforms and primary current laminae. These methods differ from previous studies four ways: (A) I divided the strata into ungraded beds on one hand, and graded beds on the other. Authors of previous studies only recognized the differences between beds or laminae, or called the graded beds couplets or couples. (B) I included a description of the sandstone/ mudstone ratio of the graded beds. Authors of previous studies did not report the sandstone/ mudstone ratios of the couplets and couples. (C) I present far more detailed descriptions of the bedforms and current laminae than were given in previous studies; and (D) The hydraulic interpretations and the interpretations of the depositional environments are based on the detailed bedform descriptions and on revised and expanded models for suspended sediment erosion, transport, deposition and compaction. Previous interpretations were based on analogy with established depositional environment models.

The locations of measured sections are shown in Figure I.1. I studied several hundred slab samples of primary and secondary sedimentary structures, and aquired more than 3000 field photographs of the different types of beds, graded beds, bedforms and primary current laminae. I studied more than two hundred thin-sections of sandy, silty, muddy and clayey graded beds to determine the character of the smaller sedimentary structures and to study the textures in sandstone and mudstone layers. These data form the basis of the descriptions in Chapter III.

The initial studies of the bedforms and primary current laminae indicated problems with applying the accepted models for suspension deposition to the structures displayed in the Helena and Wallace

11

formations. Basically. the laminae and bedforms indicate deposition occurred from currents with far higher velocities than the conventional depositional models suggest.

BEDDING DESCRIPTIONS

Descriptions of stratification profoundly impact the stratification classification, which in turn profoundly impacts the interpretations. Many previous studies of the Helena and Wallace formations employed the descriptive method of McKee and Weir (1953), who divide strata into beds and laminae based on their thickness. composition and texture. By their definition, a bed or lamina exhibits more-or-less uniform composition and texture. Their terminology implies that a graded bed actually consists of two beds; a sandstone bed overlain by a mudstone bed.

Many previous descriptions of the Helena and Wallace formations (Adshead, 1963; Harrison and Jobin,1963; Price, 1964; O' Connor, 1967; Eby, 1977; and many more) were based on McKee and Weir's (1953) approach to describing stratification. For example, O' Connor (1967, p. 127) described the undulose bedded rock type: "This rock type consists of very thin to occasionally medium beds of light olive gray, moderately sorted, dolomitic coarse siltstone, alternating with laminae of dark gray. very poorly sorted, dolomitic mudstone. The contact between the siltstone and overlying mudstone is commonly graded, with graded sets averaging approximately 1-2 cm; the contact between the mudstone and overlying siltstone is sharp. . . Soft sediment deformation structures are abundant, particularly load casts of siltstone pressed into the mudstone. The combined effects of current cross-stratification and soft sediment deformation produce strongly undulose bedding surfaces and discontinuous beds and laminae which laterally pinch and swell."

The above authors chose to emphasize the difference between the sandstone layer and the mudstone layer. But I chose to emphasize the fact that a sandstone-mudstone pair form a graded bed. It is a matter of both description and perception. Interbedded sandstone and mudstone leads to the perception of two separate events. The same strata described as a graded bed implies one event.

Lemoine (1979), Grotzinger (1981), Winston et al. (1984), Winston (1986 b, 1989, 1991, 1993) and Winston and Link (1993) recognized that the sandstone strata were genetically related to the overlying mudstone layers, and called the sandstone-mudstone pair couplets or couples. For instance: "Pinch-and-swell couples are characterized by fining-upward fine sand- and silt-to-clay couplets in which the sandy and silty layers thicken and thin across outcrops, producing uneven, pinch-and-swell stratification ... " (Winston, 1986 b, p. 99). Winston's pinch-and-swell couplet sediment type is approximately equivalent to O'Connor's undulose bedded rock type.

The couplet and couple sediment types represent an improved understanding of the genetic relationship between the sandstone layer and the mudstone layer. However, I do not use the sediment type scheme because the couple and couplet sediment types are categories of rock similar to lithofacies (Winston and Link, 1993, p. 486) and may contain several different types of graded beds.

SANDSTONE/ MUDSTONE RATIOS

The couplet and couple descriptions of the graded beds mark a great improvement in the descriptions of the sediments comprising the Helena and Wallace formations. However, these authors did not record the sandstone/ mudstone ratios of the graded beds. The sandstone/ mudstone ratios in Winston's (1986 b) pinch-and-swell couplet sediment type varies from about 90 percent sandstone at some locations to about 10 sandstone at other locations.

CURRENT LAMINAE AND BEDFORM DESCRIPTIONS

The Helena and Wallace formations contain a wide variety of well preserved current produced bedforms and primary current laminae. Many of these bedforms and laminae are either rare, absent or poorly described from other formations in the Belt Supergroup as well as on a world wide basis.

Previous workers in the Helena and Wallace formations did not describe bedforms in detail. Rarely

they called a bedform a wave ripple, oscillation ripple or current ripple, leaving to the readers' imaginations

the ripple's height, shape and spacing. Some authors describe ripple laminated beds (Lemoine, 1979;

Grotzinger, 1981; Winston, 1986 b) without giving the angle of the laminae, the thickness of the laminated

interval, or whether the internal laminae were concordant or discordant to the ripple's form. Bedform

height, shape, symmetry, spacing and the type of internal laminae provide information about the velocity

and type of current that produced the bedform.

A detailed method for describing bedforms and current laminae is presented in

Chapter III.B and C.

PROCESS MODELS

The other major difference between this dissertation and other studies concerns the hydrodynamic

models used to interpret the data. The hydrodynamic interpretations in Chapters V, VI, and VII are based on

the models presented in Chapter IV. These models describe the process of wash load erosion, transport,

deposition and compaction. Wash load is the part of the suspended load less than 100 μm in diameter

(Nordin and Prez-Hernandez, 1988). The origins of massive bedding and current laminae, and the basis for

interpreting the currents are covered in Chapter V.

Previous hydraulic interpretations (Lemoine, 1979; Grotzinger, 1981; Winston et al., 1984;

Winston, 1986 b, 1989, 1991) of the very fine-grained sandstones and mudstones that comprise the Helena

and Wallace formations were based on the competency model for suspension deposition, Chapter IV.A. The

competency model for suspension deposition describes deposition from dilute, very low velocity currents

where the current lacks either the competency to maintain the sediment in suspension (Komar, 1985) or the

competency to move the sediment along the bed (McCave and Swift, 1976). However, Bagnold (1966) and

Hiscott (1994) present a capacity model for suspension deposition that describes the mechanics of

deposition from moderate to very high velocity currents.

DATA

The data in this dissertation consist of detailed descriptions of the ungraded beds, the graded beds, and the bedforms and current laminae in the facies of Helena and Wallace formations. The descriptions extend previous descriptions by Winston (1986 b; 1989; 1991), Winston and Link (1993), Eby (1977), O'Connor (1967; 1972) Godlewski (1980) and Grotzinger (1981, 1986).

DIVISIONS OF THE HELENA AND WALLACE FORMATIONS

Figure III.1 shows the hierarchy of depositional packages that compose the Helena and Wallace formations. At the smallest scale, ungraded beds and graded beds form the thinnest discrete depositional packages. About 95 percent of the formations consist of graded beds, and 5 percent probably consists of ungraded beds. The graded beds are divided into anomalous graded and background graded beds. Anomalous graded beds have higher sandstone/ mudstone ratios and are thicker than the associated background graded beds.

A facies is composed of a complexly interbedded suite of ungraded beds, background graded beds and anomalous graded beds. The background graded beds within a facies display similar thicknesses, sandstone-mudstone ratios and primary current structures. A facies' name is based on its sandstone/ mudstone ratio of its background graded beds and their thickness.

Several facies, stacked in a particular recurring order, make up a cycle (O'Connor, 1967; Grotzinger, 1981; 1986; Winston and Lyons, 1993). Informal members of the upper Helena formation consist of either repeating cycles or thick intervals composed of a single facies (Winston, 1993).

15
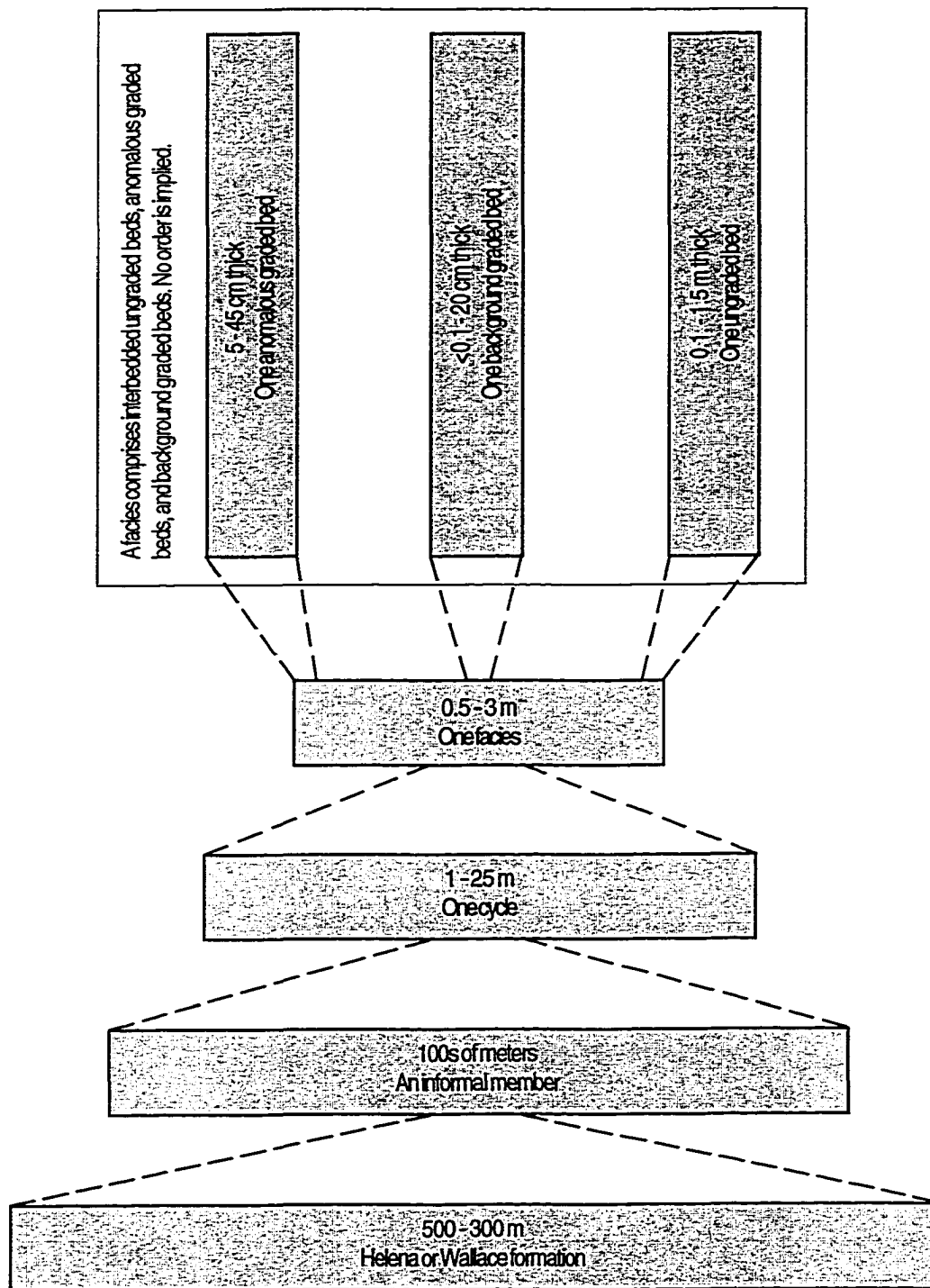
Figure III.1. *Diagrammatic hierarchy of architectural elements that compose the Helena and Wallace formations. See Winston (1993) for the division of the upper Helena Formation into cycles and informal members.*

UNGRADED BEDS. Ungraded beds are fundamental sedimentation units of the facies, composed of one lithology, displaying a uniform texture. Ungraded beds differ from the graded beds in that they lack grading and commonly contain internal reactivation and scour surfaces, absent in the graded beds. Ungraded beds are commonly thicker than the interbedded graded beds, ranging from about 10 cm to 1.5 m thick. Ungraded beds commonly occur in cosets, forming intervals up to 2 or more meters thick. The Helena and Wallace formations contain eight common types of ungraded beds, described in Chapter III.H.

GRADED BEDS. Graded beds fine upward, and range from less than 1 mm up to 45 cm thick. They contain a coarser lower layer, either of very fine sandstone or siltstone overlain, either gradationally or abruptly by a layer of mudstone or claystone.

Graded beds in the facies of the Helena and Wallace formations occur at two scales. Background graded beds are thinner and have lower sandstone/ mudstone ratios than the interbedded anomalous graded beds. Background graded beds range in thickness from less than 1 mm to 20 cm, and anomalous graded beds range from about 5 cm to 45 cm. For instance, Plate 7-a shows an interval of facies D made up of very muddy background graded beds 10-15 cm thick, interbedded with a very sandy anomalous graded bed about 30 cm thick.

I recognized 6 different types of background graded beds, described in Chapter III.F, and 5 types of anomalous graded beds, described in Chapter III.G. A facies contains several types of graded beds. But, also commonly, facies may contain thick intervals composed of a single type of graded bed. Such an interval is called a graded bed coset.

FACIES. A facies is a sedimentation unit composed of interbedded ungraded beds, anomalous graded beds and background graded beds. Different facies are distinguished by: (1) The differences in sandstone or siltstone-mudstone ratio of the background graded beds; and (2) The dominant thickness of

the background graded beds. I recognized four facies, each of which is divided into subfacies. The facies are described in Chapter III.I.

BEDFORMS

Within the ungraded beds and graded beds, the Helena and Wallace formations contain well preserved bedforms and primary current laminae. Many of these bedforms and laminae are either rare, absent or poorly described from other formations around the world. The descriptions of the bedforms and laminae used in this study make it possible to link the bedforms and laminae to different areas on the bed phase diagrams (Ashley et al., 1990; Arnott and Southard, 1990).

I describe bedforms by their height, spacing, shape, symmetry and their internal laminae. The components of the bedform description are shown on Figure III.2. The distance between the ripple crests defines a bedform's spacing. I prefer the term spacing to wavelength because dome shaped bedforms can not be said to have a wavelength (Arnott and Southard, 1990). The vertical distance from the trough to crest defines its height. The straightness, continuity and roundness of the ripple crest defines a bedform's shape. Bedforms with straight crests are called 2-dimensional (2D) bedforms, and bedforms with sinuous or discontinuous crests are called 3-dimensional (3D) bedforms (Allen, 1966). Ripple crest lines are either rounded or sharp.

Three dimensional bedforms can be recognized on vertical exposures, irrespective of outcrop orientation, because the ripple crests rise to different heights along the exposure. Two dimensional bedforms can be recognized because they reach the same height along vertical exposures.

Symmetrical bedforms give ripple symmetry indices, crest-to-trough spacing on one side of the crest divided by the crest-to-trough length on the other, less than 2.5 (Reineck and Singh, 1980). Asymmetrical bedforms give ripple symmetry indices greater than 3. Slightly asymmetric ripples lie

Figure III.2. *Components of bedform descriptions.*
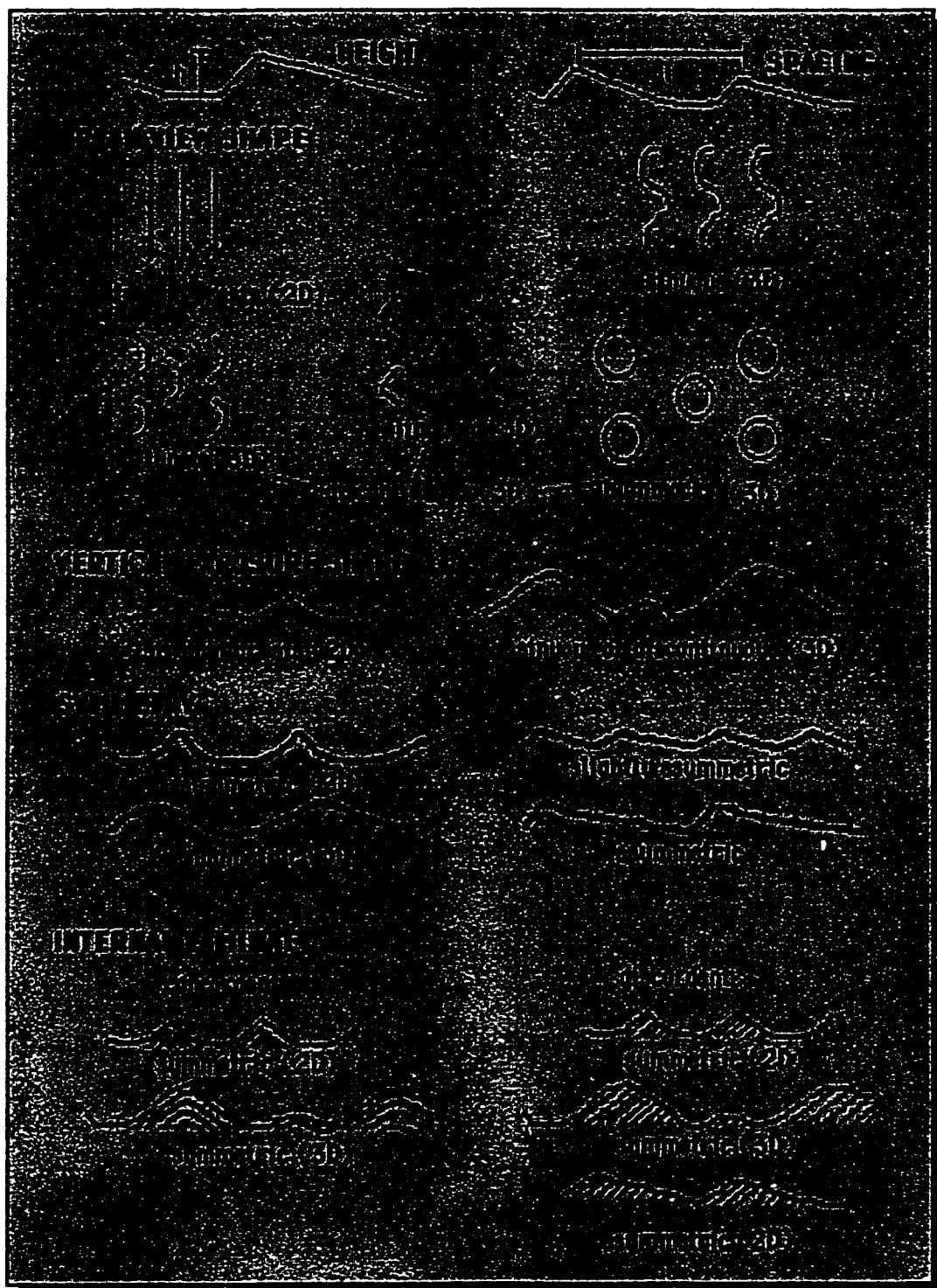
Table III.1   Descriptions of bedforms common inthe Helena and Wallace formations.

1. **Trochoidal ripples** are symmetrical, 2D forms with straight, sharp crest lines. Forms range from 0.5 to 5 cm high, and range from about 3 to 21 cm apart, but most are spaced from about 7 to 13 cm apart.

2. **Rounded trochoidal ripples** are symmetrical, 2D forms with straight, rounded crest lines. Forms range from 0.5 to 5 cm high, and from about 5 to 21 cm apart, but most are spaced about 10 to 17 cm apart.

3. **Small hummocky ripples** are symmetric, 3D forms with discontinuous, rounded crest lines. The forms range from oval to dome shaped. Forms range form 0.5 to 10 cm high, and from about 10 to 21 cm apart.

4. **Medium hummocky ripples** are symmetric, 3D forms with discontinuous, rounded crest lines. The forms are approximately dome shaped on bedding plane exposures. Forms range up to about 15 cm high, and range from 30 to 70 cm apart.

5. **High, large hummocky ripples** are symmetric, 3D forms with discontinuous, rounded crest lines. The forms are approximately dome shaped on bedding plane exposures. The forms range from about 15 to 20 cm high, and have spacings ranging from about 70 to 100 cm.

6. **Medium, large hummocky ripples** are symmetric, 3D forms with discontinuous, rounded crest lines. The forms are approximately dome shaped on bedding plane exposures. The forms are spaced between 100 and 150 cm apart and range from about 10 to 15 cm high.

7. **Low, large hummocky ripples** are symmetric, 3D forms with discontinuous, rounded crest lines. The forms are approximately dome shaped on bedding plane exposures. Formes are spaced more than about 150 cm apart and range from about 5 to 10 cm high.

8. **Small slightly asymmetric ripples** are slightly asymmetric, 3D forms with sinuous, continuous crest lines. The forms range up to 5 cm high and about 21 cm long, but most are about 1 to 2 cm high and 10 cm apart.

9. **Small current ripples** (Harms et al., 1982; Ashley et al., 1990) are very asymmetric, 3D forms with discontinuous crest lines. Forms range up to 5 cm high and 60 cm long, but most are about 0.5 cm high and about 15 cm apart.

Figure III.3. Line drawing showing vertical sections through the most common types of complete bedforms preserved in the Helena and Wallace formations.
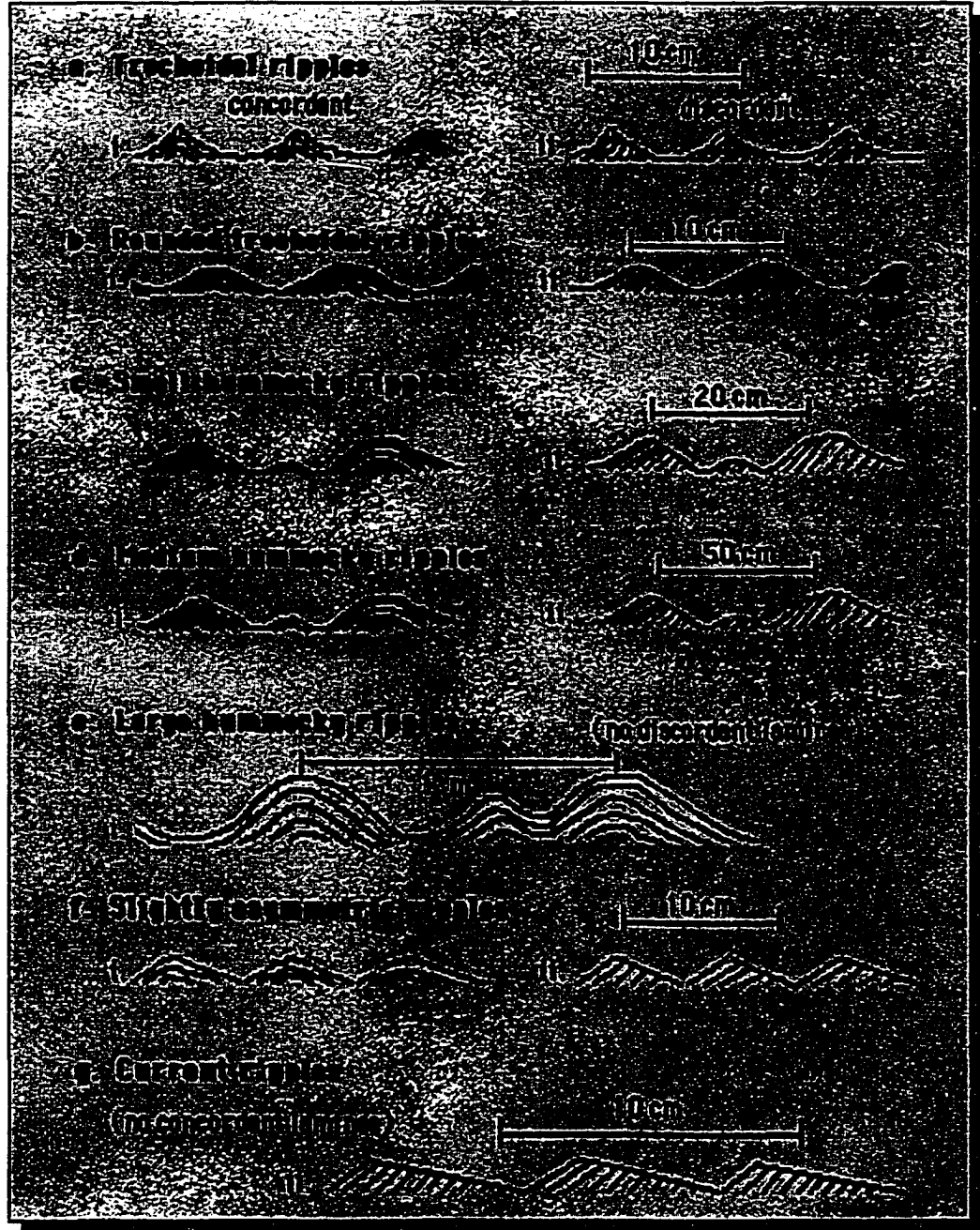
between the two end members (Harms, 1969). Symmetrical bedforms displayed on vertical exposures

display only symmetrical shapes, no matter how face intersects them. Asymmetrical bedforms only produce

asymmetrical outlines.

Laminae within bedforms can be either concordant or discordant. Concordant laminae conform to

the ripple outline and record vertical bedform growth (Rubin, 1987). Discordant laminae are truncated by

the ripple outline and record bedform migration (Rubin, 1987).

Ripple symmetry, size, shape, internal lamination style and spacing combine to produce a large

number of potential ripple types. The Helena and Wallace formations contain 9 common bedforms,

described in Table III.1 and shown in Figure III.3. Inman (1957) named the trochoidal ripples, Ashley et al.

(1990) named dunes and small current ripples, and Harms et al. (1982) named hummocky ripples. All other

terms are new. This level of detail is warranted because, as shown in Chapter V, each type of bedform

provides specific information about the current type and velocity.

CURRENT LAMINAE WITHOUT BEDFORMS

The Helena and Wallace formations contain five types of laminae without associated bedforms,

shown on Figure III.4. The Helena and Wallace formations contain rare truly planar, or horizontal, laminae.

Planar laminae in the sandstone layers of the anomalous graded beds and ungraded sandstone beds parallel

the dip of the adjacent beds and graded beds.

Arnott (1993) defined quasi-planar laminae as nearly planar laminae that rise and fall about a

centimeter along several meters of lateral exposure. Sandstone layers in the anomalous graded beds and

ungraded sandstone beds in the Helena and Wallace formations commonly display quasi-planar laminae.

Ungraded sandstone beds and the sandstone layers in many anomalous graded beds contain sets of

long low angle laminae that range from about 5 cm to 20 cm thick. Long low angle laminae dip uniformly

Figure III.4. Line drawing showing vertical sections through the most common types of laminae without associated bedforms in the Helena and Wallace formations
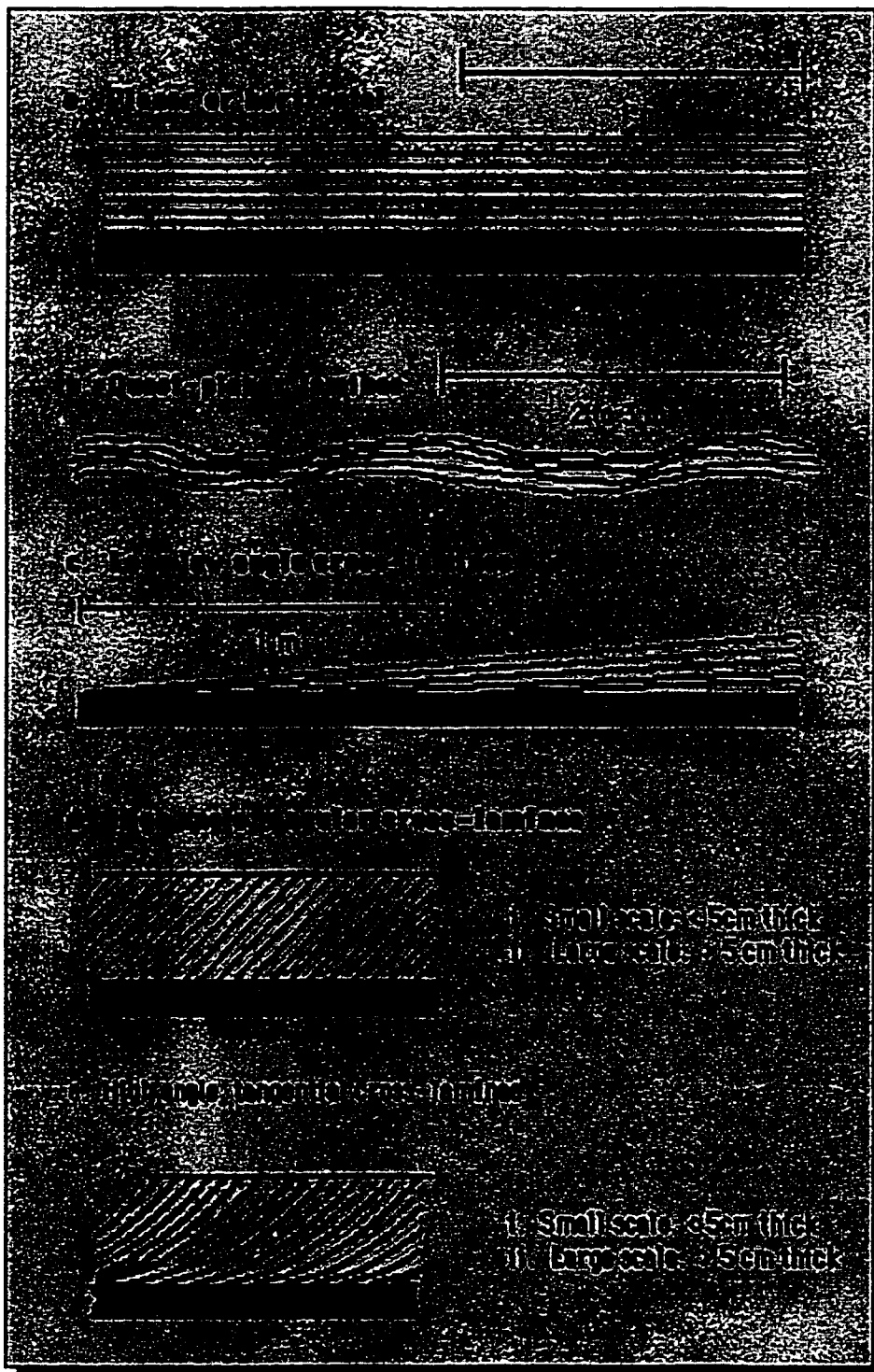
in one direction within a given bed. The laminae range from several tens of cm long to several meters long, and dip at less than 15 degrees to the bed boundaries. Long low angle laminae intersect the top of the underlying bed at a very low angle.

High angle, angular cross-laminae and high angle, tangential cross-laminae are very rare in the Helena and Wallace formations. Where they occur, one set of high angle, angular or tangential laminae completely fill a sandstone layer in background graded beds or comprise cosets in ungraded sandstone beds. Cross-laminae less than 5 cm high are called small scale current cross-lamination, and cross-laminae greater than 5 cm high are called large scale current cross-lamination (Harms et al., 1982). Vertical exposures oriented perpendicular to the current direction that intersect angular cross-laminae produce laminae that appear planar. Vertical exposures oriented perpendicular to flow that cut tangential cross-laminae produce small scale trough lamination (Harms et al., 1982).

MASSIVE BEDDING

Many sandstone beds and the sandstone layers in the graded beds in the Helena and Wallace formations contain massive bedding. ". . . massive bedding is used to describe beds that appear to be homogeneous and lacking in internal structures" (Boggs, 1987, p. 144).

VERTICAL SEQUENCES OF PRIMARY SEDIMENTARY STRUCTURES

Vertically changing sequences of laminae or bedforms are common in the graded beds and ungraded sandstone beds in the Helena and Wallace formations. Sequences range from less than 1 cm to about 45 cm thick. Six of the most common stratification sequences are given in Table III.2.

BACKGROUND GRADED BEDS

Six different types of background graded beds occur in the Helena and Wallace formations. Each is identified by the morphology of its basal contact and the morphology its of coarser-to-finer transition,

Table III.2.   *Common sequences of primary current structures in the graded beds.*

(a)

mudstone

— abrupt contact with mudstone —

vertically climbing rounded trochoidal ripple forms (Fig. III.3-b, i)

vertically climbing small hummocky ripples (Fig. III.3-c, i)

± long, low angle laminae (Fig. III.4-c)

± planar (Fig. III.4-a) or quasi-planar laminae (Fig. III.4-b)

— erosion surface —

(b) see Plate 7-a

mudstone

— abrupt contact with mudstone —

vertically climbing trochoidal ripples (Fig. III.3-a, i)

vertically climbing large hummocky ripples (Fig. III.3-e, i)

— loaded base — or — erosion surface —

(c) see Plate 1-a; Plate 1-b

mudstone

— interleaved sand and mud —

rounded trochoidal (Fig. III.3-b, i), or slightly asymmetric (Fig. III.3-f, i)

± long low angle laminae (Fig. III.4-c)

— erosion surface —

(d) see Plate 3-c; Plate 7-b

mudstone

— gradational contact, or abrupt contact with mudstone layer —

massive bedding

planar or quasi-planar laminae; rare small high-angle laminae (Fig. III.4-d)

— erosion surface, commonly guttered —

(e) see Plate 2-d

mudstone

— interleaved sand and mud laminae, or abrupt contact with mudstone layer —

vertically climbing trochoidal ripples (Fig. III.3-a, i)

vertically climbing rounded trochoidal ripples (Fig. III.3-b, i)

—little or no erosion —

(f) see Plate 2-d; Plate 7-c

mudstone

— interleaved sand and mud laminae —

vertically climbing trochoidal ripples (Fig. III.3-a, i)

— little or no erosion —

Figure III.5. Line drawings showing the morphologies of the background graded beds.
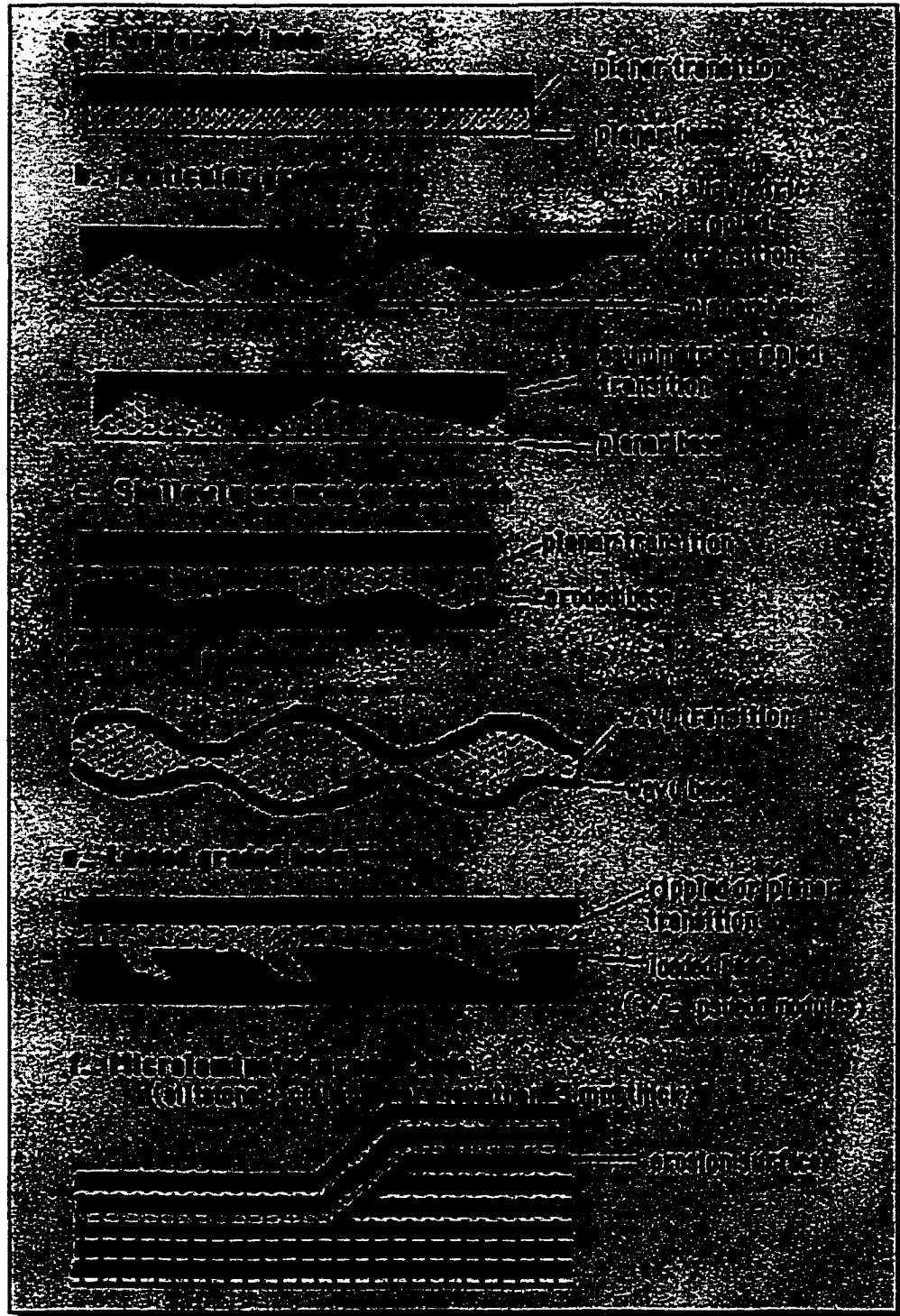
shown on Figure III.5. Individual background graded beds are also classified by their thickness and their sandstone/ mudstone ratios.

EVEN GRADED BEDS. An even graded bed consists of a tabular sandstone or siltstone layer overlain by a mudstone or claystone layer. Both the top and base of the sandstone layers are flat and planar, hence the sandstone layers maintain an even thickness across the exposure. Table III.3 gives details of the even graded beds in the different facies. Many of the graded beds shown on Plate 4 a and Plate 2 c are even graded beds. Even graded beds display mature grading, i. e., continuous grading across the coarser-finer transition (Reineck and Singh, 1980). Even graded beds most commonly occur in cosets, that is, a sequence of two or more graded beds of the same type. Even graded bed cosets are approximately equivalent to Winston (1986 b) and Winston and Link (1993) uncracked even couplet and even couple sediment types.

Sandstone layers in the even graded beds commonly display massive bedding. Rarely, even graded beds in facies B display planar laminae and rarely small scale, high angle cross-laminae in facies C. Winston (1989, p. 52) also reported planar laminae in the even couplet sediment type.

LENTICULAR GRADED BEDS. The sandstone layers in the lenticular graded beds display planar bottoms and a wavy coarser-finer transition. Plate 2-d and Plate 7-c show 50-50 and muddy lenticular graded beds respectively. Table III.4 lists the characteristics of the lenticular graded beds in the different facies. Lenticular graded beds are approximately equivalent to Reineck and Wunderlich's (1968) lenticular bedding, and to Winston's (1986 b) and Winston and Link's (1993) lenticular couplet sediment type.

Lenticular graded beds occur in several different forms, distinguished by the continuity of the sandstone layers and on the shapes of the ripples they contain. At some locations the sandstone layers are continuous across the exposure, with symmetrical ripple lenses on top of massive or long low angle

laminated sandstone. At other locations the sandstone layers are discontinuous, consisting of isolated symmetrical or slightly asymmetrical ripple forms.

Rounded trochoidal ripples, Figure III.3 -b, and trochoidal ripples, Figure III.3- a, with concordant laminae are very common. Rare asymmetric forms with discordant laminae, Figure III.3-g, occur near the Snowslip-Helena contact at Rogers Pass and Little Skunk Creek.

Lenticular graded beds commonly separate cosets of shallowly scoured or even graded beds in facies B and C, and lenticular graded beds commonly form cosets in facies D. Most lenticular graded beds in facies B and C contain immature grading (Reineck and Singh, 1980), i. e., an abrupt change in grain size across the coarser-finer transition. Mature grading from rippled sandstone to siltstone to mudstone is common in facies D, Plate 7-c. Both the siltstone and mudstone display faint, discontinuous horizontal laminae, Plate 7-c.

SHALLOWLY SCOURED GRADED BEDS. The coarser layers in the shallowly scoured graded beds have planar tops and wavy bottoms, Figure III.5-c, Plate 2-b, Plate 3-d, and are commonly composed of silt sized grains. Table III.5 lists their characteristics. Shallowly scoured graded beds have not been described before; they are a subdivision of Winston's (1986 b) and Winston and Link's (1993) pinch-and-swell couple and couplet sediment types.

The basal contacts of the shallowly scoured graded beds display low relief scour surfaces that cut into, but not through, the mudstone layer of the underlying graded bed. The scours are either angular or rounded, Plate 7-b, commonly about a centimeter or so deep and commonly 15 cm or more wide.

The siltstone or sandstone layers in most shallowly scoured graded beds are massive, and the siltstone-to-mudstone transitions are flat, displaying mature grading from massive siltstone upward into

massive mudstone. Some shallowly scoured graded beds in facies A and B contain planar laminae. Winston

(1989, p. 54) also reported planar laminae in his pinch-and-swell couplet sediment type. Shallowly scoured

graded beds commonly occur in cosets, or interbedded with even graded beds, Plate 4-a.

WAVY GRADED BEDS. The tops and bottoms of the sandstone layers in the wavy graded beds

are wavy, and the waviness of the top is out of phase with the waviness of the bottom. Table III.6 lists the

details of the wavy graded beds. The waviness at the base of the graded beds was inherited from the wavy

topography on the top of the mudstone layer of the underlying graded bed. Waviness at the top of the

sandstone layers results from ripple forms at the graded beds' coarser-to-finer transition. Wavy mudstone

layers, 1 mm to 1 cm thick, separate the thickening and thinning sandstone layers within wavy graded bed

cosets, Plate 1-a, Plate 1-b.

Wavy graded beds have not been previously described from the Helena or Wallace formations, but

are equivalent to Reineck and Wunderlich's (1968) wavy bedding. The sandstone-mudstone transitions

display mature grading, commonly with mudstone laminae interleaved with sandstone laminae in the ripple

troughs. Wavy graded beds commonly contain rounded trochoidal or small hummocky ripples with

concordant internal laminae. Less commonly they contain medium hummocky ripples.

LOADED GRADED BEDS. The sandstone layers in the loaded graded beds have wavy tops due

to the presence of ripple forms and wavy bottoms due to contemporaneous loading of sand into the mud of

the underlying graded bed, Plate 6-d, Plate 7-a. Loaded graded beds are characteristic of facies D and are

common in subfacies Bg. Table III.7 lists their characteristics in the facies.

Loading occurs in three ways, and loaded graded beds displaying the different types of loading

commonly occur interbedded with one another. (1) Load-casted ripples (Collinson and Thompson, 1989;

Blatt, Middleton and Murray, 1980) form where laminae in isolated ripple lenses deformed by sinking into

the underlying mud layer. Some graded beds display un-deformed trochoidal ripples, built on top of the load-casted ripples. (2) Pseudo-nodules of sand surrounded by mud (Blatt, Middleton and Murray, 1980) occur where ripple forms sank completely into the underlying mud, and (3) Sinking of individual sand grains into the underlying muddy layer, making the top of the underlying muddy layer appear reverse graded, Plate 7-a.

The coarser-to-finer transitions in the loaded graded beds commonly display mature grading. Loaded graded beds commonly contain well sorted lower very fine-grained sandstone that grades upward to siltstone and then to mudstone.

MICROLAMINATED GRADED BEDS: Microlaminated graded beds are named for their thickness, which is less than 3 mm for the siltstone or sandstone-mudstone pair. The microlaminated graded beds of this dissertation are equivalent to the microlaminae sediment type of Winston (1986 b) and Winston and Link (1993). Reineck and Singh (1980) called similar structures tidal bedding, laminites or rhythmites. Table III.8 lists their characteristics in the facies.

The coarser-to-finer transitions commonly display immature grading. Most microlaminated graded beds display planar coarser-to-finer transitions. Their basal contacts are commonly planar, or rarely shallowly scoured. Rarely the coarser-to-finer transitions contain trochoidal ripples or slightly-asymmetric ripple forms. Thus, the microlaminated graded beds display the same morphologies as the even, shallowly scoured and lenticular graded beds. In thin-section, some siltstone layers in even microlaminated graded beds contain small scale, high angle, angular or tangential cross-laminae.

Microlaminated graded beds occur in cosets. The cosets can be separated from other cosets by (1) a gentle scour surface with 5 to 15 cm of relief, (2) a lenticular graded bed, (3) an ungraded sandstone bed, or (4) an anomalous graded bed. Ungraded sandstone beds interbedded with microlaminated graded bed

Figure III.6. Line drawings showing the different types of contacts between an
erosion surface and the overlying microlaminated graded beds.
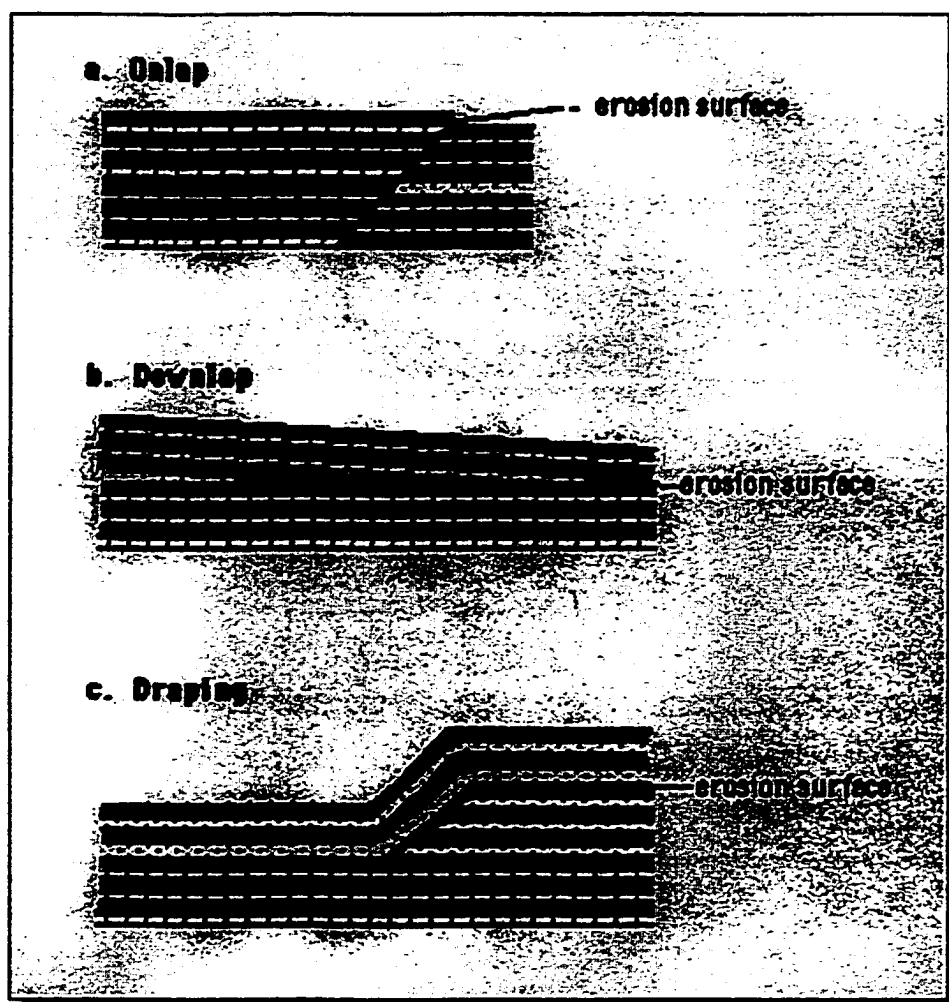
cosets commonly contain small scale angular or tangential, high angle cross-laminae cosets, and reactivation surfaces. Microlaminated graded beds onlap, downlap or drape the scour surfaces. Figure III.6. Woods (1986) described the same types of surfaces separating cosets of microlaminae in the Shepard Formation.

At some locations, the microlaminated graded beds display changes in sandstone/ mudstone ratios within a coset. At these locations the microlaminated graded beds change from an interval 0.5 to 2 cm thick composed of sandy microlaminated graded beds, to an interval 0.25 to 1 cm thick composed of muddy microlaminated graded beds, Plate 5-a, c, d, and e. However, other observers (Don Winston, 1995, personal communication) do not recognize changes in the sandstone/ mudstone ratios. Williams (1989 a; 1989 b) called similar changes in sandstone/ mudstone ratios lamina-cycles.

At some locations the microlaminated graded beds also display systematically alternating high-low sandstone/ mudstone ratios, Plate 5-d. However, other observers (Don Winston, 1995, personal communication) do not recognize alternating high-low sandstone/ mudstone ratios. The lamina-cycles and alternating high-low ratio microlaminated graded beds have not been previously described in rocks of the Belt Supergroup, and are controversial.

ANOMALOUS GRADED BEDS

The anomalous graded beds were given a different names to emphasize the fact they differ from the interbedded background graded beds. Anomalous graded beds: (1) are thicker than the interbedded background graded beds; (2) have higher sandstone/ mudstone ratios than the interbedded background graded beds; (3) commonly contain coarser-grained sand than the interbedded background graded beds; and (4) have basal contacts that commonly truncate several underlying background graded beds. Figure III.7 shows the morphologies of the different types of anomalous graded beds. Authors of previous studies of the Helena and Wallace formations made no distinction between anomalous and background graded beds.

Figure III.7. Line drawings showing the morphologies of the anomalous
graded beds.
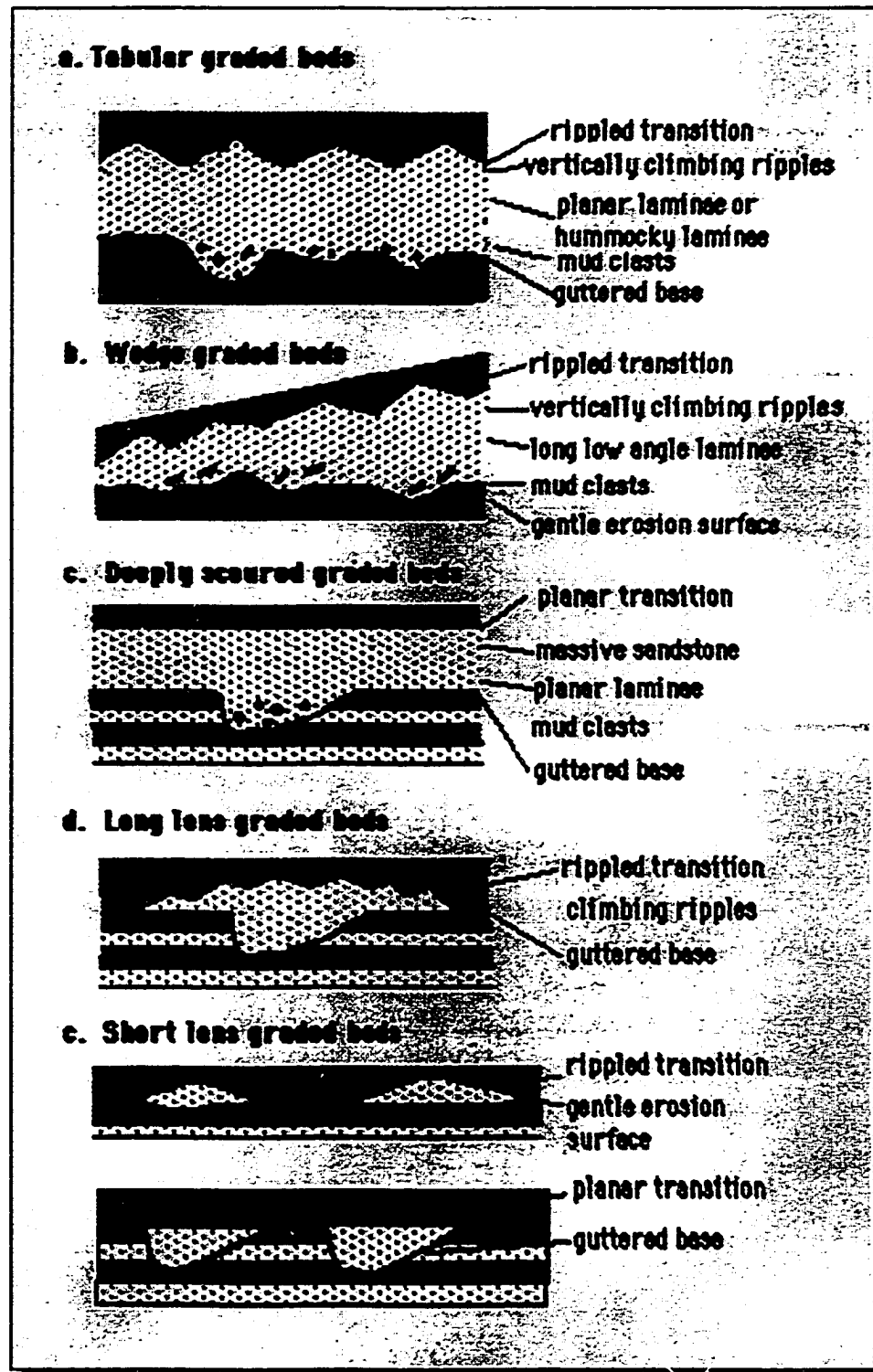
TABULAR GRADED BEDS. Tabular graded beds comprise the thickest and the sandiest graded beds found in the Helena and Wallace formations. Table III.9 lists their characteristics in the different facies. The sandstone layers of tabular graded beds maintain the same thickness across tens of meters of exposure, commonly displaying gently wavy sandstone-mudstone transitions and wavy basal contacts. Commonly, the basal contacts truncate the underlying graded beds at a very low angle. Tabular graded beds range from about 10 to 45 cm thick, including the mudstone layers which range from about 1 to 3 cm thick.

Tabular graded beds display a wide variety of laminae and ripple forms, and commonly display the vertical sequences shown on Table III.2-a and b. The coarser layers commonly display mature grading, rarely from conglomerate, or commonly from very fine-grained sand, up to silt. The siltstone-mudstone transition commonly displays immature grading.

WEDGE GRADED BEDS. As the name implies, wedge shaped graded beds thin across vertical exposures, Plate 6-b. They range from about 5 cm to about 20 cm thick, and pinch out in several meters. The basal contacts of the wedge graded beds commonly truncate the underlying graded beds at a low angle. Table III.10 lists their characteristics. The coarser layers of the wedge graded beds commonly contain upper very fine-grained sand, or rarely they contain matrix supported intraclast conglomerate. Mudstone layers commonly range from 1 to 2 cm thick.

Slightly asymmetric small scale ripples or rounded trochoidal ripples commonly occur at the sandstone-mudstone transitions. Moderately abundant planar laminae or quasi-planar laminae occur at the base of the sandstone layers. Long, low angle laminae are very common, but large hummocky ripples are absent. Laminae sequence Table III.2-c is common.

DEEPLY SCOURED GRADED BEDS. Sandstone layers in deeply scoured graded beds display planar tops and guttered bases (Woods, 1986). Between the cutters, their basal contacts commonly truncate

the underlying graded beds at a low angle. Deeply scoured graded beds range from about 5 to 10 cm thick between the gutters, but commonly reach 30 cm thick in the gutters. Table III.11 lists their characteristics in the facies. The coarser-to-finer transitions of the deeply scoured graded beds display mature grading that grades upward from massive sandstone to mudstone, over several millimeters.

Sandstone layers in the deeply scoured graded beds commonly contain upper very fine-grained sand, and rarely the gutters contain matrix supported mudstone clast conglomerate. Deeply scoured graded beds commonly display planar laminae, quasi-planar laminae, long, low angle laminae or massive bedding. The structures commonly occur in the order shown on Table III.2-d. In contrast to the other anomalous graded beds, deeply scoured graded beds do not contain symmetrical bedforms.

LONG LENS GRADED BEDS. Long lens graded beds display discontinuous sandstone layers, producing lenses up to about 15 cm, that range from about 1 meter to several meters long, Plate 6-b. Long lens graded beds commonly contain lower very fine-grained sand, overlain by a mudstone layer 1 to 2 cm thick. Characteristics of the long lens graded beds in the facies are listed on Table III.12. In facies C their basal contacts commonly truncate the underlying graded beds at a low angle, and at some locations, the basal contacts contain gutters (Woods, 1986), Plate 4-c.

Long low angle laminae are common in the lower parts of the sandstone layers. The upper part of the sandstone layers commonly contain small hummocky ripples or trochoidal ripples with concordant internal lamination, Table III.2-c lists the most common sequence of structures, but immature grading across the coarser-to-finer transition is more common than mature grading.

SHORT LENS GRADED BEDS. Short lens graded beds are similar to the long lens graded beds except the sand lenses are not so long or thick, ranging from 10 to 60 cm long, and up to 10 cm thick. Table III.13 lists their characteristics. Sandstone layers in short lens graded beds display three morphologies: (1)

as a horizon of rounded convex-up lenses 10 to 30 cm long, with more or less flat bases, resting on a low

angle truncation surface; (2) as a horizon of flat topped gutter fillings, 15 to 30 cm wide, Plate 4-c; or (3)

rarely as an horizon of trochoidal ripples. Rarely, the gutters contain matrix supported molar-tooth

clast conglomerate.

UNGRADED BEDS

I make a distinction between the graded beds and ungraded beds because the graded beds fine

upward, whereas ungraded beds do not. The different ungraded beds are recognized by their composition

and texture.

POD CONGLOMERATE. Pod conglomerate beds consist of clast supported, tabular or disk-

shaped clasts 3 cm to 20 cm long, by 0.25 to 1 cm thick. The clasts in the pod conglomerate beds have the

same compositions and textures as molar-tooth pods (O'Connor, 1967). Clasts consist of microspar calcite

cementing siliciclastic sandstone, siltstone or mudstone, set in a very fine-grained sand matrix. Some

conglomerate beds displays randomly oriented, imbricated, and radially imbricated clasts or stone rosettes

(Ricketts and Donaldson,1979). Tabular pod conglomerate beds range in thickness from about 10 cm to

about 1.5 m thick. Pod conglomerate lenses range from 20 cm to 5 m long, and from 5 cm to 30 cm thick.

Both the beds and lenses rest on erosion or truncation surfaces.

MOLAR-TOOTH INTRACLAST CONGLOMERATE. Molar-tooth conglomerate beds

contain clast supported rounded, disk or tabular shaped calcite microspar clasts, 0.5 cm to about 3 cm long

by 1 mm to 3 mm thick. Clasts are set in a very fine-grained quartz sand (O'Connor, 1967) or fine sand-

sized carbonate intraclast matrix. The calcite in the clasts is the same size and morphology as the calcite in

blobs, vertical ribbons and horizontal ribbon molar-tooth structures, and O'Connor (1967) called these beds

molar-tooth hash beds. The clasts in some beds are randomly oriented and in others they are imbricated at a

low angle to bedding, or imbricated into stone rosettes. Beds range from continuous to lenticular, from 10

cm to about 45 cm thick, and they commonly rest on truncation surfaces.

INTRACLAST GRAINSTONE BEDS. The intraclast grainstone beds are composed of carbonate cemented, fine sand-to-granule sized, siliciclastic siltstone or mudstone intraclasts. The clasts and matrix commonly contain about 50 percent calcite microspar cement. Intraclast grainstone beds range from 20 to 50 cm thick, and, in some places, are stacked into cosets that range from about 0.5 m up to about 15 m thick. Intraclast grainstone beds and cosets commonly appear massive due to recrystalization of the carbonate within the intraclasts and matrix, which tends to weld both the primary current laminae and the bedding planes into one mass. However, at some locations, planar laminae, quasi-planar laminae, long low angle laminae, trochoidal ripples or medium to long spaced hummocky ripples can still be recognized on weathered surfaces, producing complexly laminated sequences.

DOLOMITIC SILTSTONE BEDS. Dolomitic siltstone beds are composed mainly of coarse silt and minor lower very fine-grained quartz sand, cemented with subhedral to euhedral 20 to 50 μm dolomite. The total dolomite content approaches, but rarely exceeds 50 percent of the rock. Recrystalization is common, but some dolomitic siltstone beds contain planar laminae, quasi-planar laminae and long low angle laminae and small scale ripple forms and laminae, commonly producing complexly laminated sequences.

QUARTZ SANDSTONE BEDS. Two types of quartz sandstone beds occur in the Helena and Wallace formations: (1) well rounded, medium-grained quartz sandstone beds; and (2) very fine grained, angular quartz sandstone beds. The well rounded, medium-grained sandstone beds range from several centimeters to a few meters thick (Hurberger, 1986). They are very rare and occur in the lowestmost and uppermost Helena Formation, mainly in the eastern part of the basin. But, in Glacier National Park they are scattered throughout the Helena Formation (Don Winston, 1993, written communication).

The very fine-grained quartz sandstone beds occur at two thickness: thinner sandstone beds range form 7 cm to 15 cm thick, but the thicker beds are about 50 cm thick. Thick and thin sandstone beds are

commonly interbedded and cosets range from 30 cm to about 3 m thick. The tops and bottoms of the

individual beds within the cosets are wavy, Plate 1-c. Internally, the sandstone beds commonly display

planar, quasi-planar or long low angle laminae; hummocky ripples are less common.

OOLITIC LIMESTONE BEDS. Oolitic limestone beds range in composition from 100 percent

ooids to mixtures of ooids and sand-sized or granule-sized intraclasts similar to those in the intraclast

grainstone beds. Rare oolite beds in the eastern basin contain up to 5 -10 percent well rounded, medium-

grained quartz sand (O'Connor, 1967). Oolite beds range up to about 30 cm thick, and are commonly

massive. Rare meter scale oolitic limestone sequences are composed of cosets of 5 to 10 cm thick wavy

oolite beds, inclined at low angles to bedding.

MUDSTONE BEDS. The Helena and Wallace formations contain rare massive mudstone beds

that display no evidence of internal bedding or grading, Plate 6-a. Mudstone beds range from about 20 cm

to about 1 m thick and commonly contain vertical molar-tooth ribbons. Mudstone beds commonly contain

up to 50 percent carbonate microspar, either as subhedral to euhedral calcite or as euhedral dolomite, or a

mixture of both. Stained thin-sections commonly show high iron euhedral dolomite overgrowths on low

iron rounded calcite cores.

STROMATOLITE BEDS. Stromatolite beds in the Helena and Wallace range from 10 cm to

over 3 m thick. Stromatolites in the beds occur a wide variety of forms and sizes: low domes, 30 to 60 cm

in diameter and 10 to 20 cm high; large domes 1 to 2 m in diameter and 20 to 30 cm high; elongate ridges

that are dome shaped in the short dimension but are ridge like in the long dimension, producing forms 0.5

m wide by 2 to 3 m long and 30 to 40 cm high; muffin shaped domes 60 cm in diameter and 20 cm high;

straight sided columns 20 to 30 cm in diameter and 45 cm high; club shaped columns 7 cm wide at the

base, 15 cm wide at the top and about 45 cm high; branching columns (Baicalia?); columns composed of

cones (Conophyton?) about 15 cm wide and up to 50 cm high. The reader is referred to Horodyski (1976;

1989) and Stickney (1991) for more detailed descriptions of the Baicalia-Conophyton cycles in the Helena

Formation.

In addition to beds containing clearly stromatolitic structures, many intervals in the upper Helena

Formation contain cryptalgalaminite. Cryptalgalaminite beds consist of horizontal, black, crinkled,

millimeter scale, carbonate rich laminae. They are commonly interbedded with microlaminated graded

beds. Grotzinger (1981) and Winston (1986 b) included the cryptalgalaminite beds in the microlaminated

rock subtype.

FACIES

Walker (1992, p. 2) defines a facies as ". . . a body of rock characterized by a particular

combination of lithology, physical and biological structures that bestow an aspect . . . different from the

bodies of rock above, below and laterally adjacent". Furthermore, facies ". . . signify any particular kind of

sedimentary rock or distinguishable rock record formed under common environmental conditions of

deposition. . ." (Bates and Jackson, 1980, p. 220), thus the facies can be either descriptive or interpretive

(Anderton, 1985). I use the term in both ways, but the way it is used is clear.

I chose to divide the Helena and Wallace formations into four facies. Each facies is characterized

by a dominant lithology (sandstone, mixed sandstone-mudstone, or mudstone) and the dominant

thicknesses of its background graded beds. I also define subfacies within facies. Although a given facies

commonly contains several types of background graded beds, their thickness, morphology, internal

structures and sandstone/ mudstone ratios are similar. The four facies described below include most of the

major lithologic variability in the Helena and Wallace formations. By necessity many textures and

structures are lumped into a given facies.

FACIES A: THE SANDSTONE FACIES. The high sandstone content in the background graded

beds characterizes facies A and ranges from about 65 percent up to nearly 100 percent, Plate 1. Background

graded beds range from about 7 to 15 cm thick, and the anomalous graded beds range form about 15 cm to

45 cm thick. Table III.14 lists the characteristics of facies A.

At most locations facies A is composed of very sandy, wavy or lenticular background graded beds

in cosets. The sandstone layers commonly contain upper very fine-grained quartz sand. Facies A commonly

displays abundant rounded trochoidal and small and rare medium hummocky ripples, all with concordant

internal laminae. Shallowly scoured background graded bed cosets, with planar laminae, characterize facies

A at some locations (see Winston, 1989, p. 54, Fig. 16).

Tabular and wedge-shaped anomalous graded beds commonly occur in facies A; deeply scoured

graded beds are less common. Anomalous graded beds in facies A range from about 15 to 45 cm thick, and

are composed of upper very fine-grained quartz sand, or rarely clast or matrix supported, intraclast

conglomerate. Tabular and wedge-shaped graded beds commonly display large hummocky ripples, planar

laminae, quasi-planar laminae and long low angle laminae. Short spaced hummocky, rounded trochoidal

and trochoidal ripples commonly occur in the upper parts of the sandstone layers.

At some locations facies A contains ungraded molar-tooth ribbon intraclast conglomerate beds and

ungraded quartz sandstone beds (Plate 1 c). The ungraded sandstone beds commonly contain planar

laminae, quasi-planar laminae, long low angle laminae, and rarely large hummocky ripples.

Facies A has four subfacies: subfacies Aw, Plate 1-a, d, characterized by wavy background graded

bed cosets; subfacies Al, Plate 1-b, characterized by lenticular background graded bed cosets; subfacies As

(see Winston, 1989. p. 54, Fig. 16) characterized by shallowly scoured background graded bed cosets; and

subfacies Ab, Plate 1-c, characterized by ungraded quartz sandstone bed cosets. Subfacies Ab also occurs as

a dolomitic or calcitic variety, composed of ungraded dolomitic or calcitic intraclast grainstone beds or

dolomitic siltstone beds.

FACIES B: THE 50/50 SANDSTONE SILTSTONE-MUDSTONE FACIES. In decreasing order of abundance, facies B contains shallowly scoured, even, and lenticular background graded beds. The graded beds contain between 35 and 65 percent sandstone, Plate 2, and range from about 1 to 20 cm thick. Table III.15 lists facies' B characteristics.

The lenticular and even graded beds mainly occur as isolated graded beds, separating 20 to 60 cm thick cosets of shallowly scoured graded beds. Silt or mixtures of silt and lower very fine-grained sand comprise the sandstone or siltstone layers. The even and shallowly scoured graded beds contain massive bedding or rarely planar laminae. The sandstone layers in the rare lenticular graded beds commonly contain trochoidal ripples or rounded trochoidal ripples.

Facies B rarely contains wedge, long lens and deeply scoured anomalous graded beds, except in subfacies Bg, where they are common and may compose 50 percent of the facies. Facies B is the only facies in which massive bedding in the anomalous graded beds is more common or as common as current laminae. Planar, quasi-planar or long low angle laminae occur at the base of the sandstone layers, overlain by massive sandstone, which is overlain by mudstone. The coarser-to-finer transitions in the anomalous graded beds rarely display ripple forms.

Facies B displays a lot of variation and encompasses at least five subfacies. Subfacies Besl, Plate 2-b, is the most common subfacies. It is composed mainly of 2 to 10 cm thick even, lenticular and shallowly scoured background graded beds, interbedded with rare deeply scoured, long lens and wedge anomalous graded beds. Subfacies Bss, Plate 2-c, is composed mainly of 3 to 5 cm thick shallowly scoured and even graded beds and rare lenticular graded beds. Subfacies Bl, Plate 2-a, is composed of 1 to 3 cm thick shallowly scoured, lenticular and rare loaded background graded beds, interbedded with wedge and long lens anomalous graded beds with loaded bases. Subfacies Be is composed of 10 to 15 cm thick interstratified even, shallowly scoured, and loaded background graded beds, and lacks anomalous graded beds.

Subfacies Bg, Plate 3, comprises intervals ranging about 3 to 20 m thick in the Wallace formation at some locations. Subfacies Bg is composed of 3 to 5 cm thick shallowly scoured, even, lenticular and rare loaded background graded beds. The background graded beds are interbedded with common tabular, wedge and deeply scoured graded beds. The anomalous graded beds commonly rest on guttered erosional surfaces, which give the subfacies its name. At some locations, anomalous graded beds may dominate making the subfacies continuous with facies A. The high number of gutters and truncation surfaces in subfacies Bg indicates deposition in a far different environment than the other subfacies of facies B

FACIES C: THE THINLY LAMINATED MUDSTONE FACIES. Facies C contains even, shallowly scoured, lenticular graded beds 0.3 to 2 cm thick and microlaminated graded beds, composed of 35 percent or less siltstone. The microlaminated graded beds display the same morphologies as the even, shallowly scoured and lenticular graded beds. Characteristics of facies C are listed on Table III.16. Coarse silt, or rarely lower very fine sand, comprise the coarser layers. The even, shallowly scoured and microlaminated graded beds commonly contain massive bedding; rarely they contain small scale, angular or tangential cross-laminae. Interbedded lenticular graded beds contain trochoidal, rounded trochoidal, slightly asymmetric or asymmetric, 2D ripples, commonly with concordant laminae (see Winston, 1989, Fig. 17, p. 55).

The most common anomalous graded beds in facies C are short lens, long lens and wedge graded beds; commonly they display guttered basal contacts. Lower very fine-grained sand makes up the sandstone parts of the anomalous graded beds, which range form about 3 to 10 cm thick. Ripple forms or laminae commonly overlie massive bedding in the anomalous graded beds.

Facies C occurs in two varieties: subfacies Cs, Plate 4, a siliciclastic rich subfacies and subfacies Cc, a carbonate rich subfacies. The same background and anomalous graded beds described above occur in both subfacies, but subfacies Cc also contains ungraded oolitic limestone beds, ungraded cryptalgalaminite

beds, ungraded stromatolite beds, ungraded molar-tooth intraclast conglomerate beds and lenses or ungraded microspar rich mudstone beds.

At some locations subfacies Cs contains 20-30 cm deep, 2 -3 m wide bow shaped scour features. These channel-lile lenses are filled with facies C background and anomalous graded beds. Plate 4 -d shows the edge of such a channel-like lens.

FACIES D: THE MEDIUM BEDDED MUDSTONE FACIES. Most background graded beds in facies D are between 5 to 15 cm range, but some range up to 20 cm thick and some down to about 1 mm thick. The millimeter scale graded beds are similar to the microlaminated graded beds, but in facies D they occur in centimeter scale cosets. The background graded beds contain less than 35 percent sandstone, and commonly less than 10 percent. Facies D contains lenticular, even, shallowly scoured and loaded background graded beds. Details of facies D are listed on Table III.17. Coarse silt and minor lower very fine-grained sand make up the coarser-grained parts of the graded beds. Lenticular and loaded background graded beds commonly contain trochoidal ripples with concordant laminae or slightly asymmetric ripples with discordant laminae, Plate 7-c. The even and shallowly scoured graded beds contain planar laminated lower very fine-grained sandstone, or faintly horizontally laminated siltstone, Plate 7-b.

Facies D contains tabular, wedge or long lens anomalous graded beds, commonly with planar basal contacts. The anomalous graded beds in facies D rarely display gutters, truncation surfaces, or loaded bases. The sandstone layers in the anomalous graded beds contain mainly upper very fine-grained sand and range form about 3 cm to 30 cm thick.

Facies D is approximately equivalent to Winston's (1986 b; 1989) carbonate mud sediment type. Winston (1989, p. 56, Fig. 20) shows a picture of weathered facies D, composed of very faint 5 to 20 cm thick, very muddy graded beds.

I recognize three subfacies of facies D. Subfacies Desl-a, Plate 6-b. composed of even, lenticular

and shallowly scoured background graded beds, and interbedded wedge and long lens anomalous graded

beds. Subfacies Desl-m , Plate 6-a, 6-c, 7-b, 7-d , contains even, lenticular, and shallowly scoured

background graded beds and interbedded massive mudstone beds, but lacks interbedded anomalous graded

beds. The bases of the mudstone beds commonly rest on a guttered surface, Plate 6-a. Subfacies Dl, Plate 6-

c, 6-d, 7-a, 7 c, is composed of interbedded loaded, lenticular and even graded beds, and in some places,

interbedded tabular and wedge anomalous graded beds, Plate 7-a, with loaded basal contacts.

Table III. 3. Characteristics of the even graded beds in the different facies. 1 = facies. 2 = occurrence. 3 = abundance. 4 = percent sandstone. 5 = grain size in sandstone layer. 6 = thickness in cm. 7 = type of grading. 8 = internal structures. 9 = internal laminae sequences (see Table III.2); and notes.

1	2	3	4	5	6	7	8	9
A	Co	Mi	65-99% sandstone	UVFG	5-15	M	massive bedding, VC planar laminae, R	(d)
B	Co	Mi	35-65%45 sandstone	LVFG(A) Z(A)	2-10	M M	massive bedding, VC planar laminae, R	(d)
	S	A						
C	Co	VA	15-35% sandstone	Z(VA) LVFG(Mi)	0.3-2	M	massive bedding, VC small scale cross laminae, R	none; laminae seen in thin section only
	S	A						
D	Co	Mi	5-10% sandstone	Z(VA) LVFG(Mi)	0.3-20	M M	massive bedding	(d)

Note: Even graded beds do not contain bedforms. In this respect they are similar to shallowly scoured background graded beds and deeply scoured anomalous graded beds.

Abbreviations for tables III.3 to III.7

VA - very abundant	VC- very common	ss - sandstone
A - abundant	C - common	Z - siltstone, or silt
Mi - minor	R - rare	icc - intraclast conglomerate
Ab - absent		

UVFG - upper very fine-grained
LVFG - lower very fine-grained

S - graded bed occurs as a single graded bed interbedded with different graded beds
Co - graded beds occur in cosets

M - mature grading, continuous gradation from coarser layer to finer layer
I - immature grading, abrupt transition from coarser layer to finer layer

Table III.4. Characteristics of the lenticular graded beds in the different facies. See Table III.3 for abbreviations. 1 = facies. 2 = occurrence. 3 = abundance. 4 = percent sandstone. 5 = grain size in sandstone layer. 6 = thickness in cm. 7 = type of grading. 8 = internal structures. 9 = internal laminae sequences from Table III.2.

1	2	3	4	5	6	7	8	9
A	S	Mi	65-99% sandstone	UVFG	5-15	I M M M	trochoidal ripples-C rounded trochoidal ripples- VC small hummocky ripples- R long low angel laminae- R	(c), C; (a), R; (e), R
B	S	Mi	35-65% sandstone	LVFG(A) Z(Mi)	2-10	I I	massive bedding- VC trochoidal ripples- R	(c), R; rarely in cosets
C	Co S	Mi A	<15-35% sandstone	Z(A) LVFG (Mi)	0.3-2	I I	massive bedding- VC trochoidal ripples- C slightly asymmetric ripples- C discontinuous lenses- C	(I);
D	Co	VA	<10% sandstone	Z(A) LVFG (Mi)	1-20	M M	massive bedding- R discontinuous lenses- VC trochoidal ripples- C slightly asymmetric ripples-C (with concordant laminae- A) (with discordant laminae- Mi)	(I);

Notes: Laminae within the ripple forms are concordant unless other wise noted. See Figure III.3 for line drawings of ripples.

See Table III.1 for descriptions of the internal structures.

Table III.5. Characteristics of the shallowly scoured graded beds in the different facies. See Table III.3 for abbreviations.
1 = facies. 2 = occurrence. 3 = abundance. 4 = percent sandstone. 5 = grain size in sandstone layer.
6 = thickness in cm. 7 = type of grading. 8 = internal structures. 9 = internal laminae sequences from Table III.2.

1	2	3	4	5	6	7	8	9
A	S	Mi	65-75% sandstone	LVFG	5-10	M	massive bedding- VC planar laminae- R	(d) where planar laminae are present
B	S	Mi	35-65%	Z(VA)	5-10	M	massive bedding- VC	(d) where planar laminae are present
	Co	VA	sandstone	LVFG(Mi)			planar laminae- R	
C	Co	A	15-35% sandstone	Z(VA) LVFG(Mi)	0.3-2	M	massive bedding	----
D	S	Mi	<10% sandstone	Z	3-10	M	massive bedding planar laminae (seen on slabs)	(d) where planar laminae are present

Notes: Shallowly scoured graded beds do not display symmetrical bedforms or symmetrical bed forms with internal laminae. In this respect they are similar to even background graded beds and deeply scoured anomalous graded beds.

Table III.6. Characteristics of the wavy graded beds in the different facies. See Table III.3 for abbreviations.
1 = facies, 2 = occurrence, 3 = abundance, 4 = percent sandstone, 5 = grain size in sandstone layer; 6 = thickness in cm, 7 = type of grading, 8 = internal structures, 9 = internal laminae sequences from Table III.2.

1	2	3	4	5	6	7	8	9
A	Co	VA	90-99% sandstone	UVFG	5-15	M, C I, C	trochoidal ripples- Mi rounded trochoidal ripples- A small hummocky ripples- VA medium hummocky ripples- Mi long low angle laminae- Mi	(c), A
B	Co	Mi	50-65%	LVFG	3-7	M, C	trochoidal ripples- Mi rounded trochoidal ripples- Mi small hummocky ripples- VA	(c), A
C	—	Ab	—	—	—	—	—	—
D	—	Ab	—	—	—	—	—	—

Notes: See Table III.1 for bedform descriptions and Figure III.3 for line drawings of bedforms.

Table III.7. Characteristics of the loaded graded beds in the different facies. See Table III.3 for abbreviations.
1 = facies. 2 = occurrence. 3 = abundance. 4 = percent sandstone. 5 = grain size in sandstone layer. 6 = thickness in cm. 7 = type of grading. 8 = internal structures. 9 = internal laminae sequences from Table III.2.

1	2	3	4	5	6	7	8	9
A	—	Ab	—	—	—	—	—	—
B	S	Mi	35-50% sandstone	LVFG(A) Z(Mi)	3-7	M	trochoidal ripples- A small, slightly asymmetric forms- A	loaded graded beds occur only in subfacies Bg
C	.	Ab	—	—	—	—	—	—
D	S Co	A VA	<20% sandstone	Z(VA) LVFG(Mi)	5-20	M	trochoidal ripples- VA	(f); characteristic of facies D

See Table III.1 for ripple descriptions and Figure III.3 for line drawings of bedforms..

Table III.8. Characteristics of the microlaminated graded beds in the different facies. See Table III.3 for abbreviations.
1 = facies. 2 = occurrence. 3 = abundance. 4 = percent sandstone. 5 = grain size in sandstone layer. 6 = thickness in cm. 7 = type of grading. 8 = internal structures. 9 = internal laminae sequences from Table III.2.

1	2	3	4	5	6	7	8	9
A	—	Ab	—	—	—	—	—	—
B	-	Ab	—	—	—	—	—	—
C	Co	VA	10-35% sandstone	Z(A) LVFG(A)	<0.3	—	small scale, angular, cross-laminae-R small scale, tangential cross-laminae- R (mostly only seen in thin-sections) trochoidal ripples- R	occur in 5 -20 cm thick cosets, X cosets are commonly stacked into meter-scale units
D	Co	Mi	<35% sandstone	LVFG	<0.3	—	massive	occur in 1-5 cm thick cosets, cosets are not stacked

Notes: Microlaminated graded beds are recognized by the thinness of the graded beds. Microlaminated graded beds display the same morphologies as the even (very common), shallowly scoured (common) and lenticular (rare) graded beds. Except for the lenticular graded beds, ripple forms and ripple forms with internal laminae do not occur in the microlaminated graded beds. Symmetrical and slightly asymmetrical ripple forms, commonly with concordant internal laminae are common in the lenticular microlaminated graded beds.

Microlaminated graded beds commonly gradationally change from an interval 0.5 to 2 cm thick composed of sandy microlaminated graded beds, to an interval 0.25 to 1 cm thick composed of muddy microlaminated graded beds, called lamina-cycles.

Microlaminated graded beds also display systematically alternating thick and thin even microlaminated graded beds.

*Table III.9. Characteristics of the **tabular** graded beds in the different facies. See Table III.3 for abbreviations.*
1 = facies. 2 = occurrence. 3 = abundance. 4 = type of basal contact. 5 = grain size in sandstone layer;
6 = thickness in cm. 7 = type of grading. 8 = internal structures. 9 = internal laminae sequences from Table III.2.

1	2	3	4	5	6	7	8	9
A	S Co	A VA	gutters (R) low angle truncation (C)	UVFG(VA) ice(Mi)	10-45	M, (C) I, (R)	trochoidal ripples- Mi rounded trochoidal ripples- A small hummocky ripples- VA medium hummocky ripples- A large hummocky ripples-A long low angle laminae - VA quasi-planar laminae-A planar laminae- A	(b) A; (a) R; base of bed may contain matrix or clast supported ice
B	S	Mi	gutters (C)	UVFG(VA) ice(Mi)	10-20	M, (C) I, (R)	trochoidal ripples- Mi rounded trochoidal ripples- A small hummocky- A long low angle laminae - VA planar laminae- A	(c) in gutters; (c) A; occur only in subfacies Bg
C	—	Ab	—	—	—	—	—	—
D	S	Mi	loaded (C) guttered (R)	UVFG	20-30	M	trochoidal ripples- A rounded trochoidal ripples- A small hummocky ripples- VA medium hummocky ripples- A large hummocky ripples-A long low angle laminae - A quasi-planar laminae- A	(b) A; (a) R

Notes: See Table III.1 for bedform descriptions and Figure III.3 for line drawings of bedforms.

Table III.10. Characteristics of the wedge graded beds in the different facies. See Table III.3 for abbreviations.
1 = facies. 2 = occurrence. 3 = abundance. 4 = type of basal contact. 5 = grain size in sandstone layer.
6 = thickness in cm. 7 = type of grading. 8 = internal structures. 9 = internal laminae sequences from Table III.2.

1	2	3	4	5	6	7	8	9
A	S Co	VA Mi	minor scour	UVFG(VA) ice(Mi)	10-20	M	trochoidal ripples- Mi small slightly asymmetric ripples-A rounded trochoidal ripples- Mi small hummocky ripples- A medium hummocky ripples- VA long low angle laminae - VA	(c), C; rarely contains matrix supported ice
B	S Co	A Mi	minor scour; gutters	UVFG	10-20	M	trochoidal ripples- Mi small slightly asymmetric ripples A rounded trochoidal ripples- Mi small hummocky ripples- VA medium hummocky ripples- Mi long low angle laminae - A	(c), C; (d), C; occur only in subfacies Bg, commonly with guttered basal contacts
C	—	Ab	—	—	—	—	—	—
D	S	Mi	minor scour	UVFG	10-20	M	trochoidal ripples- Mi small slightly asymmetric ripples A rounded trochoidal ripples- Mi small hummocky ripples- VA medium hummocky ripples- Mi long low angle laminae - A	(c), C

Notes: See Table III.1 for bedform descriptions and Figure III.3 for line drawings of bedforms.

Table III.11. Characteristics of the deeply scoured graded beds in the different facies. See Table III.3 for abbreviations.
1 = facies, 2 = occurrence, 3 = abundance, 4 = type of basal contact, 5 = grain size in sandstone layer, 6 = thickness in cm, 7 = type of grading, 8 = internal structures, 9 = internal laminae sequences from Table III.2.

1	2	3	4	5	6	7	8	9
A	S	Mi	gutters	UVFG	5-10	M	massive bedding- VA long low angle laminae- A planar laminae- VA	(d), C
B	S	A	gutters	UVFG ice(Mi)	20-30	M	massive bedding- VA long low angle laminae- A planar laminae- VA	(d), C matrix supported ice in gutters
C	—	Ab	—	—	—	—	—	—
D	—	Ab	—	—	—	—	—	—

Notes: Deeply scoured anomalous graded beds do not display symmetrical ripple forms or symmetrical ripple forms with internal laminae. In this respect the deeply scoured anomalous graded beds are similar to the even and shallowly scoured background graded beds.

Facies D contains very rare- massive ungraded mudstone beds resting on a guttered surface cut 5 to 15 cm into the underlying thick very muddy lenticular graded beds. These mudstone beds may be related to the deeply scoured graded beds.

Table III.12. Characteristics of the long lens graded beds in the different facies. See Table III.3 for abbreviations. 1 = facies, 2 = occurrence, 3 = abundance, 4 = type of basal contact, 5 = grain size in sandstone layer, 6 = thickness in cm, 7 = type of grading, 8 = internal structures, 9 = internal laminae sequences from Table III.2.

1	2	3	4	5	6	7	8	9
A	—	Ab	—	—	—	—	—	—
B	—	Ab	—	—	—	—	—	—
C	S	A	low angle truncation; gutters	LVFG icc(R)	2-15	M I	trochoidal ripples- VC rounded trochoidal ripples- C small hummocky ripples- C long low angle laminae- C massive bedding- C	(c), C
D	S	Mi	minor scour	LVFG	2-15	M	massive bedding	—

Notes: See Table III.1 for bedform descriptions and Figure III.3 for line drawings of bedforms.
At some locations, facies D contains long lens graded beds that are regularly spaced at 20-30 cm apart.

*Table III.13. Characteristics of the **short lens** graded beds in the different facies. See Table III.3 for abbreviations.*
1 = facies, 2 = occurrence, 3 = abundance, 4 = type of basal contact, 5 = grain size in sandstone layer,
6 = thickness in cm, 7 = type of grading, 8 = internal structures, 9 = internal laminae sequences from Table III.2.

1	2	3	4	5	6	7	8	9
A	—	Ab	—	—	—	—	—	—
B	S	Mi	gutters	LVFG icc (R)	5-20	I	massive bedding planar laminae	(a), C; short lens graded beds are common in subfacies Bg, but absent in other subfacies of facies B
C	S	Mi	gutters	LVFG icc (R)	2-15	I	trochoidal ripples- R rounded trochoidal ripples -R massive bedding-VC	occur as gutter fillings and isolated ripple lenses
D	—	Ab	—	—	—	—	—	—

Notes: See Table III.1 for bedform descriptions and Figure III.3 for line drawings of bedforms.

Table III.14. Characteristics of Facies A, the sandstone facies. See Table III.3 for abbreviations and Table III.1 for ripple descriptions.
1 = type graded bed. 2 = abundance. 3 = type of grading. 4 = types of bedforms and laminae. 5 = internal laminae sequences from Table III.2.
6 = amount of scour on basal scour. 7 = occurrence, single graded beds or cosets. 8 = typical grain size. 9 = notes.

Background graded beds. *Coarser-grained layers are composed mainly of very fine-grained sand. Background graded beds range from 5 to 15 cm thick.*

1	2	3	4	5	6	7	8	9
wavy	VA	M	trochoidal ripples- Mi rounded trochoidal ripples- A small hummocky ripples- VA medium hummocky ripples- Mi long low angle laminae- Mi	(c)	high	Co	UVFG	cosets form subfacies Aw
lenticular	A	M	trochoidal ripples- C rounded trochoidal ripples- VC small hummocky ripples- R long low angle laminae- R	(c)	minor	Co,C S, R	UVFG	cosets form subfacies Al
shallowly scoured	Mi	M	massive bedding- VC planar laminae-R	(d)	moderate	Co	LVFG	cosets form subfacies As

Beds.

• Tabular molar-tooth intraclast conglomerate beds 10 to 30 cm thick are very common in subfacies Ab. Clasts are commonly randomly oriented, imbricated or in rosettes.

• Wavy and tabular sandstone beds 10 to 30 cm thick are very common in subfacies Ab.

• Wavy beds of calcitic intraclast grainstone 10 to 30 cm thick commonly form intervals up to 15 m thick at some locations.

* Tabular dolomitic siltstone beds 50 to 150 cm thick, are stacked at some places, making intervals 3 to 30 m thick.

• Columnar and domed stromatolite beds are common in the eastern most Helena and Siyeh formations.

Table III.14. Facies A continued. See Table III.3 for abbreviations. See Table III.1 for bedform descriptions.
1 = type graded bed. 2 = abundance. 3 = type of grading. 4 = types of bed forms and laminae. 5 = Internal laminae sequences from Table III.2.
6 = amount of scour on basal scour. 7 = occurrence, single graded beds or cosets. 8 = typical grain size. 9 = notes.

Anomalous graded beds. *Coarser layers are composed mainly of very fine-grained sand, with rare matrix supported or very rare clast supported dolomitic mudstone or molar-tooth intraclast conglomerate. Anomalous graded beds range from 20 to 45 cm thick.*

1	2	3	4	5	6	7	8	9
tabular	A	M	trochoidal ripples- Mi rounded trochoidal ripples- A small hummocky ripples- VA medium hummocky ripples- A large hummocky ripples-A long low angle laminae - VA quasi-planar laminae- A planar laminae- A	(a)	truncation surfaces- VC; gutters- R	S;VA Co;R	UVFG ice;VR	cosets and interbedded with wedge graded beds produce subfacies Ab matrix supported ice common at base of bed and in gutters
wedge	A	M	trochoidal ripples- Mi rounded trochoidal ripples- Mi small slightly asymmetric ripples- A small hummocky ripples- VA medium hummocky ripples- Mi long low angle laminae - VA	(c)	truncation surfaces- VC; gutters- R	S;A Co;R	UVFG ice;R	Rare matrix supported ice at base of bed and common in gutters
deeply scoured	Mi	M	massive bedding- VA long low angle laminae- A planar laminae- VA	(d)	gutters only	S	UVFG ice;C	matrix supported ice common in gutters

Table III.15. Characteristics of Facies B; the 50-50 sandstone-mudstone facies. See Table II.3 for abbreviations. See Figure II.4 for bedform descriptions. 1 = type graded bed. 2 = abundance. 3 = type of grading. 4 = types of bedforms and laminae. 5 = internal laminae sequences from Table III.2. 6 = amount of scour on basal scour; 7 = occurrence, single graded beds or cosets. 8 = typical grain size. 9 = notes.

Background graded beds. *Coarser-grained layers are composed mainly of silt and lower very fine-grained sand. Background graded beds range from about 2 to 15 cm thick, but most are in the 3 to 10 cm thick range. Very commonly the background graded beds become muddier and thinner upwards in intervals composed of facies B.*

1	2	3	4	5	6	7	8	9
even	A	M	massive bedding- VC planar laminae- R	(d)	minor	S	LVFG Z	—
shallowly scoured	VA	M	massive bedding- VC planar laminae- R	(d)	moderate	Co	LVFG Z	—
lenticular	A	l	massive bedding- VC trochoidal ripples- VC	—	minor	S	LVFG-A Z-Mi	occur as isolated graded beds
loaded	Mi	M	laminae disrupted by loading trochoidal ripples- VC	—	none	Co Z-VA	LVFG	occur mainly in subfacies Bg

Notes. Even graded beds tend to occur singly, commonly separating shallowly scoured graded bed cosets. Shallowly scoured graded beds are much more common than even graded beds.

Table III.15. Facies B continued. See Table III.3 for abbreviations. See Table III.1 for bedform descriptions.
1 = type graded bed. 2 = abundance. 3 = type of grading. 4 = types of bed forms and laminae. 5 = laminae sequences from Table III.2.
6 = amount of scour on basal scour; 7 = occurrence, single graded beds or cosets. 8 = typical grain size. 9 = notes.

Anomalous graded beds. *Coarser layers are composed mainly of lower very fine-grained sand. Graded beds range from about 10 to 30 cm thick. Anomalous graded beds are rare in facies B, except in subfacies Bg where anomalous graded beds are very common and may comprise over 50% of the facies. The characteristics given below are for subfacies Bg.*

1	2	3	4	5	6	7	8	9
tabular	A	M	massive bedding- VC planar laminae- C quasi-planar laminae-C long low angle laminae- C	(d)	truncation surfaces- C gutters- R	S	LVFG	C in subfacies Bg, with gutters
wedge	A	M	massive bedding- VC long low angel laminae- C	(d)	truncation surfaces- C gutters- R	S	LVFG	VC in subfacies Bg, with gutters
long lens	Mi	M	massive bedding- VC long low angel laminae- C	(d)	truncation surfaces	S	LVFG	C in subfacies Bg with gutters
deeply scoured	VA	M	massive bedding- VC planar laminae- VC	(d)	gutters	S	LVFG	VC in subfacies Bg with gutters

Beds. Facies B, by definition, contains no sandstone or mudstone beds. At some locations facies B is interstratified with sandstone beds of subfacies Ab. In this case the nomenclature is the problem. By my definition facies B is composed of 50-50 sandstone-mudstone; hence, the sandstone beds must be in facies A. Tabular mudstone beds 30 to 100 cm thick, resting on a scoured surface, are also rarely interstratified with facies B rocks at some locations. Again by definition, these tabular mudstone beds are placed in facies D.

Table III.16. Characteristics of facies C, the thinly graded bedded and microlaminated mudstone facies. See Table III.3 for abbreviations. See Table III.1 for bedform descriptions;
1 = type graded bed. 2 = abundance. 3 = type of grading. 4 = types of bed forms and laminae. 5 = Lamina sequences from Table III.2.
6 = amount of scour on basal scour. 7 = occurrence, single graded beds or cosets. 8 = typical grain size. 9 = notes;

Background graded beds. *Coarser-grained layers are mainly composed of silt and minor very fine-grained sand. Background graded beds range from less than 0.1 mm thick to about 2 cm thick.*

1	2	3	4	5	6	7	8	9
even	VA	M	massive bedding- VC	—	minor	S	LVFG-A Z-VA	commonly as cosets
shallowly scoured	A	M	massive bedding- VC	—	moderate	Co	LVFG-A Z-VA	as single graded beds
lenticular	Mi	I	massive bedding- VC trochoidal ripples- C	—	minor	S	LVFG-A Z-Mi	occur as isolated graded beds
micro-laminae	VA	I	massive bedding- VC small scale, angular cross-laminae- R small scale, tangential cross-laminae- R	—	minor	Co	LVFG-A Z-VA	occur in 5 to 10 cm thick cosets

Beds. The following beds are common in the eastern Helena and Siyeh formations. Their presence makes up subfacies Cc.
• Massive, calcitic microsparic mudstone beds, 50 to 150 cm thick, are rare.
• Cryptalgalaminite beds 1 to 3 m thick are commonly interbedded with microlaminated graded bed sequences.
• Oolite beds 30 cm to 150 cm thick, composed of cosets of wavy beds 5 to 15 cm thick are common.
• Domed stromatolite beds are common.
• Molar-tooth intraclast conglomerate beds and lenses, 5 - 30 cm thick, resting on an erosion surface are very common.
• Intraclast grainstone beds, 15 - 30 cm thick, are common.

*Table III.16. **Facies C** continued. See Table III.3 for abbreviations. See Table III.1 for bedform descriptions. 1 = type graded bed. 2 = abundance. 3 = type of grading. 4 = types of bed forms and laminae. 5 = Laminae sequences from Table III.2. 6 = amount of scour on basal scour; 7 = occurrence, single graded beds or cosets. 8 = typical grain size. 9 = notes.*

Anomalous graded beds. *Coarser-grained layers are mainly composed of lower very fine-grained sand; gutters rarely contain matrix supported intraclast conglomerate. Anomalous graded beds commonly range from about 5 to 15 cm thick.*

1	2	3	4	5	6	7	8	9
wedge	Mi	M	trochoidal ripples-Mi rounded trochoidal ripples-Mi small, slightly asymmetric ripples- A small hummocky ripples- VA medium hummocky ripples- Mi long low angle laminae - A	(a)	truncation surface	S	LVFG	—
long lens	A	I	trochoidal ripples- VC rounded trochoidal ripples- C long low angle laminae- R massive bedding- C	—	gutters-C, truncation surface	S	LVFG	laminae on massive bedding
short lens	A	I	trochoidal ripples- R rounded trochoidal ripples-R massive bedding-VC	—	gutters- C, truncation surface	S	LVFG	laminae on massive bedding

Notes: Wedge, long lens and short lens graded beds commonly contain massive bedding overlain by bedforms or laminae without bedforms. This is the opposite of Table III.2-d sequence.

Table III.17. Characteristics of facies D, the thickly graded bedded mudstone facies. See Table III.3 for abbreviations. See Table III.1 for bedform descriptions. 1 = type graded bed. 2 = abundance. 3 = type of grading. 4 = types of bed forms and laminae. 5 = Lamina sequences from Table III.2. 6 = amount of scour on basal scour. 7 = occurrence, single graded beds or cosets. 8 = typical grain size. 9 = notes.

Background graded beds. *Coarser-grained layers contain abundant silt and minor lower very fine-grained sand. Background graded beds range mainly from 5 to 20 cm thick, although at some locations the facies contains graded beds 0.1 to 1 cm thick.*

1	2	3	4	5	6	7	8	9
loaded	A	M	trochoidal ripples- A	—	none	Co-C S-C	Z-VA LVFG-Mi	laminae commonly distorted by loading
even	Mi	M	massive bedding- VC	—	minor	Co	Z-VA LVFG-Mi	—
shallowly scoured	Mi	M	massive bedding- VC planar laminae- R	—	moderate	S	Z-VA LVFG-Mi	—
lenticular	VA	M	trochoidal ripples- VC small slightly asymmetric ripples (with discordant laminae)- C	—	minor	Co	Z-VA LVFG-Mi	occur in cosets
microlamina	Mi	l	massive bedding	—	minor	Co	Z	occur in 0.5-2 cm thick cosets

Table III.17. Facies D continued. See Table III.3 for abbreviations. See Table III.1 for bedform descriptions.
1 = type graded bed. 2 = abundance. 3 = type of grading. 4 = types of bedforms and laminae. 5 = Lamina sequences from Table III.2.
6 = amount of scour on basal scour. 7 = occurrence, single graded beds or cosets. 8 = typical grain size. 9 = notes.

Anomalous graded beds. Coarser grained layers are composed of lower very fine-grained sand, matrix supported intraclast conglomerate is rare. Anomalous graded beds range from about 5 to 30 cm thick, but 5 to 10 cm thick graded beds are most common.

1	2	3	4	5	6	7	8	9
tabular	Mi	M	trochoidal ripples- C rounded trochoidal- C small hummocky ripples- R medium hummocky ripples- R large hummocky ripples-C long low angle laminae - Mi quasi-planar laminae- A	(b) (a)	none; truncation surface- R; gutters- R	S	LVFG UVFG	basal contacts are loaded in places
wedge	Mi	M	trochoidal ripples-Mi rounded trochoidal ripples-Mi small slightly asymmetric ripples- A small hummocky ripples- VA medium hummocky ripples- Mi long low angle laminae - A	(c)	minor truncation surface	S	LVFG	—
long lens	Mi	M	trochoidal ripples- C rounded trochoidal ripples-C small hummocky ripples-C massive bedding	—	minor truncation	S	LVFG Z	regularly spaced about 20-30 cm apart at some locations

Beds. Massive dolomitic microsparic mudstone beds, 20 to 50 cm thick, resting on a guttered surface, occur in the Wallace Formation at some locations.

SEDIMENT TRANSPORT, DEPOSITION, COMPACTION AND EROSION MODELS

The goal of this dissertation is to find out as much as possible about the currents that transported and deposited sediment in the Helena and Wallace formations. In this chapter I review the models for the erosion, transport, deposition and compaction of wash load material. Wash load material consists of debris less than 100 μm in diameter. The models are based on existing models, and models modified by observations reported in the literature.

MODEL FOR SUSPENSION TRANSPORT AND DEPOSITION.

Gilbert (1914) found that currents transport sediment in two ways: as bedload and as suspended load. The bedload encompasses grains in traction transport, ie., the rolling, sliding and saltating particles (Gilbert, 1914). Bedload transport is the result of momentum transfer through particle-particle interactions and horizontal fluid-particle momentum transfers (Bagnold, 1973). Suspension load encompasses the particles supported above the bed by fluid turbulence (Gilbert, 1914) and results from vertical momentum transfer from the fluid to the particles (Bagnold, 1973). There is yet a third type of sediment transport, namely the wash load (Einstein, 1950) which is the fine-grained part of suspension load.

Nordin and Perez-Hernandez (1988) defined the wash load as those particles that immediately go into suspension when the current's velocity exceeds the critical shear velocity for the initiation of motion of the particle. Nordin and Perez-Hernandez (1988, p. A49) calculated that wash load in water encompasses quartz density grains 100 μm diameter and smaller. Using this definition, I estimate that over 95 percent of the sediment in the Helena and Wallace formations was transported as wash load. By this definition, particles smaller than 100 μm do not travel as bed load; they are either stationary on the bed or in suspension.

64

Gilbert (1914) observed that particles on the bed did not start to move until the current reached a critical threshold velocity. Gilbert also observed that at velocities greater than the critical velocity, the amount of sediment transported increased as the third power of the current velocity. These observations led Gilbert to define the current's competency as the set of conditions at which sediment begins to move, and a current's capacity as the maximum theoretical amount of sediment a given current can transport.

It follows from Gilbert's observations that there are two modes of deposition (Hjulstrom, 1935). Competency deposition encompasses sediment deposited because the current lacks the ability to move individual particles along the bed. Capacity deposition encompasses sediment deposited because the current lacks the ability to continue to move the mass of all the particles in transport.

The difference between the suspended sediment load and the current capacity defines a current's suspended sediment saturation. Currents with loads less than their capacity are undersaturated, that is, they have the capacity to transport more sediment than they actually are. Currents with loads that equal their capacity are saturated, and currents with loads greater than their capacity are over saturated during a transport event. Presumably, currents evolve from under-saturated to moderately under-saturated to saturated as they eroded sediment from the bottom. The currents become super-saturated when the flow's velocity begins to decrease. Super-saturated flows contain more sediment in suspension than the current can support, and must deposit sediment.

Many modern evaluations of wash load deposition, based on Hjulstrom (1935), only consider the role the current's competency plays in deposition (McCave and Swift, 1976; Stow and Bowen, 1980; Hesse and Chough, 1980; Krone, 1986). The reason capacity deposition is neglected is that Hjulstrom (1935) believed that the amount of sediment suspension was only limited by how close the particles could be packed. Hence, he believed that the capacity of the suspension load and saltating part of the bedload is effectively unlimited.

Komar (1985) showed that the model for competency deposition gave current velocities about an order of magnitude lower than the minimum current velocities required to produce the current structures preserved in a Neogene turbidite. Thus. Komar (1985) concluded the competency model for suspended load deposition could not account for the primary current laminae and bedforms found in turbidite deposits. Building upon Komar's work. Hiscott (1994) contradicted Hjulstrom (1935) and showed that declining current capacity can explain the presence of current laminae and bedforms because, if the load is high. capacity deposition can occur at very high current velocities.

Hiscott (1994) linked capacity deposition in Komar's turbidite to declining current capacity using the diffusion model for suspension transport (Rouse, 1937). Hiscott (1994) showed that declining current velocity results in declining bed shear stress which causes a reduction in the total volume or mass of suspended sediment the current is able to transport.

Bagnold (1966) presented a physical model for suspension load deposition that is easier to understand than the Hiscott model. Bagnold linked the capacity of a current to an upward force generated by the turbulence in the current, and showed that gravity acting on that mass of sediment creates a downward force. Bagnold reasoned that capacity deposition must occur when the downward force is greater than the upward force of the turbulence. Unfortunately there is no accepted way to calculate the upward force of the turbulence in Bagnold's model, and thus the model is not broadly accepted.

Thus, wash load deposition results from either insufficient current competency or insufficient current capacity. Competency deposition of very fine-grained sand in the wash load occurs in currents with velocities less than 14 cm/s (Anderson and Smith, 1989), and competency deposition of clay flocs takes place at current velocities below 4 cm/s (Little-Gadow and Reineck, 1974). Deposition occurs at low velocities because the current lacks the competency to keep the particles in suspension, and once on the bed the current lacks the competency to move the particles along the bed.

But, wash load can also be deposited at velocities far above that needed to keep the particles in suspension or move them along the bed. At velocities above that needed to suspend individual particles, the total mass of particles in suspension must be supported by an upward generated force to balance the force of gravity (Bagnold, 1966). In decelerating currents, the upward force must decrease, leading to wash load deposition at far higher velocities than those predicted by the by Komar's (1985) or McCave and Swift's (1976) competency models. Hiscott (1994) showed that current deceleration caused capacity deposition from a Neogene turbidity current. He also calculated that the depositional velocities were high enough to produce the types and the sequence of current structures found in the turbidite.

SUMMATION. From the above arguments, two processes control deposition of wash load material. Dilute, low velocity currents deposit wash load material when they no longer have either the competency to maintain individual particles in suspension, or the competency to move the particles along the bed. The mass of suspended sediment is low because low velocity currents generate a weak upward force.

But wash load material can also be deposited from decelerating high velocity currents, where gravity acting on mass of suspended sediment exceeds the upward force generated by the turbulence. Thus, the often stated paradigm of wash load deposition occurring in low energy environments is not always true.

FLOW BEHAVIOR DURING CAPACITY DEPOSITION

Different types of particles in the suspension impart different behavior to the current transporting them. Quartz sand particles have little or no cohesion, and suspensions containing only quartz sand behave as Newtonian fluids even at concentrations up to 1300 g/L (Howard, 1965; Rodine, 1974). Suspensions composed of quartz silt sized particles acquire a yield strength at concentrations of about 900 g/L (Lane, 1940; Qian et al., 1980). Sand and clay mixtures containing 10 to 20 percent clay may develope a yield strength at concentrations as low as 265 g/L (Hampton, 1975). Suspensions composed only of flocculated

clay particles may begin to develope a yield strength at concentrations as low as 10 g/L (Einstein and Krone, 1962). Thus, the type of material, and their abundances control the suspensions behavior.

Flows that exhibit a yield strength behave as non-Newtonian fluids, and the processes operating in these flows are complex and poorly understood (Pierson and Scott, 1985). Newtonian flows can evolve into non-Newtonian flows by depositing sediment, and non-Newtonian flows can evolve into Newtonian flows by dilution of the suspension. Pierson and Scott (1985) suggest that sand and larger particles form one phase in the fluid and that water, silt and clay form another phase in the fluid. They also suggest that the principal control on the flow's behavior the water plus silt plus clay phase.

THE EFFECTS OF SAND. Downward moving turbulent packages in a turbulent current place suspended sediment on the bottom. If deposition is driven by insufficient capacity, then some of this sediment becomes incorporated into the bed. As long as sand dominates the sand to silt plus clay ratio in the near bed layer, then the near bed layer should act as a Newtonian fluid and particle sorting can occur on the bed. Particle sorting in the near bed layer permits the formation of primary current laminae (Arnott and Hand, 1989; Allen, 1991).

THE EFFECTS OF SILT PLUS CLAY. However, since sand is deposited first, the sand to silt plus clay ratio of the initial suspension decreases, and at concentrations above about 500 g/L the flow may evolve a mudflow (Pierson and Scott, 1985). At concentrations in the range of 5 to 50 g/L, suspensions of clay flocs may display the behavior of mobil and stationary suspensions observed by Kirby and Parker (1983), that is, the flow becomes very viscous and may behave as a Bingham plastic or psuedoplastic.

ORIGIN OF STATIONARY SUSPENSIONS

Kirby and Parker (1983) described mud deposition and the type of mud deposits that result from declining current capacity in the Severn Estuary, U. K. They observed a 2 m/s current with 5 g/L

suspended sediment concentration evolved through three stages as the current decelerated, resulting in the deposition of a 3 m thick fluid mud layer in a period of a few seconds. Although I can not demonstrate it, I believe that many of the claystones in the Helena and Wallace formations probably formed in the manner described by Kirby and Parker.

Kirby and Parker (1983) defined a mobile suspension as a moving, turbulence-supported assemblage of particles. Initially they observed a 2 m/s current with a concentration of 5 g/L, evenly distributed through the flow. As the current slowed, they observed that particles in the suspension moved downward, forming a stratified mobil suspension with abrupt jumps in suspended sediment concentration, overlain by clear water. Current velocities in the stratified mobil suspension were of the order of 0.7 to 1.0 m/s, and concentrations were on the order of 8-10 g/L. These velocities are far higher than the 0.04 m/s velocity needed to keep flocs in suspension (Little-Gadow and Reineck, 1974). Thus, the formation of the observed stratified mobil suspension must have been due to a lack of current capacity.

Kirby and Parker observed that, as the current slowed further, the entire mass of suspended sediment stopped moving, forming a stationary suspension 2-3 m thick, with a maximum concentration of about 9 g/L. A stationary suspension is a suspension that is not moving, but in which the particles are mainly supported by pore-fluid pressures and a few particle-particle contacts.

The closeness of particles in the stationary suspension hinders the escape of pore-water and creates pore-water pressures that are greater than the hydrostatic pressure (Sills and Elder, 1986). Thus, none of the particle support in a stationary suspension is due to vertical momentum transfer between the turbulence and the particles. Stationary suspensions border on being non-Newtonian fluids, but Kirby and Parker consider them true suspensions because they behave like Newtonian fluids, which have viscosity but no shear strength. Stationary suspensions evolve into mud deposits that behave like Bingham plastics or

pseudoplastics (Sills and Elder, 1986; Bryant et al., 1980; Krone, 1986) that exhibit shear strength, and finally evolve into a mud bed that behaves brittlely.

The following model for the formation of a stationary suspension is based on a combination of the floc behavior model of Partheniades (1986) and Krone (1986) and the observed behavior of a muddy decelerating current (Kirby and Parker,1983). Initially, the flocs are well mixed throughout high velocity flows (Kirby and Parker, 1983). As currents lose capacity, suspended sediment moves downward, forming a high concentration stratified suspension, overlain by clear water with very low suspended sediment concentration (Kirby and Parker, 1983).

As a result of stratification, individual flocs are forced closer together, increasing the number of floc-to-floc impacts, and increasing the viscosity of the stratified portion of the current. At cohesive particle concentrations over about 10 g/L, the increased viscosity of the current may cause it to behave as Bingham fluid (Krone, 1986, p. 67), or a psuedoplastic (Bryant et al., 1980, p. 283). At concentrations below about 10 g/L the mixture acts as a Newtonian fluid (Einstein and Krone, 1962; Bryant et al., 1980; Krone, 1986).

Some particle impacts result in the flocs sticking together, forming floc aggregates (Partheniades, 1986). Floc aggregates are weaker (less cohesive) than the individual flocs. As the concentration in the stratified suspension increases, floc aggregates become attached to other floc aggregates forming aggregate networks, which in turn are weaker then the floc aggregates.

Thus, a current may start as a well mixed current with a density of about 1030 kg/m³, assuming a sea water with a density of 1025 kg/m³, composed of isolated individual flocs with a density of about 1150 kg/m³ (Bryant and Williams, 1983). Increased viscosity in the high concentration layer may reduce turbulent shearing, forming floc aggregates (Partheniades, 1986). When the current reaches a density of

about 1080 kg/m³, (Kirby and Parker, 1983), and it becomes a stationary suspension. This model is supported by the experiments of Krone (1986).

The stationary suspensions of Kirby and Parker have also been called fluid mud, sling mud, fluff mud and creme de vase (Wells, 1983). Fluid mud deposits not only occur in estuaries, but also front many muddy coastlines of the world (Wells, 1983). Presumably Kirby and Parker's observations apply to all such deposits, and Hiscott's (1994) and Bagnold's (1966) capacity deposition models explain their origins.

MUD COMPACTION MODEL

Mud compaction and a given mud's strength are a complex function of the silt/clay ratio, the amount of clay verses the amount of clay sized quartz and feldspar, the salinity of the water, the content and type of organic material and the deposit's recent history and overburden (McCave, 1984). However, the model presented below, based on settling tube experiments of Elder and Sills (1984), Sills and Elder(1986) and the observations of fluid mud deposits in the Severn Estuary (Kirby and Parker, 1983), should apply to all mud deposits.

Elder and Sills conducted experiments in which mud slurries were rapidly pumped into the settling tubes. This procedure more-or-less duplicates the formation of a stationary suspension formed by capacity deposition. They also examined the behavior of mud, slowly pumped into the tubes, that had to settle through 3 m of water. This experimental procedure mimics the conditions of particle-by-particle deposition of the competency model. Their data show that the different modes of deposition produce mud deposits with different settling characteristics.

CAPACITY DEPOSITED MUDS. Stationary suspensions consist of three components that grade vertically into one another. When deposited, the stationary suspension has zero shear strength (Kirby and Parker, 1983; Sills and Elder, 1986). I call this layer with no shear strength the alpha mud layer. Water

is expelled from the lower parts of the mud slurry as soon as the stationary suspension is formed, and the lowest portions obtain some strength (Sills and Elder, 1986). I call the layer with some strength the beta mud layer. Given more water expulsion, the alpha-beta interface moves upward, and the lowest part of the beta layer evolves to a true mud deposit exhibiting true strength (Wells and Coleman, 1981). I call this layer the gamma layer.

Stationary suspensions must dewater through their upper surface, as a result of the downward movement of the flocs acting under the influence of gravity. This keeps the pore-water pressures between the floc aggregates and the aggregate networks in the upper part of the deposit above hydrostatic pressure (Elder and Sills, 1984). At the same time, the particles lower in the suspension become more-and-more supported within a framework of touching particles. The increasing number of particle-particle contacts results in increasing strength in the mud deposit (Krone, 1962; 1986; Partheniades, 1986).

The particles in the alpha mud layer, comprising the uppermost part of the stationary suspension, are mainly supported by the excess pore-water pressure. The alpha mud layer has no strength and acts as a Newtonian fluid, hence it can be easily eroded by the next current. Indeed, with increasing current velocity, Kirby and Parker (1983) observed entire stationary suspensions lift off the bottom, becoming mobil suspensions. Bryant and Williams (1983, p. 100) found that flocs filled 100 percent of the volume at a density of about 1150 kg/m^3. Presumably, alpha layer evolves into the beta layer at this density. The alpha layer exists as long as floc aggregate and aggregate networks exist, and the uppermost part of the stationary suspension may never evolve to the beta mud layer.

Experiments by Elder and Sills (1984) suggest the framework of particles becomes extensive enough that stationary suspension obtains some strength at about a density of 1130 kg/m^3. Note, this is in close agreement to the theoretical point at which the flocs fill the entire volume (Bryant and Williams, 1983). Compaction within the beta layer occurs by crushing the flocs, leading to the formation of the

gamma layer. The beta layer is entirely framework supported, and it continues to gain strength as more

pore-water is expelled and more of the primary particles gain contact with other primary particles.

However, the pore-water pressures remain above hydrostatic, and the deposit behaves like a Bingham

plastic or psuedoplastic (Elder and Sills, 1984). The beta mud layer probably exists in a density ranges

between about 1150 kg/m^3, the density of individual flocs, to about 1250 kg/m^3 (Wells and Coleman, 1981).

The alpha and beta layers are approximately equivalent to sling mud or fluid mud which range in

density from 1030 to 1250 kg/m^3 (Wells and Coleman, 1981). Fluid muds with these densities display

viscosities between 0.02 to 210 poises (Wells and Coleman, 1981).

Data in Wells and Coleman (1981) suggests the gamma layer forms in muds with densities above

about 1250 kg/m^3. The gamma mud layer is probably mainly composed of domains of completely crushed

and partially crushed flocs (Krone, 1962; 1986; Partheniades, 1986). Pore-water pressures within the

gamma layer approximately equal the hydrostatic pressure (Elder and Sills, 1984) and the deposit begins to

act as a very weak brittle substance. The gamma layer is equivalent of Kirby and Parker's (1983)

settled mud.

COMPETENCY DEPOSITED MUDS. Slowly deposited mud, in the settling tubes, dewatered

at a rate an order of magnitude slower than rapidly deposited mud (Elder and Sills, 1984). The slowly

deposited muds simulate competency deposition. Apparently the flocs form a relatively rigid network, so

that the overlying sediment can not drive rapid compaction. Data in Elder and Sills (1984) suggest that

competency deposits retain higher water contents for longer periods of time than the basal portions of

capacity deposits. Furthermore, pore-water pressures are approximately equal to the hydrostatic pressure,

reflecting the ridged floc structure. Since they have a ridged frame work, competency deposited muds may

behave as a Bingham plastic. But, their high water content suggests that they should behave as a

Newtonian fluid. Thus, the model for capacity deposited muds can not predict the behavior and strengths of competency deposited muds.

MUD EROSION MODEL

The critical shear stress of erosion of a mud is controlled by the type and content of organic material, stress history, grain size, fabric, age and overburden thickness (Mc Cave, 1984). In spite of many complicating factors, the data show that the degree of compaction, as expressed by the mud's density, is the primary control on the deposit's shear strength, and there is general agreement that the strength of a mud is approximately proportional to the mud's density raised to the 5/2 power (Krone, 1962).

For the following model, I assume that the critical shear stress is related to density of the mud (Krone, 1962; Partheniades, 1986; Krone, 1986; McCave, 1984). The model is based on the observations of Kirby and Parker (1983), flume experiments of Hawley (1981 a; 1981 b) and the settling tube experiments of Elder and Sills (1984) and Sills and Elder (1986).

Observed mud erosion appears to take place in three steps, that approximate the stages of consolidation out lined above. At a current velocity of about 70 cm/s in the Severn Estuary, the stationary suspension part of the deposit starts to move (Kirby and Parker, 1983, Fig. 9). At about 1.2 m/s the stationary suspension lifts off the bottom and starts to mix with the clear water (Kirby and Parker, 1983, p. 92). Hawley (1981 b) observed that the uppermost two-thirds of a mud deposit several centimeters thick was re-suspended at velocities less than 0.16 m/s. At this stage, Hawley probably observed the re-mobilization of the alpha mud layer.

In the Severn Estuary, the removal of the alpha mud layer exposes the top of the beta mud to a shear stress of about 0.5 Pa (Kirby and Parker, 1983, Fig. 9). Sonar reflections across stationary suspensions show that the surface of the beta layer is flat and horizontal (Kirby and Parker, 1983). After exposure of this flat surface, erosion appears to change from mass re-suspension to erosion of chunks of

mud (Hawley, 1981 b). Local regions of less consolidated mud appear to erode easer than regions of more consolidated mud, producing an wavy surface. Since the beta and gamma layers increase in density with depth, I presume that an increasing current velocity is required for deeper erosion.

If the current velocity is high enough, about 1.5 m/s, then the beta mud layer may be completely removed, exposing the gamma mud layer. Hawley (1981 b) reported that the most resistant mud layer was uniform in thickness, and draped over the ripple forms that the mud was deposited upon. The thinness of the mud layers in Hawley's experiments may have permitted the rapid formation of the gamma mud layer. Data in the Elder and Sills experiments suggests the 2 to 3 m thick stationary suspensions in the Severn Estuary probably did not have time to form gamma mud layers.

As with the other layers, the gamma mud layer increases in strength downward. Hawley (1981 b) observed that erosion of the gamma layer was most pronounced on the stoss side of ripple crests, where mud was slowly worn away. This suggests that the gamma layer erodes in a particle-by-particle manner. The base of the gamma mud layer may reach a density of 1,700 kg/m^3 (Wells and Coleman, 1981), and exhibit a shear strength of between 10 and 15 Pa (McCave, 1984, Fig. 7).

SUMMATION. The alpha mud layer ranges in density from about 1030 to 1125 kg/m^3, has no shear strength and is re-suspended in mass by currents between 0.5 and 1.0 m/s. The beta layer ranges in density from 1125 to 1250 kg/m^3, has moderate shear strength, and erosion occurs in chunks at velocities between 1 m/s and 2.5 m/s. The contact between the alpha and beta mud layers is planar and horizontal. The gamma layer has a density greater than 1250 kg/m^3, is very strong, and erodes particle-by-particle at velocities above 2.5 m/s. The gamma mud layer displays equal thickness and conforms to the shape of the bottom of the bed.

HYDRAULIC INTERPRETATION OF BEDFORMS AND LAMINAE

INTRODUCTION

Hydraulic interpretation is the process of extracting from the primary current laminae and bedforms information about the currents that deposited the sediment. Hydraulic interpretation can be conducted at different scales. At the finest scale, one can interpret the bedforms and current laminae, covered in this chapter. At the next largest scale one can interpret the currents that deposited individual graded beds, presented in Chapter VI. At the scale of a meter or so, one can interpret the general conditions of the deposition of a facies, presented in Chapter VII.

Given good exposures and good preservation of the laminae and bedforms, one can determine:

- current type: unidirectional, oscillatory, or combined: Chapter V.E

- initial depositional velocity of the current: Chapter V.F, Table V.1

    ◊ unidirectional current velocities: Chapter V.F.1, Figure V.1

    ◊ oscillatory current velocities: Chapter V.F.2, Figure V.2

    ◊ combined current velocities: Chapter V.F.3, Figure V.2

- the average suspended sediment concentration at the onset of deposition: Chapter V.G

- the current's velocity when mud deposition began: Chapter V.H

- the current's deceleration rate: Chapter V.I

- the relative amount of sediment bypass: Chapter V.J

- permissible water depths and wave conditions for the oscillatory currents: Chapter V.K.

BASIS FOR INTERPRETING BEDFORMS AND LAMINAE

Harms et al. (1982) linked a deformable bed's configuration to the preserved sedimentary structures formed under unidirectional currents. A bed's configuration is its morphology during deposition.

76

"In making hydraulic interpretations from primary sedimentary structures, the underlying assumptions are that a given flow over a given sediment bed will produce a definite bed configuration, and therefore a definite stratification geometry, and that the same set of flow conditions somewhere else would produce stratification which, while different in detail, would show the same average properties and the same kinds of significant features" (Harms et al., 1982, p. 2-1). Two types of bed configurations exist: plane bed and rippled bed. Rippled beds exhibit bedforms with different shapes, sizes, spacing and symmetry, depending of the type current, water depth, current velocity and grain size. Ashley et al. (1990) presented the most broadly accepted bed phase diagram for unidirectional currents, reproduced herein as Figure V.1.

Harmes et al. (1982) and Allen (1985), also linked a different set of bed configurations to oscillatory currents. Arnott and Southard (1990) linked oscillatory and combined unidirectional and oscillatory currents to specific bed configurations, and presented the first bed phase diagram for oscillatory and combined currents. A modified version of Arnott and Southard's bed phase diagram is shown in Figure V.2. The development of Figure V.2 is given in Appendix I.

ORIGIN OF CURRENT LAMINAE

The origin of internal lamination and massive bedding is controlled by the particles' behavior once they arrive at or very near the bed. One type of particle behavior leads to the formation of laminae, while the other leads to the formation of primary massive bedding. Allen (1991, p. 293) described lamination in sandy sediments as "... interleaving of particles in thin layers which differ slightly among themselves in average grain size." That is, laminae are the result of very fine scale sorting of the particles (Kuenen, 1966).

PLANAR LAMINAE. Planar lamination is a result of sorting due to particle movement in the near bed layer(Kuenen, 1966, p. 530; Blatt et al., 1972, p. 116; Boggs 1987, p. 144), and as a result of deposition on a plane bed. Particles can be transported as bedload by sliding, rolling, or bouncing along
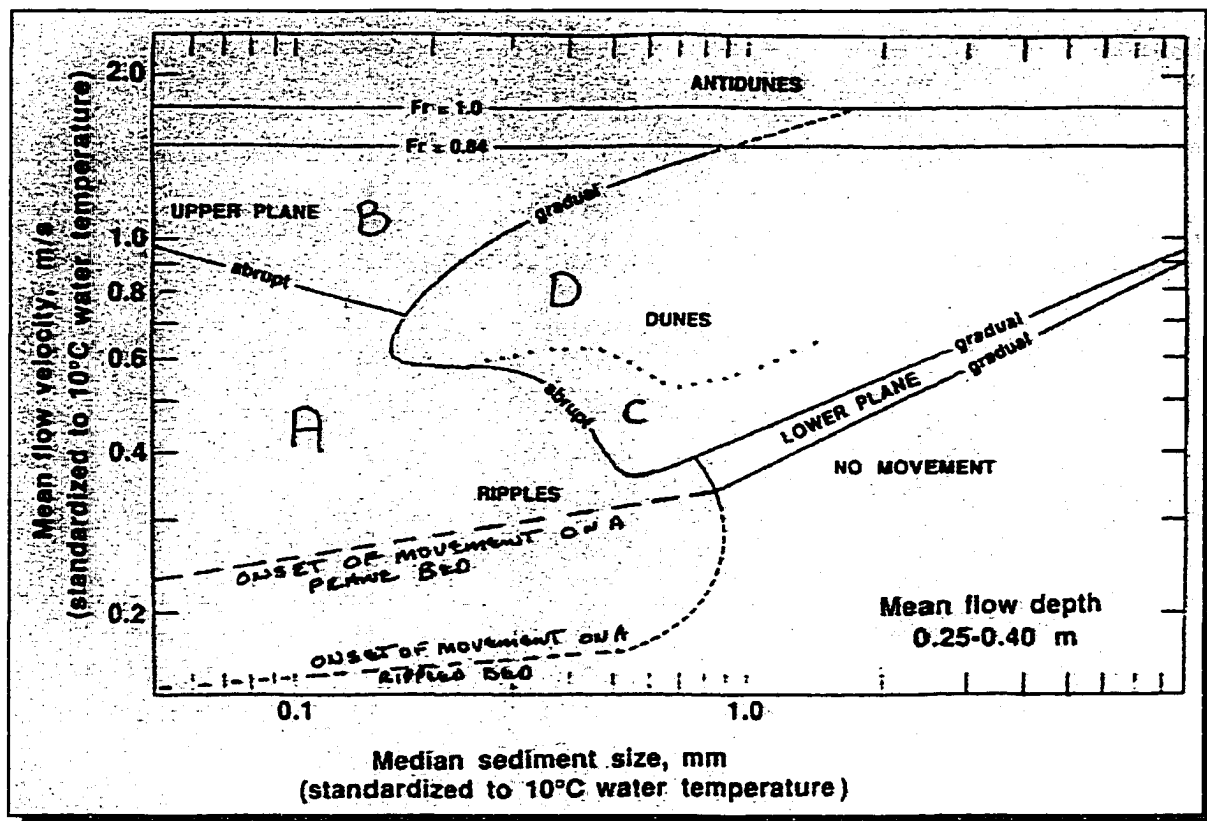
Figure V.1.

Bed phase diagram for unidirectional currents from Harms et al. (1992) and Ashley et al. (1990)

A. Small Scale Current Ripples. *< 60 cm spaced, highly asymetric, 3D ripples, or beds less than 5 cm thick with high angle, angular, or tangental cross-laminae, or trough cross-laminae. See Fig. III.3-y, and III.4-d, e.*

B. Upper Plane Bed. *Planar, horizontal laminae. See Fig. III.4-a.*

C. Large Striaght-crested Dunes. *Meters to tens-of-meters spaced, hihly asymetric, 2D dunes, or beds greater than 5 cm thick with high angle, angular cross-laminae.*

D. Large Sinuous-crested Dunes. *Meter to several meters spaced, highly asymetric, 3D dunes, or beds greater than 5 cm thick, with high angle, tangental cross-laminae.*

Figure V.2. Revised oscillatory and combined flow bed phase diagram. Based on Arnott and Southard (1990), Southard et al. (1990). Duke et al. (1991) and symmetrical bed forms observed in the Helena and Wallace formations. See the Appendix for the origin of this bed phase diagram.

LEGEND

(Figure Overleaf.)

SYMMETRICAL BEDFORMS

A. *TROCHOIDAL RIPPLES; < 21 cm spaced, symmetrical, 2D, peaked ripple forms. See Figure III.3-a.*

B. *ROUNDED TROCHOIDAL RIPPLES; < 21 cm spaced, symmetrical, rounded, transitional 2D-3D ripple forms. See Figure IIL.3-b.*

C. *SMALL HUMMOCKY RIPPLES; < 21 cm spaced, symmetric, 3D ripple forms. See Figure III.3-c.*

D. *MEDIUM HUMMOCKY RIPPLES; 30 to 70 cm spaced, 3 cm high (field), or 50 to 100 cm spaced, 5 cm high (wave tunnel), symmetrical, 3D ripple forms. See Figure III.3-d.*

E_f *LARGE HUMMOCKY RIPPLES; > 70 cm spaced, about 12 cm high (field) or 70 to 150 cm spaced, 20 cm high (wave tunnel), symmetrical, 3D ripple forms. See Figure III.3-e.*

E_x *LARGE HUMMOCKY RIPPLES; > 100 cm spaced, 7 to 10 cm high (field) or 100 to 300 cm spaced, 10 to 15 cm high (wave tunnel), symmetrical, 3D ripple forms. See Figure III.3-e.*

E_f *LARGE HUMMOCKY RIPPLES; > 100 cm spaced, < 5 cm high (field) or 150 to 300 cm spaced, < 5 cm high (wave tunnel), symmetrical, 3D ripple forms. See Figure III.3-e.*

ASYMMETRICAL BEDFORMS

F. *Less than 21 cm spaced, asymmetric, 2D ripple forms.*

G. *Less than 21 cm spaced, asymmetric, transitional 2D-3D ripple forms.*

H. *SMALL SCALE CURRENT RIPPLES; < 60 cm spaced, asymmetric, 3D ripple forms. See Figures III.3-g, and III.4-d, e.*

I. *LONG LOW ANGLE CROSS-LAMINATION; See Figure III.4-c.*

J. *Large scale, high angle cross-lamination in 90 μm sand; See Figure III.4-d. (Absent in Helena and Wallace formations.)*

PLANE BED CONFIGURATIONS

K. *QUASI-PLANAR LAMINATION; Myrow (1993) See Figure III.4-b.*

L. *PLANAR LAMINAE; See Figure III.4-a.*

Figure V.2. *Revised oscillatory and combined flow bed phase diagram. Based on Arnott and Southard (1990), Southard et al. (1990), Duke et al. (1991) and symmetrical bed forms observed in the Helena and Wallace formations. See the Appendix for the origin of this bed phase diagram.*
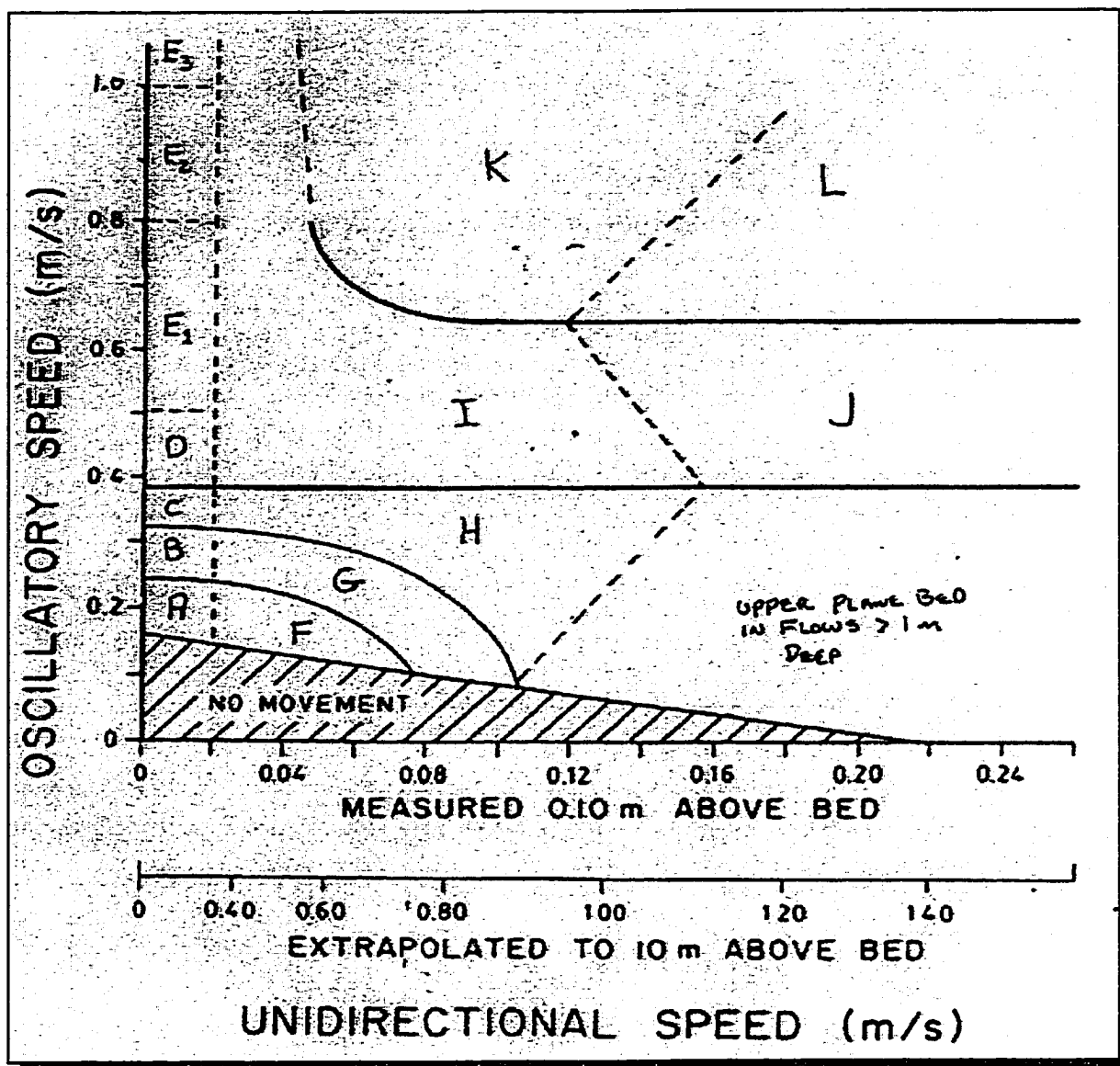
the bottom (Gilbert, 1914; Harms et al., 1982), or they can be transported by a combination of bed load and suspension processes in a near bed layer (Gilbert, 1914; Middleton and Southard, 1984). Unsupported grains, in the near bed layer of high velocity currents, settle to the bed due to a lack of flow capacity (Allen, 1991, p. 292). Allen (1991) links the sorting and formation of laminae to the multiple transfers of a grain between the population of moving grains in the near bed layer and the static bed.

Arnott and Hand (1989) suggest that sorting in planar lamination takes place in moving near bed sheets, several grain diameters thick and tens of cm long. They observed that coarser grains were located at the front of the sheet and the finer grains were located at the back of the sheet. Arnott and Hand (1989, p. 1065) hypothesized that planar lamination in Bouma B division originated by velocity fluctuations related to current surging or large-scale turbulence.

CROSS-LAMINAE. Cross-lamination also results from grain sorting. However, the sorting may be due to the above process of grain sorting in near bed layer (Allen, 1991), or to the agitation of the grains produced by avalanching down the lee side of a bedform (Harms et al., 1982).

ORIGINS OF MASSIVE BEDDING

There are three types of massive bedding: (1) The laminae are present but not observed; (2) Laminae were present but were destroyed by secondary processes such as slumping or bioturbation; and (3) Primary massive bedding, where no laminae ever existed. This section deals only with the type of primary massive bedding, where no lamination ever existed.

Two conditions exist under which primary massive bedding may form. Massive bedding may form under high velocity currents, at high sedimentation rates, where sedimentation occurs as a result of insufficient current capacity. Primary massive bedding can also form under low velocity currents, where sedimentation occurs as a result of insufficient current competency.

ORIGIN IN CAPACITY DEPOSITS. The literature contains two models to explain the origin of primary massive bedding under high velocity currents where deposition results from a lack of capacity. Both models are based observations in flume experiments.

Middleton (1967) suggested that rapid sedimentation from suspension causes the viscosity of the near bed layer to increase. He further suggested that the near bed layer stops behaving as a Newtonian fluid and begins to behave as a Bingham plastic and acquires some shear strength when the sediment concentrations become high enough. Middleton suggested that the near bed region freezes when the shear stress produced by the current falls below the shear strength of the near bed layer.

This process has been linked to the deposition of debris flows, mud flows and the massive bedding in turbidites (Harms et al., 1982, p. 3-6; Middleton 1967). However, this process probably does not apply to the deposits in the Helena and Wallace formations. Bryant et al. (1980), Howard (1965) and Rodine (1974) found that colloidal quartz suspensions and quartz sand suspensions behaved as Newtonian fluids at concentrations up to 1300 g/L. With increasing amounts of clay, the suspensions may acquire a yield strength. Clay-rich mixtures may exhibit yield strength at concentrations of the order of 265 g/L (Hampton, 1975). Thus, high clay concentrations appear to be required for bed freezing (Pierson and Scott, 1985; Scott, 1988).

The second model is based on experiments of Arnott and Hand (1989). Arnott and Hand found sorting was suppressed in the near bed layer when the bed aggradation rate was greater than about 4 cm per minute. They suggested that sorting was suppressed by the caging or boxing in of the particles by newly arriving particles. Allen (1991) suggested that at high aggregation rates, the particles do not have the opportunity for multiple transfers between the bed and the near bed layer, and hence do not undergo sorting and produce a massive bed. Lowe (1988) also linked the formation of massive bedding found in some turbidites to very high bed aggradation rates, and Collinson and Thompson (1989, p. 104) suggested that no

sorting can take place where the particles can not move along the bed.

ORIGIN IN COMPETENCY DEPOSITS. Deposits that are the result of the declining current competency also produce massive bedding. Harms et al. (1982, p. 3-5) suggest that deposition from suspension occurs at very low current velocities, by particle fallout without traction transport. Sand deposited from currents less than 13 cm/s (Anderson and Smith, 1989) stops moving as soon as it hits the bed because the current lacks the competency to move it along the bed. Because there is no near bed layer, particles deposited in this manor produce a massive bed because they can not shuffle between the bed and the near bed layer.

DETERMINING THE CURRENT TYPE

Before one can interpret a paleo-current conditions from a bed phase diagram, one must establish the type of current responsible for deposition of the primary structures. There are three types of currents: oscillatory, unidirectional, or combined oscillatory and unidirectional currents. A bedform's symmetry is a direct function of the type of current it formed under (Tanner, 1967; Harms, 1969), and stoss length to lee length ratio is independent of the orientation of a vertical exposure. The ratio of the stoss length to the lee length is called the ripple symmetry index, RSI (Tanner, 1967).

Tanner (1967), Harms (1969), de Raaf et al. (1977), Reineck and Singh (1980), and Harms et al. (1982) present well documented studies on the recognition of the current type, based on bedform symmetry. Internal lamination within bedforms do not always define the type of current because migrating symmetrical ripples contain unidirectional dipping cross-laminae (Newton, 1968).

The ripple heights on a vertical exposure indicate the dimensionality of the bedforms. Bedforms exposed on a vertical plane through a bed of 2D ripples rise to the same height. But, bedforms on a vertical plane through a bed of 3D ripples rise to different heights. Also, de Raaf et al. (1977) presented a suite of recognition criteria for structures deposited from oscillatory currents on vertical exposures.

OSCILLATORY CURRENT BEDFORMS. A large number of field and laboratory

observations confirm that symmetric oscillatory currents produce symmetric bedforms (Inman, 1957;

Komar et al., 1971; Carstens et al., 1969; Arnott and Southard, 1990). However, photos in Southard et al.

(1990) suggest that some small 3D ripples, may form under purely oscillatory current, particularly when

they occur on the flanks of larger symmetric bedforms. Also, the bed may display slightly asymmetric

bedforms, oriented in opposite directions, and separated by several symmetric bedforms. Thus, a ripple

horizon containing opposed asymmetric bedforms also record purely oscillatory currents. The occurrence

of rare sandstone beds in the Helena and Wallace formations with opposed asymmetric ripples shows that

they are not an artifact of the wave tunnel experiments as Arnott and Southard (1990) suggested.

Reineck and Singh (1980, fig. 35, fig. 36) suggested that ripples with a ripple index, length

divided by height, less than 4 indicates the ripples were formed under purely oscillatory currents. However,

the ripple index can be affected by differential compaction and should be used with caution. Tanner (1967)

suggests that a ripple symmetry index, the length of the long side divided by the length of the short side,

less than 2.5 indicates the ripples formed under symmetrical oscillatory currents.

Low velocity oscillatory currents produce symmetrical ripples with straight and continuous crests

that divide in a simple Y-shaped junction on bedding planes (Harms, 1969). Wave tank experiments show

that oscillatory current bedforms change progressively with increasing orbital velocities. Carstens et al.

(1969) observed a progression from: (a) straight and sharp crested ripples, to (b) straight but rounded

crested ripples, to (c) sinuous crested ripples, to (d) discontinuous crested ripples, to (e) symmetrical,

dome-shaped ripple forms.

Thus, wave tank experiments show that the various types symmetrical ripple forms shown on

Figure III.2 and listed on Table III.1, record different orbital velocities. Symmetrical, sharp crested forms,

that rise to the height along a vertical exposure, record low velocity oscillatory currents. Symmetrical,

rounded crested forms, that rise to the height along a vertical exposure, record moderate velocity oscillatory

currents. Symmetrical forms that display varying heights along a vertical exposure record high velocity

oscillatory currents.

UNIDIRECTIONAL CURRENT BEDFORMS. Reineck and Singh (1980, fig. 35, fig. 36)

suggest that a ripple index greater than 15 indicates purely unidirectional current ripples. Tanner (1967)

suggests a ripple symmetry index grater than 3 records the ripples formed under purely unidirectional

currents.

In plan view, Harms (1969) found that low velocity unidirectional currents produce sinuous but

continuous crested ripple forms, but high velocity unidirectional currents produce short, discontinuous

ripple crests. Allen (1968) divided asymmetric discontinuous crested ripples into linguoid, cuspate and

lunate forms.

COMBINED CURRENT BEDFORMS. Unidirectional current ripples and oscillatory current

ripples represent end members of a continuum of ripple shapes that range from highly asymmetrical to

symmetrical (Harms, 1969; Harms et al., 1982). Ripple indices between the end member ripples record

deposition from combined oscillatory and unidirectional currents (Harms, 1969). "Intermediate-flow

[combined oscillatory and unidirectional currents] ripples are intermediate in both geometry and behavior

between the end-member cases. Only slight asymmetry of flow is needed to make the ripple profiles

moderately asymmetrical. . . All of the aspects of ripple geometry—height, spacing, indexes, and plan

pattern—seem to vary smoothly with degree of flow asymmetry as well" (Harms et al. 1982, p. 2-45).

Tanner (1971), Komar et al. (1972) and Tietze (1978, 1979) also document increasing ripple asymmetry

with increasing unidirectional current velocity relative to the maximum near-bed orbital velocity.

Ripple asymmetry is induced by asymmetric waves. Stokes and cnoidal waves induce asymmetric

oscillatory currents (Clifton et al., 1971; Reineck and Singh, 1980, p. 31), and this induces net sediment transport in one direction, producing asymmetric ripples. Differentiation between asymmetrical ripples formed under asymmetric oscillatory currents and those formed under combined oscillatory and unidirectional currents may not be possible (Reineck and Singh, 1980, p. 34; Clifton and Dingler, 1984).

DETERMINING THE CURRENT'S VELOCITY

The bed's configuration is a function of the current type, grain size, water depth and current velocity (Harms et al., 1982). The type current can be determined from the symmetry of the bedforms, and grain size can be measured. The water depth has little effect, slightly moving the regions of the bed phase diagram to higher current velocities in deeper water (Boguchwal and Southard, 1990). Thus, it is possible to estimate the current's velocity by inferring the bed's configuration from the preserved bedforms and current laminae, and relating that bed configuration to the bed phase diagrams, Figures V.1 or V.2.

The evaluation of a current's depositional velocity presumes the current velocities, as indicated by the bed phase diagrams, truly reflect the velocities of the currents at the time of deposition. Komar (1985) reviewed the reasons that bed phase diagrams can not be trusted to provide accurate current velocities during suspension deposition, and found that these reasons posses little merit. Knowing of no valid reasons to disregard the bed phase diagrams, I assume Figures V.1 and V.2 provide realistic estimates of the depositional velocities. Table V.1 lists the current velocities inferred from the different types of bedforms described in Chapter III.B, and the different types of laminae without bedforms, described in Chapter III.C.

Some graded beds contain a vertically changing sequence of laminae and bedforms, the more common sequences are shown on Table III.2. Assuming the bedforms and laminae reflect the current's velocity, these vertical sequences record changing current velocities during deposition. In general the changes in laminae or bedforms record deposition from slowing currents.

Table V.1.   Type of currents and near bed current velocities as infered from the bed configurations.

OSCILLATORY CURRENT BED CONFIGURATIONS

bed configuration	example	current type/ velocity
Trochoidal ripples	Figure III.3-a	oscillatory 16-24 cm/
Rounded trochoidal ripples	Figure III.3-b	oscillatory 24-32 cm/s
Small hummocky ripples	Figure III.3-c	oscillatory 32-38 cm/s
Medium hummocky ripples	Figure III. 3-d	oscillatory 38-50 cm/s
High, large hummocky ripples	Figure III.3-e	oscillatory 50-80 cm/s
Medium high, large hummocky ripples	Figure III.3-e	oscillatory 80-100 cm/s
Low, large hummocky ripples	Figure III.3-e	oscillatory > 100 cm/s

COMBINED CURRENT BED CONFIGURATIONS

Planar	Figure III.4-a	oscillatory > 65 cm/s unidirectional > 12 cm/s
Quasi-planar	Figure III.4-b	oscillatory > 65 cm/s unidirectional 1-12 cm/s
Long low angle forms	Figure III.4-c	oscillatory 38-65 cm/s unidirectional 1-12 cm/s
Slightly asymmetric ripples	Figure III.3-f	oscillatory 16-24 cm/s unidirectional 1-8 cm/s
Asymmetric ripples	Figure III.3-g	oscillatory 32-38 cm/s unidirectional > 1 cm/s

UNIDIRECTIONAL CURRENT BED CONFIGURATIONS

Planar	Figure III.4-a	unidirectional > 80 cm/s
Small scale current ripples	Figure III.4-g Figure III.4-d, e	unidirectional 17-80 cm/s
Dunes	Figure III.4-d, e	unidirectional 35-120 cm/s

The laminae or bedforms, at the base of an ungraded bed or graded bed, reflect the current's velocity at the onset of deposition. The bedforms or laminae at the sandstone-mudstone transition in the graded beds provide a realistic estimate of a current's velocity when mud deposition began. In particular, planar sandstone-mudstone transitions suggest that mud deposition began when the current was in the upper plane bed phase; whereas ripple forms imply the current velocity was in the ripple field when mud deposition commenced. In general, the thicker graded beds within a given facies, contain higher velocity bedforms or laminae at their bases' than the thinner graded beds within the same facies.

Planar laminae can form under either unidirectional or under combined currents. Thus, their origin is ambiguous. However, in some graded beds, planar laminae are associated with bedforms or laminae without bedforms, see Table III.2. Where this occurs, the type current can be inferred from the other structures in the graded bed.

Highly asymmetric ripples are also ambiguous. They can form under either purely unidirectional currents or under high velocity unidirectional currents combined with moderate velocity oscillatory currents. Table V.1. Fortunately, they are very rare in the Helena Formation and virtually absent in the Wallace Formation.

AVERAGE SUSPENDED SEDIMENT CONCENTRATION

The average suspended sediment concentration of a current is a function of the current type, the current's velocity and distribution of particle sizes in the suspension. The current must generate an upward force to maintain the mass of sediment in suspension, and that upward force is a function of the current's velocity (Bagnold, 1966; Vincent et al., 1982; Hiscott, 1994). It follows that high suspended sediment concentrations require high current velocities to maintain the mass of sediment in suspension. Since the initial depositional velocity is reflected by the laminae or bedforms at the base of a graded bed, then those bedforms also indirectly reflect the suspended sediment concentration.

Grant and Madson (1979) showed that the type of current affects the suspended sediment concentration. An oscillatory current can maintain more sediment in suspension than a unidirectional current at the same velocity. Furthermore, a combined oscillatory and unidirectional current maintain can more sediment in suspension than the sum of its individual parts would suggest (Grant and Madson, 1979; Vincent et al., 1982).

The suspended sediment concentration is also a function of the size of the particles in suspension. A current with a given velocity can maintain much more 16 µm silt in suspension than 64 µm silt. However, the models contain no mechanism that permits one to estimate the relative amounts of the different sediment size classes in suspension; they must be imposed from outside the model (Hiscott, 1994; Einstein, 1950). Therefore, there is no rational method for estimating suspended sediment concentration for the currents that deposited the sediment in the Helena and Wallace formations.

Normal suspended sediment concentrations in most modern sedimentary environments range from < 0.001 g/L to about 5 g/L. Hill and Nadeau (1989) report suspended concentrations of 5 g/L under storm waves with periods of 8 s, heights of 4 m in 5 m deep water. For the sake of this discussion I assume an upper limit of 25 g/L. This value is 5 times higher than the highest average suspended sediment concentrations observed in 2 m/s tidal currents in the Severn Estuary (Kirby and Parker, 1983), 5 times higher than that reported under fair weather waves off the coast of Surinam (Wells and Coleman, 1981) and 5 times that observed under storm waves in the Beaufort Sea (Hill and Nadeau, 1989). Pierson and Scott (1985) report concentrations ranging from 4.5 to 33 g/L during storm events Toutle River, Washington. Pierson and Scott (1985) also report the formation of hyperconcentrated flows with concentrations of 1050 to 1300 g/L. But, these hyperconcentrated flows evolved from debris flows. Hiscott (1994) estimated that a 15.8 m/s turbidity current, composed of clay-to- medium-grained sand, had an initial suspended sediment concentration of about 140 g/L.

Theoretical models for estimating suspended sediment concentrations are very complex and require the imposition of arbitrary suspended load particle size distributions (Einstein, 1950; Hiscott, 1994). There is no accepted method for estimating the upward force generated by flowing water, but Bagnold (1966) and Hiscott (1994) related the average suspended sediment concentration to the current's velocity. Table V.2 gives hypothetical suspended sediment concentrations for different bed configurations based on the assumption that storms can suspend a maximum of 25 g/L. The anomalous graded beds in a facies contain higher velocity laminae or bedforms than the interbedded background graded beds. This confirms that the suspended sediment concentrations are at least qualitatively related to the initial depositional velocity.

CURRENT VELOCITY AT THE ONSET OF MUD DEPOSITION

Assuming the bed configuration reflects the current's velocity during deposition, then the configuration of the coarser-to-finer transition reflects the current's velocity at the onset of mud deposition. Trochoidal ripples at the transition reflect low oscillatory current velocities and hummocky ripples reflect high oscillatory current velocities. A planar coarser-to-finer transition records plane bed configuration, either under high velocity combined currents, or high velocity unidirectional currents.

ESTIMATING A CURRENT'S DECELERATION RATE

The model for capacity deposition, Chapter IV.A, and the model for the formation of laminae, Chapter V.C, show that primary current laminae form at low to moderate bed aggradation rates, and primary massive bedding forms at very high bed aggradation rates. The aggradation rate is a function of the rate the sediment is supplied to the bed from the suspension, which is a function of the degree of overloading or supersaturation of sediment in suspension.

Given two currents with the same amount of sediment in suspension, a rapidly decelerating current must deposit the same amount of sediment in less time than a slowly decelerating current. That is, the rapidly decelerating current must be more super-saturated with sediment than the slowly decelerating

Table V.2. Hypothetical average suspended sediment concentrations, ASSC, for the different types and velocities of currents that deposited sediment in the Helena and Wallace formations.

bed configuration	current type/ velocity	ASSC

UNIDIRECTIONAL CURRENT BED CONFIGURATIONS

small scale current ripples	unidirectional 17-80 cm/s	1-5 g/l
dunes	unidirectional 35-120 cm/s	1-5 g/l
planar	unidirectional > 80 cm/s	> 5 g/l

OSCILLATORY CURRENT BED CONFIGURATIONS

trochoidal ripples	oscillatory 16-24 cm/s	1-4 g/l
Rounded trochoidal ripples	oscillatory 24-32 cm/s	4-7 g/l
Small hummocky ripples	oscillatory 32-38 cm/s	7-10 g/l
Medium hummocky ripples	oscillatory 38-50 cm/s	10-13 g/l
Large hummocky ripples	oscillatory > 50 cm/s	13-25 g/l

COMBINED CURRENT BED CONFIGURATIONS

Asymmetric ripples	oscillatory 32-38 cm/s unidirectional > 1 cm/s	8-12 g/l
Slightly asymmetric ripples	oscillatory 16-24 unidirictional 1-8 cm/s	2-5 g/l
Long low angle forms	oscillatory 38-65 cm/s unidirectional 1-12 cm/s	8-20 g/l
Quasi-planar	oscillatory > 65 cm/s unidirectional 1-12 cm/s	20-25 g/l
Planar	oscillatory > 65 cm/s unidirectional > 12 cm /s	20-25 g/l

current. Thus, a change from planar laminae upward to massive sandstone, Table III.2, records an increase

in the deposition rate, which implies an increase in the rate at which the current decelerated.

SEDIMENT BYPASSING

Planar laminae, quasi-planar laminae, long low angle laminae and the different types of cross-

laminae record either unidirectional currents or combined oscillatory and unidirectional currents.

Unidirectional and combined currents imply at least part of the suspended sediment load bypassed the site

of deposition. Graded beds containing vertically climbing bedforms imply little or no sediment bypassed

the site of deposition.

PERMISSIBLE WAVE HEIGHTS AND WATER DEPTHS

As shown in Chapter V.E, symmetrical ripples form under oscillatory currents. Wave equations

(Clifton and Dingler, 1984; Komar, 1976; Shore Protection Manual, 1977) can be used to calculate the

minimum and maximum wave heights, and the maximum and minimum water depths for the waves under

which the symmetrical ripples could have been produced. If one assumes the wave tunnel experiments

provide accurate orbital velocities, Appendix I, then the wave calculations can be based on the orbital

velocities suggested on Figure V.2. If one assumes that the ripples are orbital ripples (Clifton and Dingler,

1984), then one can use the spacing of the ripple forms to calculate wave conditions and water depths.

The most common approach (Fritz, 1991; Aspler et al., 1994) for calculating permissable wave

conditions is based on the relationship between the ripple's spacing and the orbital diameter of the waves

that deposited the ripples (Clifton and Dingler, 1984, Fig. 5). In this method, one plots $\neg$ /D verses d_0/D

where $\neg$ is the ripple spacing, D is the grain size and d_0 is the orbital diameter, all in cm. If the ripples in

the study area plot in the orbital ripple field, then the ripples are assumed to be orbital ripples. If the ripples

are orbital ripples, the near bed orbital diameter d_0 is related to the ripple spacing s by,

$$s = 0.65 \, d_0. \qquad\qquad\qquad\qquad (V.1)$$

(Miller and Komar, 1980 a). Once one estimates the orbital diameter, one can calculate the wave

conditions using Equation V.2 (Clifton and Dingler,1984, eq. 18),

$$H = d_0 \sinh (2\Pi h/L) \qquad (V.2)$$

where H is the wave height, d_0 is the orbital diameter, h is the water depth, and L is the wave length. In

equation V.2, the wave height, orbital diameter and wave length change as the waves travel from open

water into shallower water. Thus, one picks a particular wave period, and then calculates how the wave

changes with water depth. The Shore Protection Manual (Vol. III, 1977) provides tables of changing

hyperbolic functions needed to make the calculations.

However, due to the fineness of the sand in the Helena and Wallace formations, the ¬ /D ratios

range from 1500 to 10,000. These large ratios make it impossible to determine if the ripples were orbital,

suborbital or anorbital ripples. Furthermore, data presented in Miller and Komar (1980 b) show that ripples

in sand 177 μm or less in diameter are spaced at 9 cm under wave trains displaying one wave period, and

are spaced at 20 cm under wave trains displaying multiple wave periods. This very strongly suggest that

the ripple spacing is independent of orbital diameters in sand 177 μm or less in diameter.

Therefore, one can not use Equation V.2 to calculate wave conditions in the Helena and Wallace

formations. But, assuming that the wave tunnel experiments provide accurate orbital velocities for the

different bedforms, one can calculate the wave conditions from the orbital velocities using,

$$H = [U_m T \sinh (2\Pi h/L)] / \Pi \qquad (V.3)$$

(Clifton and Dingler,1984, eq. 18), where U_m is the maximum near bed orbital velocity.

I used a different method to calculate permissable wave heights, periods and water depths than that

previously used by Clifton and Dingler (1984), Fritz (1991) and Aspler et al. (1994). These authors limit

the deep water wave height to the deep water wave breaking limit H_{bd}, given by,

$$H_{bd} = 0.142 \ L \ tnah \ (2\Pi h/L) \qquad\qquad (V.4)$$

(Komar, 1976). Clifton and Dingler (1984) and Fritz (1991) limited the shallow water wave height to the shallow water breaking limit (H_{bs}) expressed by,

$$H_{bs} = 0.78 \ h \qquad\qquad (V.5)$$

(Komar, 1976).

However, the deep water breaking limit and the shallow water breaking limit includes wave shapes other than Airy waves. Thus, these limits are not as restrictive as the conditions placed upon Airy waves, and only Airy waves produce symmetrical ripples. The deep water wave height limit for Airy waves H_{A-S} is defined as the transition from a wave best described by the Airy formula to a wave best described by the Stokes formula.

$$H_{A-S} = 0.0625 \ L \ tanh \ (2\Pi h/L) \qquad\qquad (V.6)$$

(Komar, 1976). The shallow water wave height limit for Airy waves H_{A-C} is defined as the transition from a wave best described using the Airy formula to a wave described by the cnoidal formula,

$$H_{A-C} = (h^3 \ 32\Pi^{2/3}) / L^2 \qquad\qquad (V.7)$$

Komar (1976). Equations V.6 and V.7 are somewhat more restrictive than Equations V.4 and V.5.

Permissable wave conditions are also limited by the minimum near bed orbital velocity needed to initiate movement of 100 µm sand (Clifton and Dingler, 1984). Komar and Miller (1973) defined the

threshold of movement of grains smaller than 500 μm with the equation,

$$\frac{p \, U_T^2}{(p_s - p) \, g \, D} = 0.30 \, (d_0/D)^{1/2}, \qquad\qquad (V.8)$$

where p_s is the density of the solids, p is the density of the fluid, U_T is the threshold velocity, and D is the grain size. For 100 μm quartz sand in water the equation reduces to

$$U_T = 2.202 \, (d_0/D)^{1/4} \qquad\qquad (V.9)$$

(Clifton and Dingler, 1984).

Figures V.3 -V. 6 slow the permissible range of water depths and wave heights for the trochoidal ripples, small hummocky ripples, medium hummocky ripples and large hummocky ripples. The figures also show the significant wave periods and heights produced by a typical cold front in the Yellow Sea, the average hurricane on the Mississippi Delta, a 10 year Yellow Sea typhoon, and a 100 year Yellow Sea typhoon. The maximum permissible deep water wave, 34 m, is based on the highest waves ever observed (Komar, 1976).

Trochoidal ripples do not form under waves with periods greater than about 15 s because the threshold of sediment movement is in part a function of wave period (Clifton and Dingler, 1984). Large hummocky ripples can not form under waves with periods less than about 6 s, and small and medium hummocky ripples can not form under waves with periods less than 4 s. This is because the waves either become Stokes or cnoidal waves, or they break, before they reach the orbital velocities needed to produce the bedform.

Figure V.7 is a compilation of the permissible water depths for waves with different periods.

Figure V.3.

Minimum and maximumwave heights and permissible water depths for the formation of trochoidal ripples, assuming troichoidal ripples form at $U_o = 0.2$ m/s
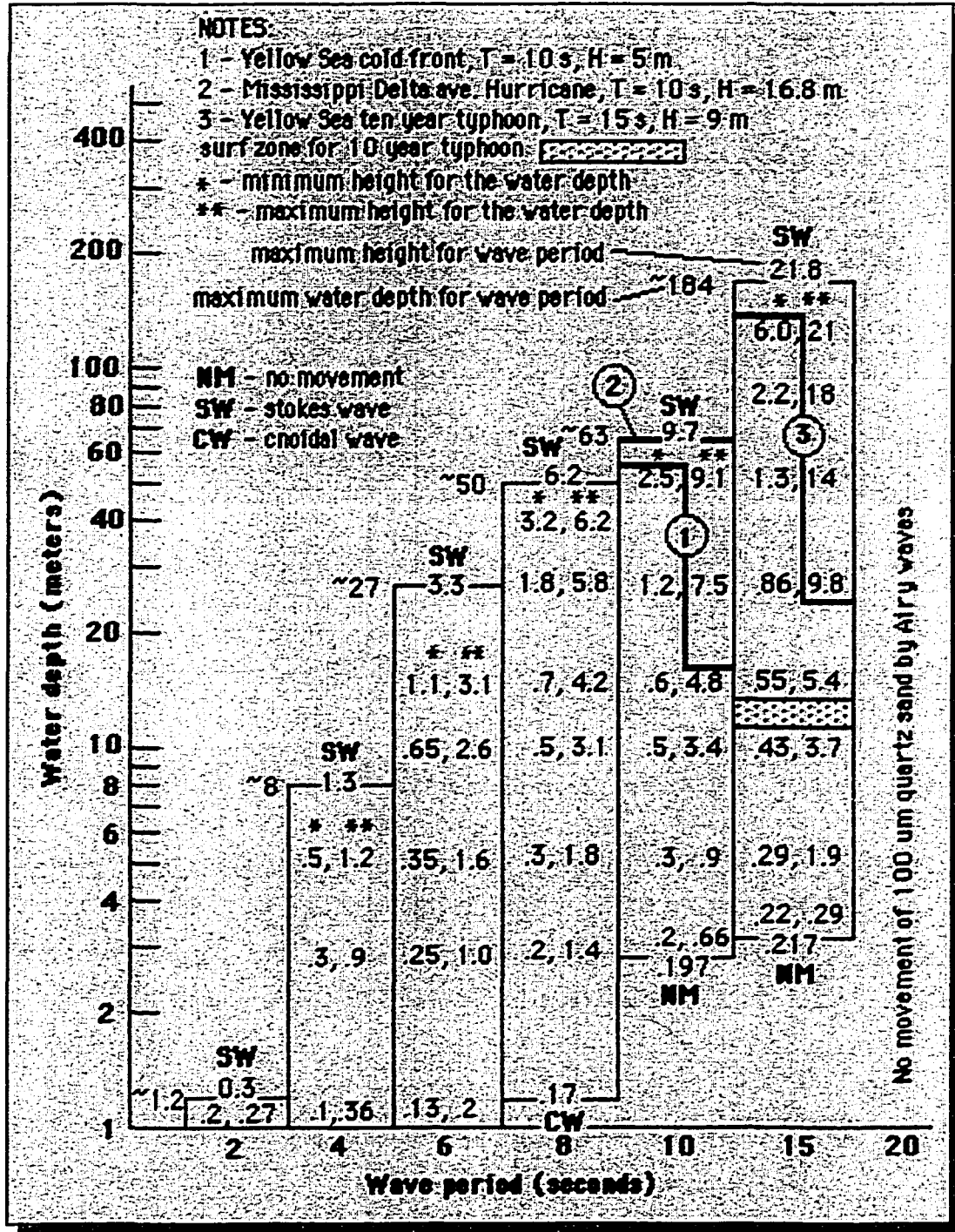
Figure V.4.

Minimum and maximum wave height and permissible water depths for formation of small hummocky ripples, assuming orbital velocities = 0.35 m/s
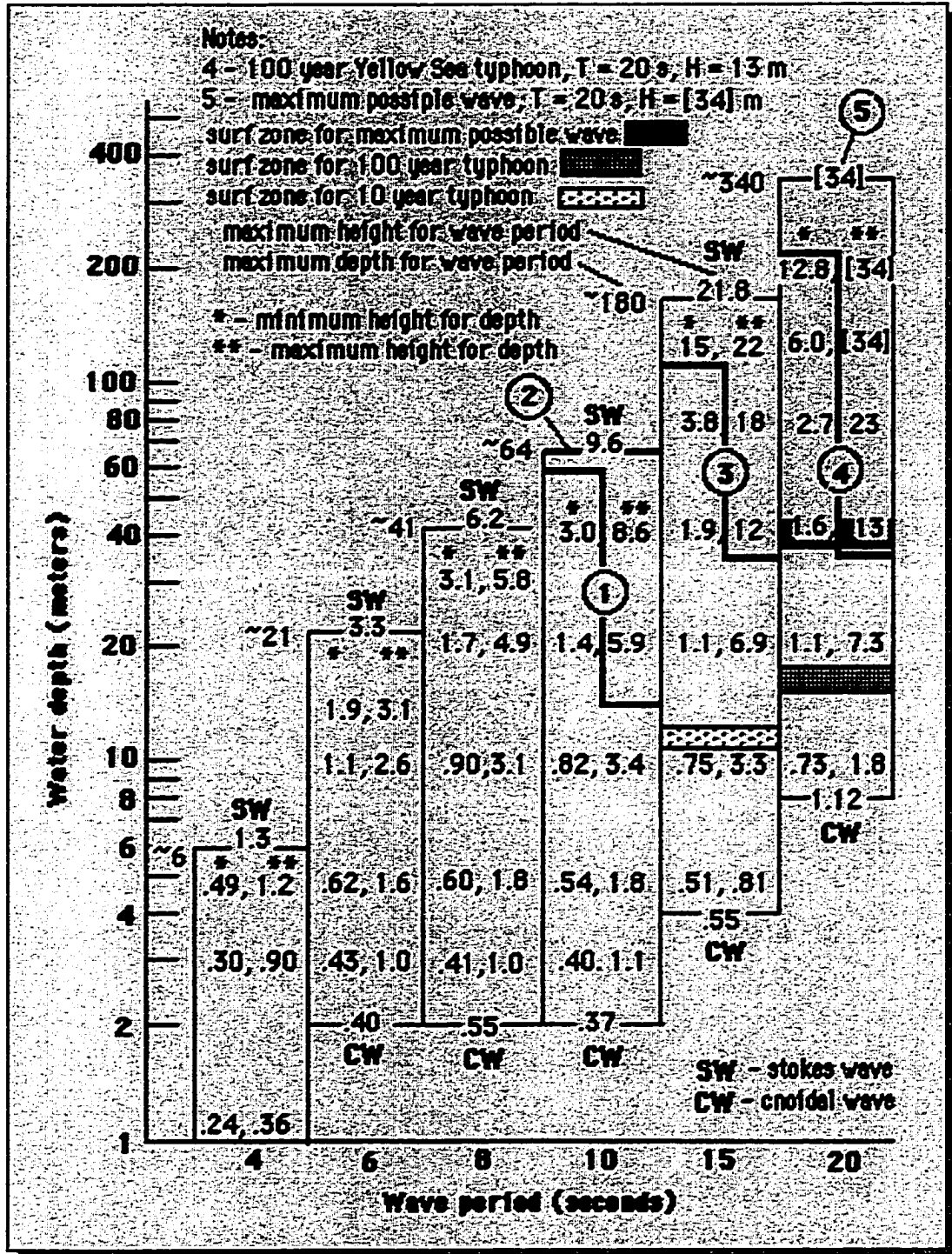
Figure V.5.
Minimum and maximum wave height and permissible water depths for medium hummocky ripples, assuming orbital velocities = 0.45 m/s
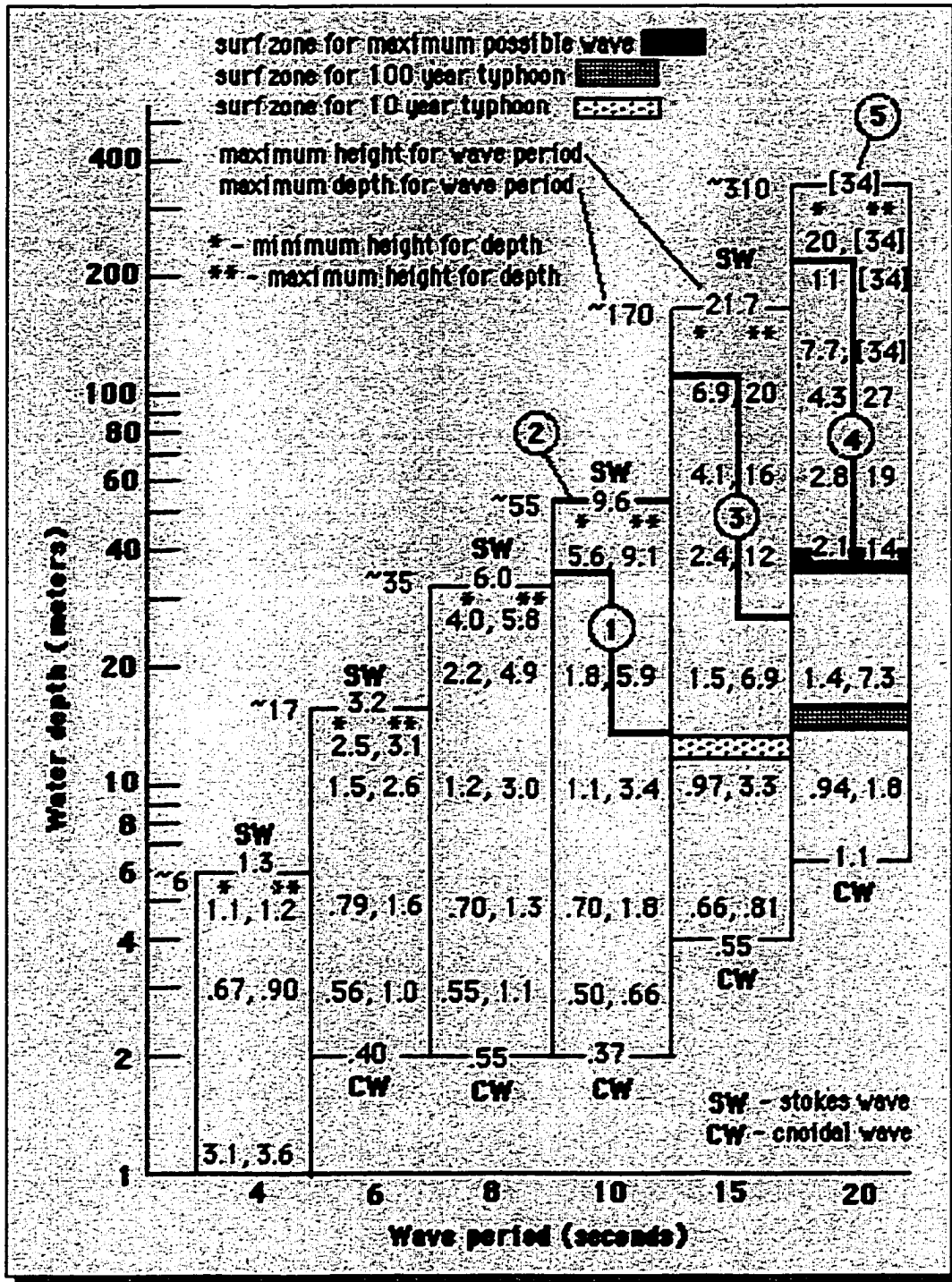
Figure V.6.

Minimum and maximum wave height and permissible water depths for high, large hummocky ripples, assuming orbital velocities = 0.65 m/s
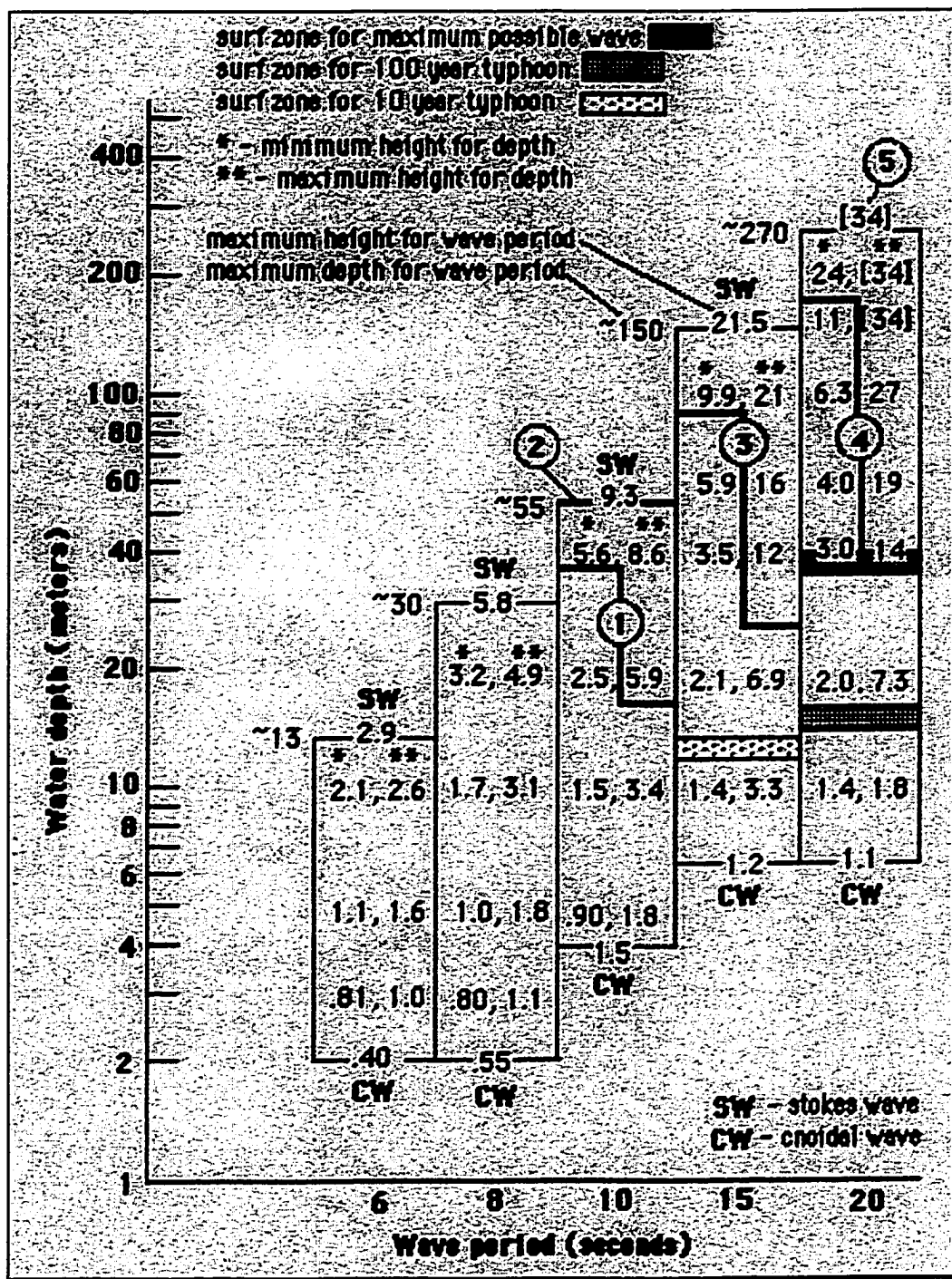
Figure V.7

Permissible water depths and wave periodicity for the formation of symmetrical ripples.
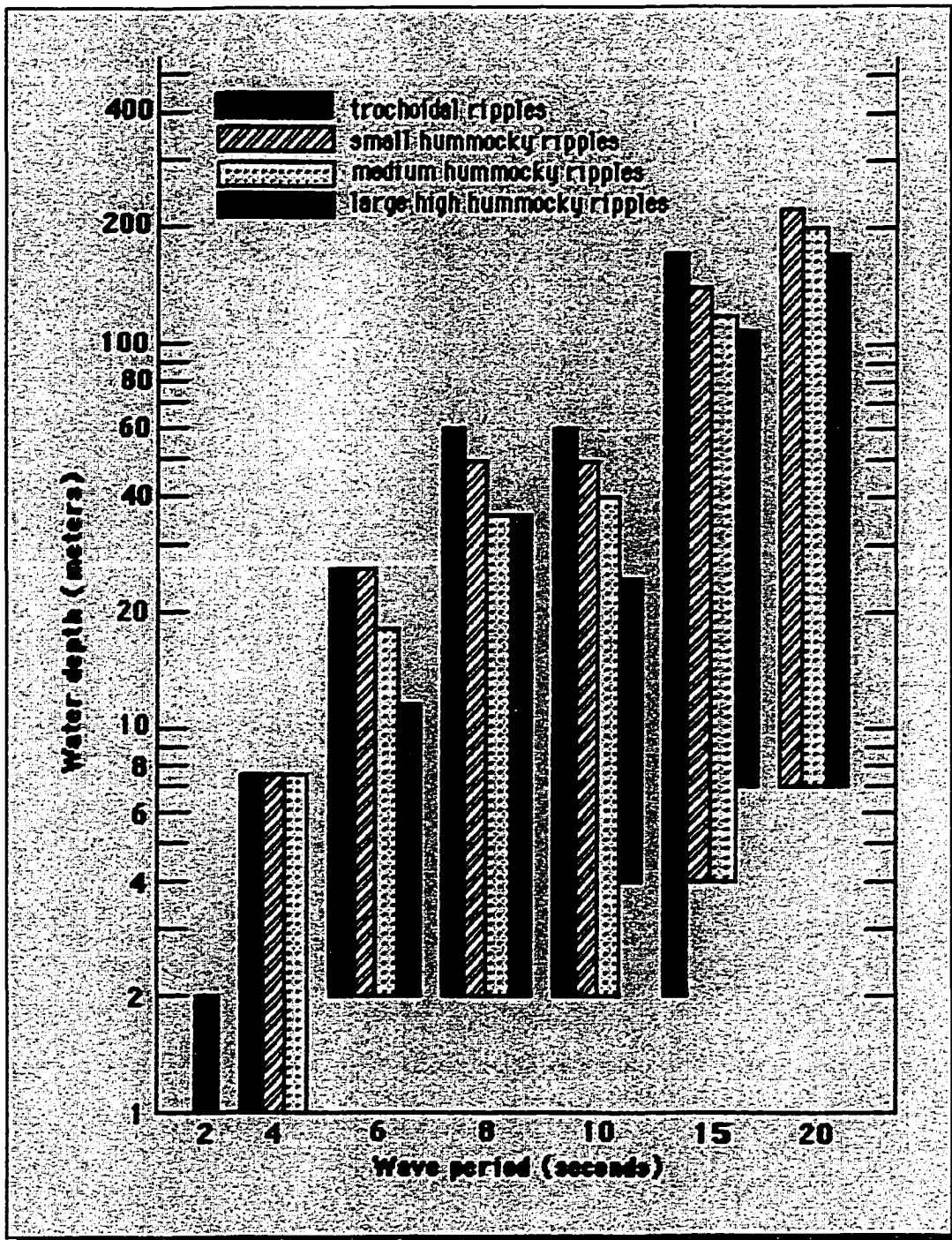
SUMMATION

Sand, silt and clay are supplied to the bed from suspension as a result of a lack of current capacity. As the sediment is supplied to the bed, it is molded into a bed configuration that reflects the type of current and the current's velocity. By definition, molding of the bed and the formation of laminae can only occur when the current is competent enough to move the particles along the bed. Bed phase diagrams provide reasonably accurate estimates of current velocities during deposition of the sediment.

Therefore: (1) The symmetry of preserved bedforms record the type of current that deposited the sediment. (2) The lowest laminae or bedforms in the sandstone layers of the graded beds provide a valid estimate of the initial depositional velocity of the current. (3) The initial depositional velocity qualitatively reflects the suspended sediment concentration. (4) Massive bedding records either very rapid capacity deposition, from rapidly decelerating currents, or very slow currents where deposition was the result of insufficient competency. (5) The bedforms or laminae at the sandstone-mudstone transition provide realistic estimates of the current's velocity when mud deposition began, and (6) The type of laminae and bedforms indicate the presence or absence of sediment bypassing.

HYDRODYNAMIC ANALYSIS OF GRADED BEDS

INTRODUCTION

The goal of this chapter is to interpret the origins of the different types of graded beds. Grading in a graded bed, and the changing vertical sequences of sedimentary structures within the sandstone layer of that graded bed, indicate deposition from a decelerating current. Thus, a sequence of graded beds record a series of decelerating currents, and implies deposition during episodic events, and not deposition from steady, uniform flows.

Dott (1983, 1988) linked episodic deposition to recurring episodic current generating events. This suggests each graded bed in the Helena and Wallace formations records the attributes of one sedimentary episode or event. A graded bed's thickness, the morphology of its basal contact, and its sandstone/ mudstone ratio provides information on the relative magnitude of the event. In general, the thickest graded beds also contain the highest velocity bedforms and laminae and the most erosive basal contacts, confirming a general link between an event's magnitude and the thickness of the resulting graded bed. Furthermore, the abundance of a particular type of graded bed provides information on the relative frequency of that type of event.

In this chapter I review the models for the deposition of graded beds. I then review and discuss episodic sedimentation. Given good exposures, one can obtain information about the sedimentary events from: (a) the graded bed's thickness, (b) the morphology of the graded bed's basal contacts, and (c) their sandstone/ mudstone ratios. Combining this information, I interpret the origin of: (a) the anomalous graded beds, (b) the origin of the lenticular and wavy background graded beds, (c) the origin of loaded background graded beds, and (d) the origin of the microlaminated graded beds. I also show that the shallowly scoured

102

and even background graded beds were deposited from current x, and I describe the characteristics of current x.

ORIGIN OF GRADED BEDS

Vertically decreasing grain size in the graded beds implies deposition from decelerating currents (Allen, 1973; Leeder, 1982; Collinson and Thompson, 1987). Dott (1983, 1988) related single graded beds to erosion, transportation and deposition during a single sedimentary episode. Furthermore, in order to become graded, all of the sediment in a graded bed must have been transported to the depositional site during a single event. Thus, the coarser-grained layers in the graded beds are genetically related to the finer-grained layers, because the sediment in both layers was transported to the site during a single event.

Most graded beds in the Helena and Wallace formations record suspension deposition from decelerating currents with insufficient capacity. However, very thin graded beds, with massive sandstone and mudstone, may record competency deposition. Capacity and competency deposition are discussed in Chapter IV.A.

SUSPENSION TRANSPORT. Over 99 percent of the sediment in the graded beds in the Helena and Wallace formations is equal to, or less than about 100 μm in diameter, i.e., it is wash load sediment according to Nordin and Perez-Hernandez's (1988) definition. In a 1 m deep unidirectional current, 100 μm quartz sand begins to move on a rippled bed when the current reaches 17 cm/s (Anderson and Smith, 1989), and goes into suspension as soon as it begins to move (Nordin and Perez-Hernandez, 1988). Thus, in any current with the competence to move 100 μm quartz sand, all particles 100 μm and smaller are transported suspension.

DECELERATING CURRENTS. Hiscott (1994) linked the formation of graded beds to decelerating currents, and Myrow and Southard (1991) used bed phase diagrams to link slowing currents to

different vertical bedform sequences. Table III.1 shows the vertical succession of bedforms and current lamination within the sandstone layers of the graded beds; recording deposition from successively lower velocity currents.

CAPACITY DEPOSITION. The presence of bedforms and laminae in the graded beds record sorting in the near bed layer. Since, sorting is produced by multiple transfers between the bed and the near bed layer, then deposition occurred from currents with velocities higher than that needed to keep the sediment in suspension. Thus, much of deposition in the Helena and Wallace formations occurred as a result of declining current capacity, not competency. This is supported by the relatively common occurrence of interleaved sandstone and mudstone laminae in ripple troughs and on ripple crests, that records simultaneous mud and sand deposition.

COMPETENCY DEPOSITION. Massive sandstone or siltstone can form under capacity driven deposition where the depositional rates are greater than 4 cm per minute. Or massive bedding can form at low depositional rates where deposition is competency driven. Thus, the processes driving deposition in graded beds that contain only massive sandstone or siltstone layers is ambiguous. However, since low velocity currents can only maintain low average suspended sediment concentrations, they should only deposit thin graded beds. Thus, graded beds with massive bedding less than about a centimeter thick may record competency deposition. Graded beds over a few centimeters thick, with massive sandstone and mudstone layers, probably record capacity deposition.

CHARACTERISTICS OF SEDIMENTARY EPISODES

Sediment can be transported and deposited either continuously from steady, uniform currents (Middleton and Southard, 1984) or episodicly during sedimentation events (Dott, 1983; 1988). The graded beds, or couplets and couples of Winston (1986 b, 1989) and Winston and Link (1993), in the Helena and Wallace formations clearly record episodic sedimentation. Since the sediment in the graded beds was
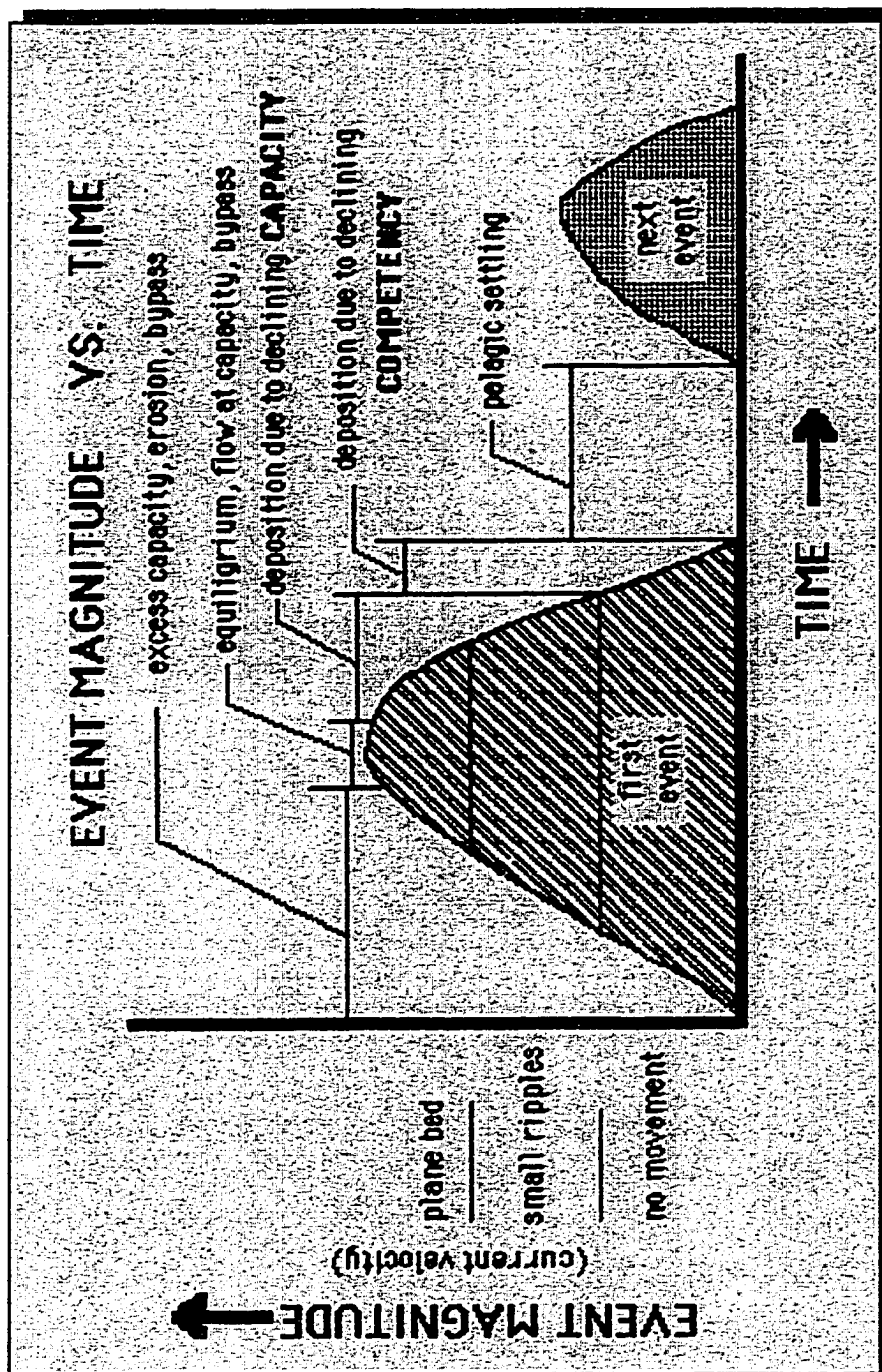
Figure VI.1. Diagram showing event magnitude (current velocity) vs. time, and the processes controlling deposition of the graded beds.

deposited from suspension, then some processes must have generated currents with the competence to erode and the capacity to transport very large volumes of very fine sand, silt and clay.

Most sedimentation is episodic, and ". . . can result from any event whose magnitude deviates from the norm for a given environment" (Dott, 1988, p. 4). Currents produced by episodic events consist of two parts: (1) an accelerating part, when erosion possibly occurred; and (2) a decelerating part when deposition occurred. Figure VI.1 is a schematic diagram of two flow events, showing the different processes operating during an event. Flow events are not only characterized by their magnitude, but their frequency or recurrence interval dictates the number of events per unit time (Dott, 1988).

SUBDIVISIONS OF THE EVENTS. The first part of each flow event records a time when the current was accelerating from the conditions that constitute the norm in the given environment. Although no deposition takes place during the accelerating part, the fact that the graded beds exist proves its existence. If the bed was erodible, then the amount of sediment in suspension increased along with the current's velocity.

During the decelerating part of the event, slowing of the current leads to a condition of oversaturation and sediment deposition. The bedforms and laminae record the conditions during the decelerating part of the flow event.

MAGNITUDE. Event magnitudes are reflected by: (a) the thicknesses of the graded beds; (b) the initial depositional velocities; and (c) the amount of erosion at the base of the graded beds. Anomalous graded beds are thicker, have higher velocity current laminae and exhibit more erosion at their bases than the interbedded background graded beds. Thus, the anomalous graded beds record higher magnitude events than the events that deposited the interbedded background graded beds.

FREQUENCY. Dott (1983) showed that very high magnitude events are less frequent than low magnitude events. Dott (1983) went on to show that high volume turbidity currents are less common than low volume turbidity currents, and extreme storm events are less common than average storm events. Thus, by inference, the anomalous graded beds record lower frequency events than the events that deposited the background graded beds. In general this is supported by the relative abundances of anomalous and background graded beds within a facies. However, this is not true where not all of the background events were preserved.

PRESERVATION POTENTIAL. The deposits of high frequency, low magnitude events tend to have a lower preservation potential than the deposits of low frequency, high magnitude events (Dott. 1983; 1988). This is true for three reasons. (1) Preservation of the deposits of the high frequency events rapidly builds the area to base level; a level where non-deposition and sediment bypass must dominate. (2) The rare high intensity events are capable of eroding the sediment deposited by many low magnitude, high frequency events. (3) Individual low magnitude events are not capable of re-suspending all the sediment deposited during a single high magnitude event.

Thus, stacked anomalous graded beds in the Helena and Wallace formations record either non-deposition of background graded beds, or the erosion of the background graded beds, or both. Furthermore, intervals that contain no anomalous graded beds must record locations that were sheltered from currents generated by the anomalous events.

GRADED BED THICKNESS

A graded bed's thickness is a function of the water depth, the average suspended sediment concentration, and the amount of sediment removed by subsequent erosion. Water depth and average sediment concentration together define the load, covered in Chapter VII.A. I showed in chapter V.G that the

average suspended sediment concentration is a function of the current's velocity. The amount of subsequent

erosion can be estimated from the morphology of the succeeding graded bed's basal contact.

MORPHOLOGY OF THE BASAL CONTACTS

The amount of erosion is a function of the current's suspended sediment saturation, the current's

velocity and the strength of the bed material. The current's velocity and the strength of the bed material

determine whether erosion is permissible or not. However, erosion only occurs if the current is under-

saturated in suspended sediment, Chapter IV.A.

As shown in Chapter IV.E, the consolidating mud of the previously deposited graded bed is

composed of alpha, beta and gamma mud layers. Loaded basal contacts imply no erosion, and direct

deposition on the alpha mud layer, because the alpha mud layer has zero strength. Since saturated flows

have no excess capacity, they are incapable of eroding the substrate, no matter how weak the mud.

Therefore, loads indicate currents that were saturated with sediment during the accelerating phase of the

events. This implies these currents obtained all their sediment at some other location.

The planar contacts beneath the even and lenticular graded beds document the removal of only the

alpha mud layer. The alpha mud layer may be removed by currents just strong enough to erode the alpha

mud layer, or by nearly saturated currents, or both. The shallow scours beneath the shallowly scoured

graded beds records the activity of under-saturated currents, with velocities strong enough to remove only

parts of the beta mud layer.

The thin mud layers that separate the wavy graded beds imply strong, under-saturated currents.

But, the currents were not strong enough to erode completely through the gamma mud layer. The truncation

surfaces that underlie many anomalous graded beds imply current velocities high enough to erode old, well

consolidated gamma layers, and possibly currents strong enough to erode highly consolidated mud.

SANDSTONE/ MUDSTONE RATIOS

As described, Chapter III.I, the background graded beds within a facies display a narrow range of sandstone/ mudstone ratios. The sandstone/ mudstone ratios are a function of: (a) current velocity, (b) the current's source area, (c) the amount of subsequent erosion, and (d) transport conditions that separate sand from mud.

High velocity currents can carry more sand than low velocity currents, thus, graded beds with high sandstone/ mudstone ratios imply high velocity currents. However, the sand/ mud ratio of the source area also influences the sand/ mud ratio of the suspension. For instance, a mud rich source area will produce only mud rich currents. Also, the sandstone/ mudstone ratio can also be effected by removal of part of the mud layer during a subsequent event.

However, the fact that the background graded beds within a facies display a limited range of sandstone/ mudstone ratios implies that all these factors must have acted in a systematic manner. Thus, the background graded beds within a facies reflect erosion, transportation and deposition from similar current types, current velocities, source areas and transport conditions.

THE ORIGIN OF ANOMALOUS GRADED BEDS

Tabular and wedge anomalous graded beds contain high velocity, wave generated bedforms and laminae, Table III.9 and III.10. The oscillatory currents indicate wave generated currents. The presence of laminae and bedforms in the sandstone layers record slow current deceleration, and deposition resulted from declining current capacity.

High velocity oscillatory currents can only be generated by high amplitude and/or long period waves, Figure V.7, and this implies deposition form currents generated by large and extreme storm events. Common truncation surfaces beneath the anomalous graded beds and their thickness also indicate the activity of high velocity currents, produced by large and extreme magnitude events. Thus, the tabular and

wedge anomalous graded beds probably record extreme storms events, possibly with recurrence intervals of tens to hundreds of years.

Conversely, the long lens and short lens anomalous graded beds, Table III.11 and III.12, contain lower velocity oscillatory bedforms and laminae. Low to moderate velocity oscillatory bedforms can form in either in deep water under high amplitude, long period waves, or in shallow water under moderate, intermediate period waves, Figure V.7. Thus, the long lens and short lens graded beds could record deep water deposition, offshore of the tabular and wedge anomalous graded beds, during the same large or extreme events. Or they could record shallow water deposition, during lower magnitude storms.

Gutters and truncation surfaces underlying the anomalous graded beds record erosion by under-saturated, sediment starved accelerating currents. Gutters, truncation surfaces and combined current laminae indicate sediment bypassing. Combined currents can be produced by either Stokes, cnoidal or breaking waves (Komar, 1976), or by Airy waves combined with a storm induced current (Duke et al., 1991). The rare loaded bases under anomalous graded beds in facies C record transport and deposition from saturated accelerating currents.

ORIGIN OF THE LENTICULAR AND WAVY BACKGROUND GRADED BEDS

Lenticular graded beds contain common vertically climbing, trochoidal ripples and rounded trochoidal ripples, Table III.4. These bedforms record initial deposition from oscillatory currents in the 16 to 24 cm/s and 24 to 32 cm/s respectively, Table V.1. The wavy background graded beds commonly contain vertically climbing, small hummocky ripples, Table III.6, indicating initial deposition from oscillatory currents in the 32 to 38 cm/s range, Table V.1.

The laminae show that the currents decelerated slowly throughout ripple deposition. Interleaving of sandstone laminae on the ripple crests with mudstone laminae in the ripple troughs records

contemporaneous sand and mud deposition due to declining current capacity. Vertically climbing ripples record little or no sediment bypassing at the depositional surface.

Deposition from oscillatory currents and the evidence for slow deceleration suggest that deposition of wavy and lenticular graded beds occurred from low to moderate velocity storm generated currents. I consider them average storms because they were less powerful than the extreme storm events that deposited the anomalous graded beds, but I can not tell whether the storms were actually average storms or not.

ORIGIN OF LOADED BACKGROUND GRADED BEDS

The base's of many loaded graded beds contain bedforms that appear to be distorted trochoidal ripples, Table III.7, and at some places, trochoidal ripples are built upon the loads. Trochoidal ripples record initial oscillatory current velocities between 16 and 24 cm/s, and imply low average suspended sediment concentrations. Laminae in the ripple forms implies capacity deposition from slowly decelerating currents.

Loads at the bases of the loaded graded beds show that the accelerating part of the flow events were incapable of eroding the very soft, alpha layer mud the loaded graded beds were deposited upon. The lack of erosion under the loaded graded beds suggests the currents were saturated with sediment, and the area acted as a sediment sink.

Slow deceleration, low suspended sediment concentrations and the low velocity symmetrical ripple forms suggest deposition occurred in deep water, from oscillatory currents generated by average storm events. Given waves with the same heights and periods, wave generated currents are weaker in deep water than in shallow water. Thus, a single storm could deposit a thick, sandy wavy graded bed in relatively shallow water at the same time it deposited a thinner and muddier loaded graded bed in deeper water. It is also possible that some loaded background graded beds were deposited from extreme storm events, but at distal locations, in very deep water.

Table VI.1.   Table summarizing the characteristics of the of the background and anomalous flow events and the properties of the graded beds that provide the information.

current characteristic	graded bed property

1. type of current
    oscillatory
    combined flow
    unidirectional
	bedform symmetry
	    symmetrical, concordant 2D ripples,
	        hummocky ripples
	    planar laminae, quasi-planar laminae,
	        long low angle laminae
	    large scale cross-laminae, small scale
	        cross-laminae

2. suspended sediment saturation
    saturated
    moderately under-saturated
 	
    under-saturated
	degree of erosion of the underlying mud layer
	    no erosion- loaded graded beds
	    minor erosion- even and shallowly
	        scoured graded beds
	    moderate erosion-wavy graded beds

3. initial depositional velocity
    high, > 65 cm/s
        > 50 cm/s
    medium, 24 - 65 cm/s
    low, 18 - 24 cm/s
	type of laminae at base of sandstone layer
	    planar laminae, quasi-planar laminae
	    large hummocky ripples
	    small and medium hummocky ripples
	    small scale 2D and 3D ripples,
	        small scale cross-laminae

4. average suspended sediment concentration
    high, > 5 g/l
 	
    medium, 2 to 5 g/l
    low = 1 g/l
	initial depositional velocity of current
	    planar laminae, quasi-planar laminae
	    large hummocky ripples
	    short and medium hummocky ripples
	    small scale ripples

5. suspended sediment load (average
    concentration times the depth)
    very high
    high
    medium
    low
	thickness of the graded beds
	
	    20 to 45 cm thick
	    15 to 20 cm thick
	    5 to 10 cm thick
	    microlaminated graded beds

6. current deceleration
    rapid
    slow followed by rapid
    slow
	lamination or massive bedding in the graded bed
	    massive bedding
	    laminae overlain by massive bedding
	    laminae or sorting throughout graded bed

ORIGIN OF SHALLOWLY SCOURED
AND EVEN BACKGROUND GRADED BEDS

The structures in the even and shallowly scoured background graded beds record deposition from fundamentally different currents than those that deposited the wavy, lenticular and loaded graded beds. The very common massive bedding in the shallowly scoured and even background graded beds, Tables III.3 and III.5, precludes high confidence identification of the type of currents they were deposited from. I call the current that deposited the shallowly scoured and even background graded beds current x because its exact origin is unknown. However, I will show that it probably was not a storm generated current or a turbidity current, Chapter IX.B; and I can show that it was possibly a tidal current.

CHARACTERISTICS OF CURRENT X

In order to interpret the origin of the shallowly scoured and even graded beds, I must document the characteristics of current x. Table VI.2 presents a summary of the characteristics of current x, and gives the evidence for each characteristic.

VELOCITY IN FACIES B. Rare planar laminae in the sandstone layers in the shallowly scoured and even graded beds in facies B suggest velocities in the upper plane bed regime. Planar laminae can form under either combined currents or unidirectional currents, Table V.1.

VELOCITY IN FACIES C. The rare small scale, high angle, cross-laminae in the shallowly scoured and even graded beds in facies C suggests current x had a lower velocity in facies C than in facies B. Small scale cross-laminae indicates current x was either an unidirectional or a combined current, and this is consistent with the planar laminae in shallowly scoured and even graded beds in facies B.

RAPID DECELERATION. Even and shallowly scoured graded beds commonly contain massive sandstone or siltstone layers, Chapter III.F. Massive sandstone or siltstone can form during capacity

Table VI.2   *Characteristics of current x.*

current x characteristic	evidence
1. current x was a unidirectional or a combined current	(a) planar laminae do not form under purely oscillatory currents; (b) small scale, high angle cross-laminae record deposition from either unidirectional or combined currents
2. if combined current, then velocity > 65 cm/s in facies B; if unidirectional current, then velocity > 80 cm/s in facies B	rare planar laminae in sandstone layers of even and shallowly scoured graded beds in facies B
3. if combined current, then velocity 18 to 38 cm/s in facies C; if unidirectional current, then velocity 18 to 80 cm/s in facies C;	rare high angle, small scale cross-laminae in microlaminated graded beds in facies C
4. rapid deceleration	very common massive sandstone layers in the even and shallowly scoured graded beds
5. higher frequency of occurrence than average storm events	high number of even and shallowly scoured graded beds relative to the number of lenticular graded beds
6. average suspended sediment concentrations were about the same as those in the average storm events	interbedded shallowly scoured, even, and lenticular graded beds are all about the same thickness
7. current x was near saturation	(a) removal of only the alpha mud layer under the even graded beds; (b) shallow erosion into beta mud layer under the shallowly scoured graded beds

deposition where the deposition rate is greater than 4 cm per minute (Arnott and Hand, 1989), or during competency deposition, where the low current velocity can't induce sorting on the bed.

Rare even and shallowly scoured graded beds in facies B contain planar laminae and suggest capacity deposition from very high velocity currents. Thus, I infer that the very common massive bedding in the sandstone layers of the even and shallowly scoured graded beds in facies B records rapid capacity deposition and not slow competency deposition. This implies that current x decelerated more rapidly than the storm generated currents that deposited the rare interbedded lenticular graded beds.

RECURRENCE FREQUENCY. Rare lenticular graded beds are interbedded with the even and shallowly scoured graded beds in facies B and C. This interbedding shows that the events that deposited the even and shallowly scoured graded beds must have been much more frequent than the events that deposited the lenticular graded beds. Since the lenticular graded beds were probably deposited during average storm events, then the process that generated current x must have had a much higher recurrence rate than the average storm events.

AVERAGE SUSPENDED SEDIMENT CONCENTRATION. The interbedded lenticular, even and shallowly scoured graded beds are all about the same thickness. This means current x must have contained about the same average suspended sediment concentration as the average storm event generated currents .

SEDIMENT SATURATION. The inferred amount of scour beneath the even and shallowly scoured graded beds suggests that current x was near saturation. The planar basal contacts of the even graded beds implies that only the alpha mud layer of the underlying graded bed was removed before deposition commenced, Chapter IV.D and IV.E. The shallow scours beneath the shallowly scoured graded beds suggests that all of the alpha mud layer and chunks of the beta mud layer of the underlying graded bed

were removed before deposition. The relatively small amount of mud removal, combined with the high velocities indicated by the rare planar laminae, imply that current x was near saturation throughout the accelerating part of the flow event. This means current x probably obtained most of its suspended sediment load at some other location.

SEDIMENT BYPASS. Planar laminae and small scale cross-laminae indicate either unidirectional or combined currents, and indicate sediment bypass. That is, at least some of the sediment in suspension bypassed the site.

SUMMATION. Current x was either a unidirectional or combined current, with a higher velocity in facies B than facies C. Current x was a rapidly decelerating current with a much higher recurrence interval than the average storm events.

ORIGIN OF THE MICROLAMINATED GRADED BEDS

Microlaminated graded beds display the same morphologies as the even, shallowly scoured and lenticular graded beds, but, they are less than 3 mm thick. Since they have the same morphologies, they probably were deposited by the same types of currents. Thus, the lenticular microlaminated graded beds probably reflect deposition from low velocity oscillatory currents generated by average storms, while the even and shallowly scoured microlaminated graded beds reflect deposition from current x.

The thinness and lack of erosion of the mudstone layers imply low velocity currents in shallow water, and this suggests the massive bedding may be the result of competency deposition. But rare small scale cross-laminae in the sandstone layers of the even microlaminated graded beds record capacity deposition from either combined or unidirectional currents.

A TIDAL ORIGIN FOR THE MICROLAMINATED GRADED BEDS

Sequences composed of millimeter to centimeter scale graded beds are commonly called

rhythmites (Reineck and Singh, 1980, p. 123). Cosets of microlaminated graded beds in the Helena and

Wallace that occur in facies C are similar to, and have been compared to rhythmites (Woods, 1986, p. 50).

Rhythmites have been reported from deltas, tidal flats, estuaries, deep marine basins, fjords, restricted bays

and lakes. Individual graded beds in the rhythmite record periodic (seasonal, annual, diurnal, semi-diurnal)

sediment transporting events, or aperiodic events (Reineck and Singh, 1980). Rhythmites produced by tidal

currents are called tidal rhythmites (Reineck, 1967).

Since rhythmites can be deposited in such a wide range of environments, by such a wide range of

episodic events, the presence of the rhythmites, by themselves, do not indicate any particular depositional

environment. However, graded beds displaying systematicly changing sandstone/ mudstone ratios probably

reflect systematic changes in current strength, and deposits that reflect systematic changes in current

strength are characteristic of tidal environments (Allen, 1985 a; Nio and Yang, 1991).

TIDAL TRANSPORT MECHANICS. Deposition of tidal rhythmites, or very thin graded beds,

occurs in the shallower parts of tidal environments (Reineck, 1967 a; Thompson, 1968; Knight and

Dalrymple, 1975; Larsonneur, 1975; Klein, 1970). Four mechanisms are responsible for rhythmite

deposition in shallow tidal environments: (1) Flood tidal currents are commonly stronger than ebb tidal

currents (G. P. Allen, 1991). Thus, sediment deposited by the flood tide is not eroded by the ebb tide. (2)

Maximum tidal current velocities are higher in the deeper parts of the tidal environment and lower in the

shallower parts of the tidal environment (G. P. Allen, 1991). Thus, erosion is more likely in deeper water

than in shallow water. (3) Settling lag (van Straaten and Kuenen, 1958: Postma, 1967) induces deposition

of the finest sediment in the shallowest water; and (4) The scour lag (van Straaten and Kuenen, 1958;

Postma, 1967) model accounts for the preservation of the very thin graded beds, because ebb currents are

not strong enough to erode the cohesive fine sediment deposited by the flood currents.

ORBITAL MECHANICS. Earth-moon-sun orbital mechanics produce systematic changes in tide heights at two different time scales (Archer et al., 1991). Systematic changes in tide heights, induced by tidal mechanics, may be recorded in systematic changes in the thickness of graded beds deposited by tidal currents (Allen, 1985 a; Williams, 1989 a; 1989 b; Kvale and Archer, 1991; Kvale et al., 1989).

Over a period of 24 hours, tidal processes produce alternating high and low high tides, called the semi-diurnal inequality (Archer et al., 1991). Over a period of 14 days, systematicly changing tidal heights are produced by neap-spring tidal variations (Archer et al., 1991). Given ideal deposition and preservation conditions, both time scales appear to be reflected by systematic changing sandstone/ mudstone ratios in the microlaminated graded beds in the Helena and Wallace formations. Chapter III.F.6.

ORIGIN OF LAMINA-CYCLES. According to my observations, millimeter scale graded beds in the Helena and Wallace formations (Plate 5 a, c and e) rarely exhibit systematicly changing sandstone/ mudstone ratios on a centimeter or so scale. I believe this produces a series of graded beds with high sandstone/ mudstone ratios, followed by a series of graded beds with low sandstone/ mudstone ratios. D. Winston (1995, personal communication) observing the same outcrops, sees no evidence of systematically changing sandstone/ mudstone ratios. These systematic changes resemble the lamina-cycles of Williams (1989 a) and Kvale and Archer (1990; 1991). Lamina-cycles may record deposition from currents that varied systematicly in strength as a result of neap-spring tidal cycles (Allen, 1985 a, p. 256; Nio and Yang, 1991; Williams, 1989 a; Williams, 1989 b; Kvale and Archer, 1991).

Neap-spring tidal variations are produced by either tropical half month or the synodic half month variations in the Earth-moon-sun system (Archer et al., 1991). High- high tides are produced when the Earth, moon and sun line up, which occurs during the full moon and during the new moon. This alignment produces spring tides (Allen 1985 b). Low- high tides are produced when the moon lies 90° to a line drawn

between the Earth and the sun. This miss-alignment produces neap tides (Allen 1985 b), and there is a gradual change form the high spring tides to the low neap tides.

Alternatively, Williams (1981; 1985) suggested each individual graded bed in the lamina-cycles records an annual flood event, ie., he interpreted each graded bed as an annual varve and not a daily or twice daily event. Williams (1981; 1985) went on to link the lamina-cycles to climatic variations, induced by the 13 year variations in sunspot activity .

The lamina-cycles do not provide compelling evidence for tidal deposition. But, given the frequency of occurrence of the interbedded lenticular graded beds, a neap-spring tidal origin is more likely than a sunspot induced climate change that affected varve thicknesses.

ORIGIN OF ALTERNATING HIGH-LOW SANDSTONE/ MUDSTONE RATIOS. The Helena and Wallace formations also contain very thin graded beds with millimeter scale siltstone layers that alternate with graded beds displaying siltstone layers only a grain diameter of two thick. Plate 5-d contains an interval of three thick-thin graded bed pairs. This produces graded beds with alternating high and low sandstone/ mudstone ratios. Kvale et al. (1989) and Kvale and Archer (1991) attributed similar variations in thin graded beds in Pennsylvanian age tidal deposits to current velocity changes induced by the semi-diurnal tidal inequality.

Dalrymple and Makino (1989, p. 168) observed the formation of graded beds with silt layers one or two silt or sand grains thick on a modern tidal flat, and called them sandy-stringer couplets. Dalrymple and Makino (1989) also observed that the sandy-stringer couplets alternated with graded beds displaying thicker sand layers. Thus, by direct observation, Dalrymple and Makino (1989) linked graded beds with alternating high-low sand/ mud ratios to the pattern of successive high-high and low-high tides produced by the semi-diurnal tidal inequality.

SUMMATION. High frequency combined or unidirectional currents, current x, deposited the even and shallowly scoured microlaminated graded beds. Interbedding of even and shallowly scoured graded beds with rare lenticular graded beds show that current x had a far higher recurrence rate the average storm currents. Thus, the frequencies and the types of currents are at least permissive of tidal current origin for the even and shallowly scoured microlaminated graded beds.

Intervals I observe containing lamina cycles and alternating high-low sandstone/ mudstone ratios in microlaminated graded beds are rare in the Helena and Wallace formations, and even their existence is sharply disputed. The lamina-cycles could record deposition from annual sediment influxes, and thereby record climatic changes induced by sun spot activity (Williams 1981; 1985). Or they could record deposition from currents induced by tidal processes, and thus record neap-spring tidal cycles. But, the three pairs of microlaminated graded beds with alternating high-low sandstone/ mudstone ratios strongly imply deposition influenced by the semi-diurnal tidal inequality.

Tidal systems are capable of producing systematic variations in sand/ mud ratios in graded beds at two time scales. My interpretation that the microlaminated graded beds in Helena and Wallace formations record both time scales provides the most compelling evidence for tidal processes driving current x.

Hydrodynamic Analysis of the Facies

INTRODUCTION

Each facies is characterized by suite of background graded bed types that display a characteristic sandstone/ mudstone ratio and thickness. The similarities indicate repeated deposition from the same type currents, with the same maximum current velocities, and the same suspended sediment concentrations. Furthermore, similarities in basal contacts and internal laminae within a facies suggest each event also induced about the same amount of mud erosion and about the same amount of sediment bypassing. Thus, the background graded beds within a facies record repeated deposition from similar currents.

At most locations, the facies contain interbedded anomalous graded beds as well as background graded beds. The anomalous graded beds are thicker and contain higher velocity bedforms and laminae than the interbedded background graded beds. The anomalous graded beds thus record lower frequency, higher magnitude events than the background graded beds.

The differences between the facies indicate each was deposited at a location characterized by different types of currents, with different velocities, and different sediment loads. Indeed, it is these differences that were responsible the set of unique characteristic of each facies. The goal of this chapter is to determine as much as possible about those currents. The hydrodynamic analysis of the individual facies as a whole provides information on:

- the primary and secondary types of currents that deposited the background graded beds
- the principal type current that deposited the anomalous graded beds
- initial depositional velocities of the background and anomalous events
- driving mechanisms for the background and anomalous currents
- relative energies of the background and anomalous current producing events
- whether the area was a sediment sink, the site of bypass or the site of erosion

Table VII.1. Summary of facies interpretations.

FACIES A

- wavy and lenticular background graded beds

transporting currents
transporting currents were under-saturated, with much excess capacity
eroded the underlying alpha, beta and most of gamma mud layer
depositing currents
oscillatory currents generated by averageTable VII.1. Continued.

FACIES B

- background graded beds
    even and shallowly scoured graded beds

transporting currents
transporting currents near saturation
erosion of alpha layer (even) & parts of beta layer (shallowly scoured)
depositing currents

current x
initial depositional velocities about 80 cm/s
currents contained average concentrations of about 5 g/l?
currents decelerated rapidly
    lenticular graded beds

transporting currents
transporting currents near saturation
erosion of alpha mud layer only

depositing currents
average oscillatory storm currents
initial depositional velocities between 24 - 32 cm/s
currents contained average concentrations between 5-7 g/l?
currents decelerated slowly
- anomalous graded beds (for subfacies Bg only)

transporting currents
greatly under-saturated, with large excess capacities
formation of truncation surfaces and gutters
depositing currents
combined unidirectional and oscillatory extreme storm currents
initial depositional velocities commonly greater than 50 cm/s
currents contained average concentrations greater than 13 g/l?
currents decelerated slowly at first, then decelerated rapidly

Notes: Facies B records deposition from three types of currents. Even and shallowly scoured back-
ground graded beds record deposition from current x. Lenticular background graded beds record
average storms, and anomalous graded beds record extreme storms.
Facies B (except subfacies Bg) acted mainly as a sediment sink, displaying little erosion during either
the anomalous and background events. Subfacies Bg acted as a source area and an area of sediment
bypass during extreme events
Anomalous graded beds were probably deposited within the extreme storm wave build-up and surf zone.

Table VII.1. Continued.

FACIES C

- even and shallowly scoured background graded beds
                    transporting currents
          transporting currents near saturation
          erosion of alpha layer (even) & parts of beta layer (shallowly scoured)

                    depositing currents
      current x
      initial depositional velocities between 18 -80 cm/s, about 50 cm/s?
      currents contained average concentrations between 1-3 g/l?
      currents decelerated rapidly

- lenticular background graded beds
                    transporting currents
          transporting currents near saturation, little or no erosion

                    depositing currents
      average storm oscillatory currents
      initial oscillatory velocities between 16-24 cm/s
      currents contained average concentrations between 1-3 g/l?
      currents decelerated slowly

-microlaminated graded beds
                    transporting currents
          transporting currents near saturation, little or no erosion

                    depositing currents
      current x, and average storm currents
      initial unidirectional velocities between 17- 80 cm/s, ≈ 20 cm/s?
      initial orbital velocities between 16-24 cm/s
      currents contained average concentrations between 0.5-1 g/l?

- anomalous graded beds
                    transporting currents
          transporting currents were under-saturated, and probably sand starved
          erosion of wavy truncation surfaces and gutters

                    depositing currents
      combined and purely oscillatory extreme storm currents
      initial depositional velocities 16-38 cm/s
      currents contained average concentrations between 1-10 g/l

Notes: Facies C records deposition from three types of currents. Even and shallowly scoured back-
          ground graded beds record deposition from current x. Lenticular background graded beds record
          average storms, and anomalous graded beds record extreme storms.

Table VII.1. Continued.

FACIES D

- lenticular and loaded background graded beds
                    transporting currents
        transporting currents were saturated, and were at or very near capacity
        currents caused little or no erosion of underlying mud layer, formed loads

                    depositing currents
        purely oscillatory average storm currents
        initial depositional velocities ranged between 16 -24 cm/s
        currents contained average concentrations between 0.5-3 g/l
        currents decelerated slowly

- even and shallowly scoured background graded beds
                    transporting currents
        transporting currents near saturation
        erosion of alpha layer (even) & parts of beta layer (shallowly scoured)

                    depositing currents
        current x
        initial depositional velocities between 18 -80 cm/s, about 30 cm/s?
        currents contained average concentrations of about 1 g/l?
        currents decelerated rapidly

- anomalous graded beds
                    transporting currents
        transporting currents were at saturation
        no erosion of underlying mud layer, formation of loaded basal contacts

                    depositing currents
        combined and purely oscillatory extreme storm currents
        initial depositional velocities commonly greater than 50 cm/s
        currents contained average concentrations greater than 13 g/l?

Notes: Facies D was deposited mainly from storm generated currents. Rare even and shallowly
        scoured background graded beds indicate current x played a minor role in deposition of the facies.

        Facies D acted as a sediment sink during the deposition of both the background and
        anomalous graded beds.

        The background graded beds were deposited far offshore of the average storm surf zone, just above
        average storm wave base.

        The anomalous graded beds were deposited offshore of the extreme storm surf zone, but well above the
        extreme storm wave base.

EROSION, BYPASSING, LOCAL SOURCE AREAS AND SEDIMENT SINKS. Structures in the facies provide evidence for sediment erosion and bypassing. Furthermore, some facies must have acted, at least part of the time, as local source areas, but others appear to act only as a sediment sink. I use the morphology of the base of the background and anomalous graded beds to estimate the amount of erosion during background and anomalous events.

Facies dominated by vertically climbing bedforms and background graded beds with little or no erosion record little or no bypassing or erosion. Such facies as sediment sinks. Facies containing low angle truncation surfaces and gutters record sites of deep erosion.

Planar laminae, quasi-planar laminae and long low angle laminae record deposition from currents with net lateral velocities greater than 30 cm/s measured 10 m above the bed, Figure V.2. Therefore, graded beds containing these current laminae document considerable amounts of net sediment transport past the site of deposition.

Graded beds containing only vertically climbing symmetrical bed forms were deposited from combined flow currents with a maximum unidirectional component of 30 cm/s measured 10 m above the bed. Thus, these bed forms record either a small amount of sediment bypassing or no sediment bypassing. Graded beds that contain planar, quasi-planar or long low angle lamination at their bases, overlain with symmetrical bed forms record the evolution of currents with large amounts of sediment bypass to currents with no sediment bypass.

FACIES A

The most striking feature of facies A, the sandstone facies, is the thinness of the mudstone layers in the background graded beds. By definition facies A contains less than 35 percent mudstone, but at most places, the facies contains less than 5 percent mudstone. At these locations the mudstone layers occur as 1 -

5 mm thick, mudstone partings, separating 5 to 15 cm thick sandstone layers. Since the background graded beds in facies B, C and D average over 50 percent mudstone, I assume the currents that deposited the background graded beds in facies A contained more than 5 percent mud in suspension. If so, this raises two questions: (1) What process removed the mud from facies A? and, (2) Where was that mud deposited?

BACKGROUND GRADED BEDS. Wavy and lenticular graded beds are the most common background graded beds in facies A. Moderate depositional velocities, dominance of oscillatory currents and high average suspended sediment concentrations suggest deposition of background graded beds occurred from currents generated by average storms. I covered the evidence for storm deposition in Chapter VI.H.

Rounded trochoidal and small hummocky ripples in the wavy graded beds record initial depositional velocities in the 24 to 32 cm/s and 32 to 38 cm/s range respectively. The symmetry and vertical climb of the bedforms in the wavy graded beds shows that the sediment was deposited from either purely oscillatory currents, or oscillatory currents combined with a weak unidirectional component, hence little or no sediment bypass at the site of deposition. Primary current laminae commonly occur throughout the sandstone layers of the wavy graded beds, recording slow deposition and slowly decelerating currents. The removal all of alpha and beta mud layers, and the preservation only a portion of the gamma mud layer, implies the presence of undersaturated erosive currents during the accelerating part of the events.

Lenticular graded beds occur mainly as individual graded beds in facies A, but at some locations they form cosets. Long low angle laminae in them record deposition from high velocity combined flow currents and indicate sediment bypass. The currents had oscillatory components between 38 and 65 cm/s, and unidirectional components greater than 30 cm/s measured at 10 m above the bed. The sequence of internal structures in the lenticular graded beds in facies A show that the currents evolved from high velocity combined flow currents to low velocity, purely oscillatory currents. This records deposition from

currents that evolved from either asymmetric waves to symmetric waves, or currents that evolved form

combined flow to purely oscillatory currents as the storms waned. Erosion during the accelerating part of

the events removed only the alpha mud layer, suggesting a nearly saturated currents.

ANOMALOUS GRADED BEDS. Tabular and wedge graded beds are the most abundant

anomalous graded beds in facies A. Planar and quasi-planar laminae record deposition from combined flow

currents with near bed orbital velocities greater than 65 cm/s and unidirectional components between 30

and 100 cm/s measured 10 m above the bed, Figure V.2. These bed configurations and velocities indicate

extreme sediment bypass. Hummocky ripples spaced more than 70 cm apart document deposition from

purely oscillatory currents with orbital velocities greater than 50 cm/s, and imply no sediment bypass. The

long low angle cross-laminae in the wedge graded beds record deposition from combined flow currents

with oscillatory velocities between 38 and 65 cm/s and a unidirectional component between 30 and 100 cm/

s measured 10 m above the bed, and record sediment bypass.

The great thickness and high velocity bedforms in the anomalous graded beds record deposition

from currents with higher initial depositional velocities and higher suspended sediment concentrations than

the currents that deposited the interbedded background graded beds. Since the wavy and lenticular graded

beds are interpreted to be the product of deposition from average storm events, then the anomalous graded

beds are interpreted to record deposition from currents generated by stronger than average storms. I call

these extreme storm events.

The common gutters and truncation surfaces underlying the anomalous graded beds in facies A

document pronounced erosion and sediment bypassing during the accelerating parts of the extreme storm

events. Long low angle, planar and quasi-planar laminae also record sediment bypassing during deposition.

DEPOSITION INSHORE OF THE STORM SURF ZONE. Applying my hydrodymanic interpretation to a permissible depositional environment, it is possible the background graded beds were deposited inshore of the average storm surf zone. By this scenario, deep water waves evolved to highly asymmetric waves, which then broke offshore, within the storm surf zone. After breaking the waves reformed into smaller, shorter period symmetric Airy waves that deposited the wavy and lenticular background graded beds. However, as the storms waned, the storm surf zone would have moved onshore, thereby eroding the sediment just deposited. Thus, it is not likely that the background graded beds in facies A were deposited inshore of the storm surf zone.

DEPOSITION OFFSHORE OF THE STORM SURF ZONE. The hummocky ripples in both the background and anomalous graded beds in facies A suggest deposition from storm currents that lacked strong unidirectional components. Furthermore, the oscillatory currents must have been generated by Airy waves. In general Airy waves become Stokes or cnoidal waves when $H/d = 0.2$ (Clifton et al., 1971) where H is the wave height and d is the water depth. Waves break in shallow water at $H/d = 0.78$ (Komar, 1976). Furthermore, the area offshore of the storm surf zone experiences declining current velocities as the storm wanes, permitting preservation of the graded bed. Thus, the hummocky ripples in the wavy graded beds most likely were deposited offshore of the storm surf zone during average storms.

DEPOSITION IN THE STORM SURF ZONE. Planar, quasi-planar and long low angle laminae in the anomalous graded beds record either wave asymmetry or strong combined flow currents. These laminae were probability formed by wave asymmetry induced by asymmetric or breaking waves within, or just offshore of the storm surf zone. Since the planar laminae and long low angle laminae are commonly overlain by hummocky ripples, the anomalous flow events must have evolved from strong, combined flow currents to weaker, nearly pure oscillatory currents. In some instances, this succession of laminae and bedforms probably record decreasing wave amplitude and the onshore migration of the surf zone as the

storm waned and wave heights decreased. In other instances, this succession may record the weakening of storm generated, geostropic currents induced by coastal setup and a change to wave dominated deposition.

The truncation surfaces that underlie many anomalous graded beds in facies A also suggest a location within the storm surf zone. The surf zone experiences the highest current velocities and most erosive currents (Komar, 1976; Blatt, Middleton and Murray, 1980). Also, the greatest amount of sediment transport occurs in the surf zone (Komar, 1976).

LACK OF MUD IN FACIES A. Background graded beds in facies A contain the thinnest mudstone layers of all the facies, commonly comprising less than 5 percent of the individual graded beds. The lack of mud in facies A can be accounted for by three hypothetical explanations: (1) The mud bypassed facies A and was deposited in an adjacent facies; (2) The flow events contained less than 5 percent mud in suspension; or (3) The storm events deposited a thick mud stationary suspension, but most mud in the stationary suspension was subsequently eroded and transported out of area by some other type of current.

There is no real way one can evaluate possibilities (2) and (3), but, mud bypass is not a probable explanation for the lack of mud in facies A. The form concordant laminae, Figure III.3, within the wavy and lenticular background graded beds indicate that the bedforms were either stationary or migrating very slowly through out sand deposition. Thus, since the water column was either stationary or moving very slowly, the mud in suspension at the onset of sand deposition could not have bypassed the site of deposition.

EROSION AND SEDIMENT BYPASS. The anomalous graded beds and sandstone beds resting on low angle truncation surfaces or with guttered bases in facies A record the removal of entire graded beds. The internal laminae in the anomalous graded beds record sediment bypass. The thinness of the

mudstone layers of the background graded beds indicates mud erosion. Thus, facies A was deposited at a site where episodes of major erosion induced by extreme storms were common, and moderate erosion by average storms was even more common. But, even though erosion was very common, facies A was dominated by deposition during average and extreme storm events. The large number of erosive events makes facies A a likely source area for the sediments in the other facies.

FACIES D

The most striking features of facies D are: (a) The extreme muddiness of the graded beds, commonly containing more than 90 percent mudstone; and (b) The thickness of the background graded beds, commonly over 10 cm. Table VII.1 presents an overview of facies D interpretations.

BACKGROUND GRADED BEDS. Continuous grading through the graded beds shows the sediment in facies D was deposited from individual decelerating flow events. The very common trochoidal ripples in the lenticular graded beds indicate deposition from oscillatory currents with orbital velocities between 16 to 24 cm/s. Slightly asymmetrical ripple forms, Plate 7-c, record deposition from oscillatory currents combined with a very weak unidirectional component.

The loaded background graded beds, common at some locations, indicate the transporting currents were not capable of eroding even very weak, alpha layer mud. This shows the currents were saturated with sediment when they reached the site of deposition. Thus, all of the sediment in the background graded beds in facies D must have originated at some other site.

The thickness of the background graded beds, up to 20 cm, combined with the low suspended sediment concentration, indicated by the low velocity bedforms, implies facies D was deposited in deep water. Deep water deposition is supported by the near total lack of erosional surfaces. Together, these features indicate deposition just above storm wave base.

ANOMALOUS GRADED BEDS. Large hummocky ripples in tabular graded beds,Plate 7-a, record deposition offshore of the storm surf zone, from purely oscillatory currents with orbital velocities greater than 50 cm/s. Common planar and quasi-planar laminae record combined flow currents with orbital velocities greater than 65 cm/s. Long low angle laminae record combined flow currents with orbital velocities greater than 38 cm/s. The more common sequence of planar laminae, or quasi-planar laminae. upward to large hummocky ripples to small trochoidal ripples records the evolution of the currents from a combined current to current dominated by oscillatory currents. This suggests sediment bypass occurred during the anomalous events, probably induced by geostropic storm currents combined with the oscillatory currents. It appears the geostropic currents waned to pure or nearly pure oscillatory currents as the storms waned. The symmetrical ripple forms, vertical climbing bedforms, high current velocities and great thickness of the anomalous graded beds all point to deposition from currents generated by extreme storm events. Deposition occurred in deep water, well above extreme storm wave base. This is consistent with background graded bed deposition from average storm generated currents.

EROSION AND SEDIMENT BYPASS. Loads at the bases of some tabular graded beds, Plate 7-a, show that the strong combined flow currents generated by extreme storm events were not able to erode very weak mud deposited during the previous event. This indicates that the anomalous currents were saturated, or very nearly saturated, with sediment before they reached the site of deposition.

The lack of erosion beneath the anomalous and background graded beds shows that the sediment deposited from the average and extreme storm generated currents must have come from a location other than facies D. The lack of erosion also implies that very little or no sediment bypassed facies D.

FACIES B

The main characteristics of facies B are the 50-50 sandstone/mudstone ratios and the thicknesses of the background graded beds. Anomalous graded beds are rare at most exposures of facies B; except

subfacies Bg which commonly contains over 50 percent anomalous graded beds. The following

hydrodynamic interpretations are for facies B in general, excluding subfacies Bg.

BACKGROUND GRADED BEDS. The following interpretation of the background graded beds

applies to both facies B and C because both facies contain the same types background graded beds.

However, the background graded beds in facies B are 2 to 15 cm thick and somewhat sandier than the

background graded beds in facies C which range from less than 1 mm to about 2 cm thick. Since the

morphology of the background graded beds is the same in both facies, then both facies were probably

deposited by the same types of currents. The principal differences between facies B and facies C are: (a)

Facies B was deposited from higher velocity currents; and (b) Facies B was deposited in deeper water.

Background graded beds in facies B and C contain two types of sedimentary structures indicating

deposition from two different types of currents. Facies B and C contain minor numbers of isolated

lenticular graded beds, recording deposition from oscillatory currents, probably produced by average storm

events. Facies B and C also contain very common even and shallowly scoured graded beds that record

deposition from current x.

The vertically climbing trochoidal and rounded trochoidal ripple forms in the rare lenticular

graded beds indicate orbital current velocities of 16 to 24 cm/s and 24 to 32 cm/s respectively. Concordant

internal laminae record pure oscillatory currents. Slight asymmetry and uniformly dipping internal laminae

in rare lenticular graded beds record oscillatory dominated combined currents. The moderate oscillatory

current velocities suggests deposition from waning storm generated currents. Note, these velocities are

lower than the current velocities that deposited the wavy and lenticular background graded beds in facies A,

which are interpreted as the deposits of currents generated by average storms. Thus, lenticular graded beds

in facies B and C may record deposition from smaller than average storms.

Primary sedimentary structures show that the shallowly scoured and even graded beds in facies B

and C were deposited from current x. Interpretation of current x was given in Chapter VI.K, and the

characteristics of current x are summarized on Table VI.2. Most even and shallowly scoured graded beds in

facies B contain massive bedding indicating rapid deceleration of the current. A few even and shallowly

scoured graded beds in facies B contain planar laminae (Winston, 1986 b) indicating deposition from

unidirectional currents greater than 80 cm/s or combined currents with orbital velocities greater than 65 cm/

s. Rare even and shallowly scoured graded beds in facies C contain small scale, high angle cross-laminae

indicating unidirectional currents with velocities between 17 and 80 cm/s. Thus, current x was a higher

velocity current in facies B than in facies C, and current x velocities were higher than those that deposited

the rare interbedded lenticular graded beds.

SUBFACIES Bg-ANOMALOUS GRADED BEDS. Anomalous graded beds are rare in facies B,

except in subfacies Bg. Tabular, wedge and long lens graded beds with guttered bases, are the most

common anomalous graded beds in subfacies Bg. Facies Bg also contains the same types of background

graded beds as facies B, recording deposition from current x.

The anomalous graded beds in subfacies Bg contain planar, quasi-planar or long low angle

laminae at the base of the sandstone layer which are overlain by massive bedding. The sequence of laminae

overlain by massive sandstone indicates the currents initially decelerated slowly and then decelerated

rapidly, Plate 3-c. Planar laminae, quasi-planar laminae and long low angle laminae record deposition from

high velocity combined flow currents. The fact that massive sand deposition is gradational into mud

deposition across a planar sandstone/ mudstone transition suggests that mud was initially deposited from

combined flow currents with oscillatory velocities greater than 38 cm/s.

Without symmetrical ripple forms, common in the anomalous graded beds in other facies, it is not

possible to prove the currents were generated by extreme storm events. The principal of parsimony suggests

the currents were probably generated by extreme storms. But, it is possible that the anomalous graded beds in subfacies Bg were deposited from a combination of current x and storm generated currents.

EROSION AND SEDIMENT BYPASS. Planar laminae and long low angle laminae in the background and anomalous graded beds show that the currents contained a strong unidirectional component. This suggests that facies B was the site of sediment bypass during both the extreme storm events and current x events. The vertically climbing ripple forms in the rare lenticular graded beds suggests little or no bypass during the average storm events.

The thick mud layers in the background graded beds also imply very little erosion of the mud layers. This is supported by the shallowness of the scours under the shallowly scoured graded beds and the lack of scours under the even graded beds. However, the lack of loads under the even graded beds show that the alpha mud layer was not eroded. The minor erosion by current x combined with its high velocity, suggests current x was nearly saturated with sediment.

The low amount of erosion under the even and shallowly scoured graded beds implies that the sediment in facies B and C did not come from facies B. Therefore, facies B was principally a site of bypass and deposition during current x and average storm events, but subfacies Bg was mainly a site of erosion and bypass during extreme storm events.

FACIES C

The principal characteristics of facies C are the thinness of its graded beds, ranging from less than 1 mm to about 2 cm thick, and the thickness of graded bed's mudstone layers which make up more than 65 percent of the individual graded beds. Otherwise, facies C contains the same types of background graded beds that comprise facies B. Table VII.1 contains a summary of facies C interpretations.

BACKGROUND GRADED BEDS. The same types of background graded beds occur in facies C as in facies B, they are just somewhat muddier and thinner in facies C than in facies B. Since the lenticular, even and shallowly scoured graded beds in facies C have the same morphologies as those in facies B, they were most likely deposited by the same types of currents as those that deposited these graded beds in facies B.

Facies C also contains very common sequences composed of microlaminated graded bed cosets. In thin-section, the microlaminated graded beds display the same morphologies as the even, shallowly scoured and lenticular graded beds. The principal differences are: (a) The combined thickness of the sandstone and mudstone layers in microlaminated graded beds is less than 0.3 mm; and (b) Even microlaminated graded beds are far more common than the shallowly scoured microlaminated graded beds. As in sequences composed of thicker graded beds, the lenticular microlaminated graded beds are rare. Since the microlaminated graded beds display the same morphologies as the thicker background graded beds, they are interpreted to have had the same origins. But, the increased numbers of even microlaminated graded beds at the expense of the shallowly scoured microlaminated graded beds suggests that the erosive power of current x was lower in the microlaminated graded beds.

Rare even microlaminated graded beds contain small scale, high angle cross-lamination. This type of cross-lamination shows that current x was probably a unidirectional current with velocities between 17 and 80 cm/s. This suggests the microlaminated graded beds were deposited from currents with lower velocities than those that deposited the thicker even and shallowly scoured graded beds. The thinness of the microlaminated graded beds also supports deposition from lower velocity currents, because low velocity currents can carry less suspended sediment.

In Chapter VI.L, I made the case the alternating high-low sandstone/ mudstone ratios and the lamina cycles were produced by the semi-diurnal tidal inequality (Dalrymple and Makino, 1989; Kvale et

al., 1989). I also linked the lamina cycles to neap-spring tidal cycles (Kvale et al., 1989; Brown et al., 1990; Kvale and Archer, 1991; Williams, 1989 a, 1989 b). These systematic changes in the sandstone/ mudstone ratios provide the most compelling evidence current x was driven by tidal processes. However, the presence of the lamina cycles and alternating high-low sandstone/ mudstone ratios is strongly contested (D. Winston, 1995, personal communication). If they do not exist, then there is no evidence for tidal currents in the Helena and Wallace formations.

ANOMALOUS GRADED BEDS. As is the case in the other facies, the anomalous graded beds in facies C record deposition from currents produced by extreme storms. Long lens and short lens graded beds, commonly with guttered bases, are the most common anomalous graded beds in facies C. Plate 5-e shows two long lens graded beds at about the middle of the photo, the lower one pinches out in series of symmetrical ripple forms. Also, the base of the lower long lens anomalous graded bed intersects the underlying graded beds at a low angle, producing a low angle truncation surface, and recording the presence of very powerful erosive currents. Long low angle laminae in the anomalous graded beds indicate most were initially deposited from high velocity combined flow currents indicating sediment bypassing, that then evolved into low velocity oscillatory currents with no sediment bypassing.

Facies C also contains common 10 to 30 cm deep erosion surfaces that are not overlain by an anomalous graded bed, as in facies A, B and D, but are overlain by more background graded beds. Several of these surfaces are shown on Plate 5-b, and 5-e. These erosion surfaces also document the presence of very powerful currents facies C. By inference, the currents that cut these surfaces were probably the same as those that produced the guttered surfaces under the long lens and short lens anomalous graded beds.

Together, the erosion surfaces without an overlying anomalous graded bed and the erosion surfaces beneath the long lens and short lens graded beds record the activity of extreme storm events. But,

the currents in facies C appear to have been more sand and silt starved than comparable currents in facies A and D and subfacies Bg.

EROSION AND SEDIMENT BYPASS. The high mud content of facies C suggests that erosion during the accelerating parts of current x was less important than in facies B and A. Also, the larger number of even graded beds in facies C, relative to facies B, documents less erosion during current x events in facies C than in B.

However, the truncation surfaces without an overlying anomalous graded bed and the truncation surfaces under some anomalous graded beds indicate that facies C acted as a source area during extreme storm events. Thus, facies C was mainly a site of sediment deposition during the background events, and mainly the site of erosion during the extreme storm events.

The main differences between current x and the average storm currents are: (a) Current x was a unidirectional or combined current, but the storm currents were oscillatory currents; (b) Current x had a much higher recurrence frequency than the average storm currents; and (c) Current x decelerated faster than the average storm currents. But, current x and the average storm generated currents carried about the same amount of sediment in suspension.

DEPOSITIONAL ENVIRONMENTS

INTRODUCTION

This chapter integrates the hydrodynamic interpretations of primary sedimentary structures, the thickness and sandstone/ mudstone ratios, and the type, magnitude and frequency of the depositional events into a depositional environment systems tract. The goals are: (1) Determine the approximate water depth range for each facies. (2) Establish the relative positions of the facies based on their depths of deposition. (3) Establish the principal driving mechanism behind the currents responsible for sediment transport and deposition, and (4) Based on the driving mechanisms behind the currents, determine the depositional environments of the facies. The principal tools for interpretations are the types of currents, the relative magnitude of the events, the relative frequency of the events and estimates of suspended sediment concentrations.

Altogether, the hydrodynamic interpretation leads to the conclusion that the sediment in the Helena and Wallace formations was deposited in two distinct environments. The evidence shows facies A and D were deposited in a moderate to deep water, shelf-like environment that was dominated by average and extreme storm events. Less compelling evidence suggests facies B and C were deposited in a shallower environment dominated by tidal currents. But, tidal deposition in facies B and C was periodically punctuated by deposition from average and extreme storm events.

Depositional environments are geomorphic or physiographic units, defined by a particular set of physical, chemical and biological processes (Blatt, Middleton, and Murray, 1980, p. 617; Boggs, 1987, p. 305). These processes produce a characteristic set of physical primary sedimentary structures, secondary sedimentary structures, chemical products, biological structures and biologic remains. Thus, interpreting of

138

a set of products in an interval of ancient rocks should yield a set of physical, chemical and biological processes that are unique to a particular physiographic unit.

Grotzinger (1981), Winston, Woods and Byer (1984), Winston (1986 b; 1989; 1991) and Winston and Link (1993) determined that the lithologies, depositional processes and stratigraphic sequences found in the Helena and Wallace formations compared favorably with the sedimentary structures, depositional processes and the succession of lithologies found in lake environments. Winston, Woods and Byer (1984) and Winston (1986 b) decided against a tidal environment based on the lack of features commonly included in the tidal environment model. But, O'Connor (1967) and Eby (1977) concluded that the Helena and Wallace sediments compared well with a tidal depositional model. No previous authors suggested the Helena and Wallace formations were deposited on a storm dominated shelf environment.

Sedimentology by analogy is broadly accepted (Walker, 1979; 1984; 1992 a; Collinson and Thompson, 1989; Anderton, 1985). The basic premise behind the approach is that one or several facies models serve as: (1) a norm for purposes of comparison; (2) a framework for future observations; (3) a predictor in new geological situations; and (4) an integrated basis for interpretation for the system that it represents (Walker, 1992 a, p. 7). However, this thesis evaluates how much information one can gather about the depositional environments from the hydrodynamics of the currents, then places those hydrodynamic interpretationsinto a depositional environment framework.

ABSOLUTE WATER DEPTHS AND RELATIVE POSITIONS OF THE FACIES

The primary current structures and the thicknesses of the background graded beds suggest the four facies were deposited in different water depths. The suggested absolute water depths presented below are based on the hypothetical average suspended sediment concentration of the depositing currents, listed on Table VIII.1, and the measured thicknesses of the background graded beds within each facies, listed on Table VIII.2.

Table VIII.1. Hypothetical average suspended sediment concentrations. ASSC-average suspended sediment concentration.

facies-type graded bed	current type	velocity (cm/s)	ASSC (g/l)
A-wavy	oscillatory	24-32	5
		32-38	8
A-lenticular	combined	38-65	10
A-wedge	combined	38-65	10
A-tabular	oscillatory	≈ 60	17
B-even	unidirectional	≈ 80	5
B-shallowly scoured	unidirectional	≈ 80	5
B-lenticular	oscillatory	24-32	5
C-microlaminated			
even	unidirectional	17-80, ≈ 20?	1?
sh. scr.*	unidirectional	17-80, ≈ 20?	1?
lenticular	oscillatory	16-24	1
C-even	unidirectional	17-80, ≈ 50?	3?
C-shallowly scoured	unidirectional	17-80, ≈ 50?	3?
C-lenticular	oscillatory	16-24	1-3
C-long lens	oscillatory	32-38	7-10**
C-short lens	oscillatory	16-24	2**
		24-32	5**
D-lenticular	oscillatory	16-24	1-2
D-loaded	oscillatory	16-24	1-2
D-tabular	oscillatory	≈ 60	17
D-wedge	oscillatory	38-50	10-13

* sh. scr. = shallowly scoured graded beds.

** Sediment starved anomalous graded beds, resting on a truncation surface. Erosion velocities probably much higher than initial depositional velocities.

Table VIII.2. Water depths of the facies. Depths are based on the assumed average suspended sediment concentrations (ASSC) of currents that deposited the background graded beds, given on Table VII.1

DEPTH CALCULATION

Load = bed thickness * bed density (assumed to = 2400 kg/m^3)
Depth = load / concentration.

facies	thickness (cm)	ASSC (kg/m^3)	load (kg/m^2)	depth (m)
A	background 7-15	5	168-360	30-50
	anomalous ≈ 30*	17	720	42
B	background 2-15	5	48-360	10-50
C***	0.01-0.3	1	2.4-48	2.4-48
	anomalous 5-15	5	120-360	24-72
D	background 5-20	2	120-480	60-240
	anomalous ≈ 45**	17	1080	64

* Anomalous graded beds in facies A range from 20 to 45 cm thick. Most show evidence of sediment bypass. The thin mudstone layers also suggest subsequent mud re-suspension.

** Anomalous graded beds in facies D range from 5 to 45 cm thick. The 45 cm thickness was used because one example contained hummocky ripples, indicating no sediment bypass. Thinner anomalous graded beds usually contain long low angle cross-laminae, indicating bypass.

*** Facies C depths based on the thickness of the microlaminated graded beds.

**** All thicknesses assume no erosion or sediment bypassing.

AVERAGE SUSPENDED SEDIMENT CONCENTRATION. Average suspended sediment

concentration is a function of the size material available to the current, the bed shear stress and the bed

roughness. Bed shear stress is a function of the current's velocity and the type of current: both of which

can be estimated from the type of bedforms and laminae in the sandstone layers of the graded beds.

Chapter V.G provides a complete discussion on estimating the average suspended sediment concentration.

Table VIII.1 lists the hypothetical average suspended sediment concentrations for the different types of

graded beds in the different facies. The average concentrations are based on the bedforms and laminae

commonly found within the graded beds in the facies, given on Table V.2.

Given the theoretical problems of estimating a current's average concentration, estimates of the

average concentrations are only hypothetical, and only poorly constrained by measurements from modern

environments. I assume the suspensions contain a mixture of very fine-grained sand, silt and clay.

SUSPENDED SEDIMENT LOAD. The total thickness of a graded bed, assuming no sediment

was removed by erosion during a subsequent flow event, indicates the total suspended sediment load of the

event. The suspended sediment load is the product of the average concentration, as estimated by the initial

depositional velocity, and the water depth or the current's thickness if the flow event was a turbidity current

or an underflow. By inferring the average concentration from the initial depositional velocity, the water

depth can be estimated from the thicknesses of the background graded beds.

According to diffusion theory (Blatt, Middleton and Murray, 1980, p. 114-116; Hiscott, 1994) the

average suspended sediment concentration depends only on the velocity of the current and the size material

in suspension, and is independent of the flows depth. But, a current in 10 m deep water that deposits its

entire load instantly will deposit a bed ten times thicker than the same velocity current in 1 m deep water

that deposits its load instantly because the total sediment load of the current is the product of the depth and

the average suspended sediment concentration. Thus, given deposition from currents with the same

velocities and same average suspended sediment concentrations, the thickness of the deposited graded bed

is a direct function of the water depth.

WATER DEPTHS. Table VIII.2 gives the hypothetical depths of the facies, using the observed

graded bed thicknesses and the hypothetical suspended sediment concentrations for the different current

types and current velocities shown on Table VIII.1. The suspended sediment load L is equal to the

thickness T of the graded bed times the bed's density p, estimated at 2400 kg/m^3, and assuming no

sediment bypass at the depositional site and no subsequent erosion.

$$L = T * p \,,(VII.1)$$

where the load is the mass of sediment suspended over each square meter of bottom (kg/m^2). The

water depth d is equal to the suspended load divided by the average suspended sediment concentration C.

$$d = L / C \,.(VII.2)$$

Based on the average suspended sediment concentrations and the thickness of background graded

beds, facies D was deposited in the deepest water, and facies A was deposited in the next deepest water.

Table VIII.2 suggests facies C was deposited in the shallowest water, and depending on the concentrations,

the depositional depths of facies C overlap with facies B, which overlaps with facies A which may overlap

with facies D. The water depths indicated by the anomalous graded beds in the facies are consistent with

those indicated by the background graded beds. This shows the hypothetical average concentrations listed

on Table VIII.1 are at least internally consistent.

RELATIVE POSITIONS OF THE FACIES. The range of the depths of the facies are plotted

on Fig. VIII.1, and it also places the facies in their probable positions relative to the shore line. The

suggested relative positions of facies A, B and C shown in Figure VIII.1 are supported by their stratigraphic

relationships. Winston (1986 b) and Winston, Woods and Byer (1984) placed the microlamina sediment

type, equivalent to the microlaminated graded beds in facies C, in a deeper water environment than the other facies. Winston (1989; 1991;1993) and Winston and Link (1993) revised this interpretation, suggesting facies A deposition occurred in deeper water than facies B, and facies C deposition occurred in the shallowest water. This interpretation agrees with O'Connor (1967). Also, none of these authors recognize facies D as a separate facies from facies C.

DEPOSITION OF FACIES A AND D
IN A STORM DOMINATED ENVIRONMENT

The current types, current velocities and the calculated water depths provide compelling evidence that facies D deposition occurred offshore of facies A. Also, the evidence shows that the background and anomalous graded beds in both facies were deposited from storm generated currents. Since both facies are dominated by symmetrical bedforms deposited from wave generated currents, then both environments must have been in a standing body of water, within storm wave base but offshore of the storm and fair-weather wave build-up and surf zones. Only a storm dominated environment satisfies all these restrictions.

Figure VIII.2 shows a diagrammatic cross-section of a modern siliciclastic shelf environment, compiled from Clifton et al. (1971), Elliott (1986) and Johnson and Baldwin (1986) with snady shore lines. Wells and Coleman (1981) and Hill and Nadeau (1989) present a different model for muddy shore lines. The probable depositional sites of facies A and D are based on the calculated water depths of deposition of the background graded beds shown on Table VIII.2.. The depth and lateral ranges for the large hummocky ripples produced by 65 cm/s oscillatory currents predicted from the wave equations, Chapter V.K, are also shown. Large hummocky ripples occur in the anomalous graded beds in both facies, and they provide an independent estimate of the range of permissible water depths. Note that the water depths predicted by the thicknesses of the graded beds are consistent with the permissible depths of formation of large hummocky ripples.

Figure VIII.1.
Relative positions of the facies and the depths of formationn of the surf zones.
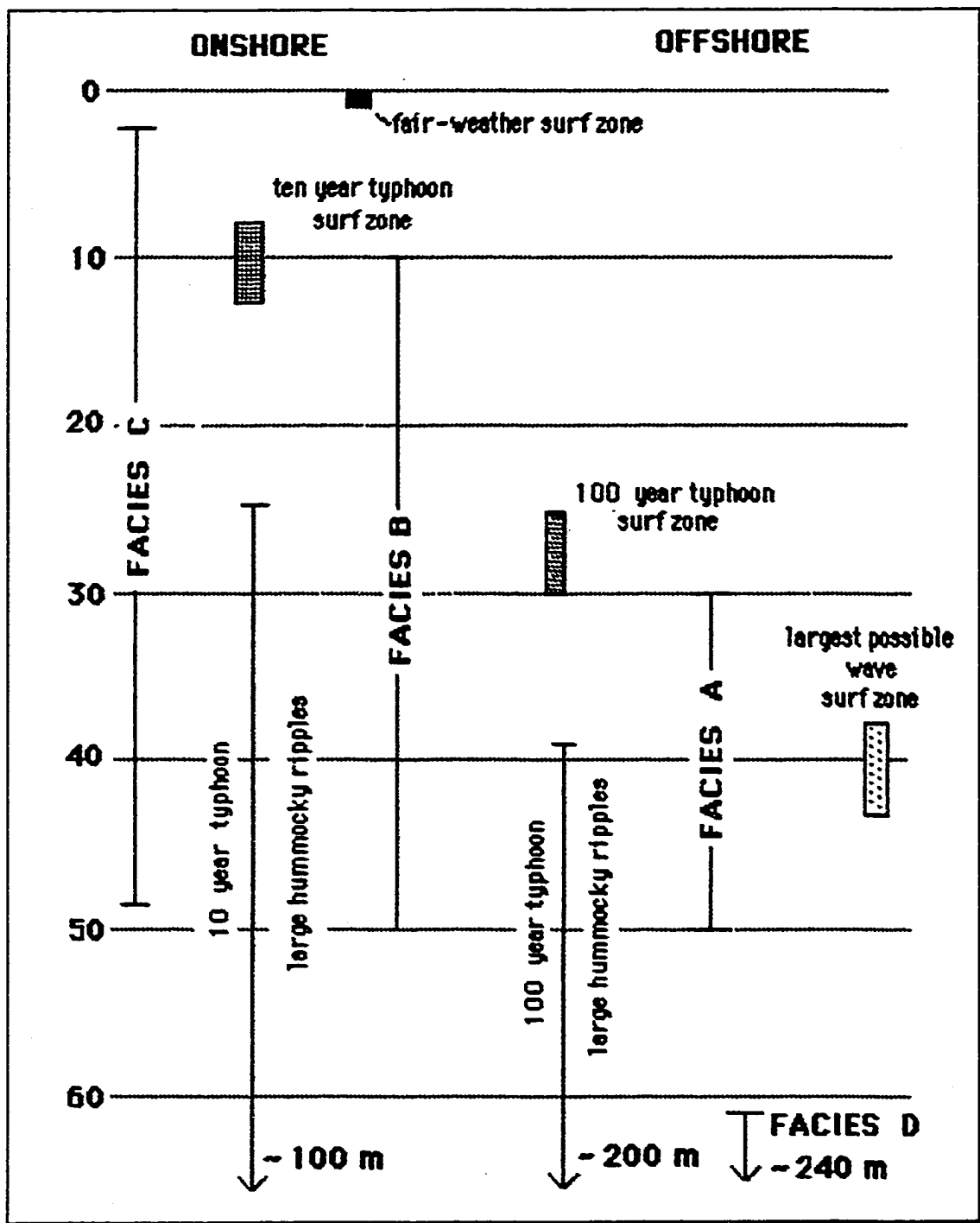
FACIES A. The very common small hummocky ripples in facies A provides an independent evaluation of the water depth. Small hummocky ripples record oscillatory currents with velocities between 32 and 38 cm/s. Assuming that the waves were produced by a storm equivalent to a typical Yellow Sea cold front, Airy wave equations show that these bedforms most likely formed in water between 4 and about 50 m deep, Figure V.4. This agrees reasonably well with the 30 to 50 m deep estimate based only on the thickness of the background graded beds.

Facies A was deposited offshore of the shoreface and shoreface transition because storm waves are asymmetric in these zones. The fair-weather wave build-up zone occurs in the shoreface shown on Figure VIII.2. Asymmetric oscillatory current ripples form in the wave build-up zone (Clifton et al., 1971), and record the sediment deposition from Stokes waves. Vertically climbing, small, medium and large hummocky ripples in the graded beds record deposition from strong oscillatory currents combined with less than 2 cm/s near bed unidirectional currents, and rule out formation under Stokes or cnoidal waves. Thus, facies A must record deposition offshore of the shoreface. Furthermore, the lack of evidence for sediment reworking and deposition from small waves in facies A also supports deposition offshore of the fair-weather wave base.

Storm waves start building up and becoming asymmetric in deeper water than fair-weather waves; hence the formation of asymmetric waves and bedforms moves offshore during storms. The depth at which wave build-up begins is a function of the deep water wave height and wave length. The wave build-up zones during an average cold front, 10 year and 100 year typhoons in the Yellow Sea are also shown on Figure VIII.2. As shown, the zone of breaking waves also moves offshore with increasing wave heights and lengths.

Elliott (1986) defined the offshore-shoreface transition boundary as the location of mean storm wave base. The offshore-shoreface transition boundary occurs at different water depths along different

coasts and is a function of the wave environment of the coast. On the Georgia shelf the transition occurs in water about 10 m deep, it occurs in water about 18 m deep on the California shelf, and about 100 m deep on the Bering shelf (Johnson and Baldwin, 1986).

The high oscillatory current velocities and the inferred high suspended sediment concentrations in the background graded beds in facies A provide compelling evidence for facies A deposition inshore of facies D. Medium hummocky ripples can only form under large waves that induce moderate oscillatory current velocities on the bottom. The lack of medium hummocky ripples in the background graded beds in facies D shows this interaction did not occur in facies D. The deep erosion indicated by the truncation surfaces observed in facies A and the lack of such surfaces in facies D also suggest facies A was deposited in shallower water than facies D.

FACIES D. Three characteristics of the background and anomalous graded beds in facies D provide compelling evidence that facies D was deposited offshore of facies A. First, the background graded beds in facies D were deposited from lower velocity oscillatory currents than those that deposited the background graded beds in facies A. Second, the average suspended sediment concentrations in facies D are lower than the implied average suspended sediment concentrations in facies A. Third, thick background graded beds coupled with low concentrations strongly imply facies D deposition in deeper water than facies A.

Finally, the lack of erosion during the accelerating part of the average and extreme storm events in facies D shows that the sediment transported by the currents must have originated elsewhere. That is, facies D acted as a sediment sink; once the sediment was deposited it was rarely, and at some locations never, re-suspended. As shown, facies A was the site of erosion during average and extreme storm events. Thus, the degree of erosion during the accelerating parts of the current generating events support the interpretation that facies D was deposited offshore of facies A.

Figure VIII.2.
Diagramic cross-section of modern siliciclastic shelves and the probable depositional environments of facies A and D.

AVERAGE STORM, period = 10 s, height = 5 m

10 YEAR STORM, period = 15 s, height = 9 m

100 YEAR STORM, period = 20 s, height = 13 m

surf zone

0 m

50 m

100 m

FACIES A

FACIES D

——— AIRY WAVES

— — AIRY WAVE BUILD-UP, large hummocky ripples

· · · STOKES WAVES, asymmetric forms, planar laminae, quasi-planar laminae

① ② ③ ④ ⑤ ⑥

① = subaerial environments

① = backshore

② = foreshore: zone between mean high water and mean low water

③ = shoreface: zone between mean low water and fair-weather wave base, 2 to 9 m deep, slope = 1:200

④ = shoreface transition: zone between fair-weather wave base and storm wave base, slope = 1:2000

⑤ = offshore: zone between fair-weather wave base and shelf break, shape = 1:2000

It is possible that facies D was deposited in a protected shallow water lagoon-like environment. In this model large storm waves would be broken in some other environment, and facies D experienced only low velocity currents, with low suspended sediment concentrations. But, at most locations facies D contains tabular, wedge or long lens anomalous graded beds interbedded with the background graded beds that contain internal structures produced by high velocity, symmetrical oscillatory currents. These structures clearly show facies D was the site of high amplitude, long period waves, since these structures could not have been produced by broken waves.

DEPOSITION OF FACIES B AND C IN A TIDE DOMINATED ENVIRONMENT

In this section I will show that facies B and C were probably deposited in a tide dominated environment that also experienced deposition during less frequent storm events.

EVALUATION OF A TIDAL CURRENT ORIGIN FOR CURRENT X. As shown, the systematic changing sandstone/ mudstone ratios in the microlaminated graded beds may have been produced by systematic changes in tidal currents. Given the similarities in morphologies between the microlaminated even and shallowly scoured graded beds and the thicker even and shallowly scoured graded beds in facies B and C, the thicker ones were also probably deposited from current x. However, D. Winston (1994, personal communication) feels that the lack of tidal channels in the Helena and Wallace formation shows the absence tidal currents and tidal processes.

In addition, four other features of facies B and C also suggest that current x was a tidal current: (1) Current x was a higher velocity current offshore in facies B than onshore in facies C. (2) The sandstone/ mudstone ratios decrease from facies B to C, in an onshore direction. (3) The graded beds thin from facies B to C, in an onshore direction, and (4) Current x had a higher recurrence rate than either the average or extreme storm events. Table VIII.3 lists the characteristics exhibited by the even and shallowly scoured graded beds and their origin as explained by tidal currents.

The thicker graded beds deposited from tidal currents are called tidal bedding, and thinner graded beds, equivalent to the microlaminated graded beds, are called tidal rhythmites (Reineck and Singh, 1980). Deposition of tidal rhythmites takes place in the shallower parts of tidal environments at the same time tidal bedding is deposited in the deeper parts (Reineck, 1967 a; Thompson, 1968; Klein, 1970; Knight and Dalrymple, 1975; Larsonneur, 1975).

Onshore thinning and fining of tidal bedding and tidal rhythmites are attributed to two characteristics of tidal systems. First, the maximum tidal current velocities occur in the middle of the tidal environment and lower velocity currents occur in both the deeper and in the shallower parts of the tidal environment (G. P. Allen, 1991). This feature is responsible for depositing sand in the highest energy part of the environment and the thickest and highest sand/ mud ratio graded beds onshore of the highest energy part of the environment. The onshore decreasing thickness and sand content of the tidal bedding result from the decreasing maximum current velocities, lower average suspended sediment concentrations and shoaling across the environment. Some sedimentation may involve settling lag (van Straaten and Kuenen, 1958; Postma, 1967) which also produces onshore fining across tidal flats.

Preservation is the second characteristic of tidal environments controlling the onshore thinning and fining of tidal deposits. Preservation of tidal bedding and tidal rhythmites results from scour lag (van Straaten and Kuenen, 1958; Postma, 1967). According to this model, the flood tidal currents in tidal environments are commonly stronger than ebb tidal currents (G. P. Allen, 1991). Thus, the accelerating part of the ebb currents are not strong enough to erode the beta and gamma mud layers deposited during the decelerating part of the flood currents. This induces net lateral and vertical accretion of the tidal environment, and tide flats prograde under conditions of low subsidence rate and high sediment supply rate.

However, D. Winston (1994, 1995, personal communications) feels that the lack of recognizable tidal channels precludes the application of tidal processes to deposits in the Helena and Wallace formations.

Table VIII.3. List of characteristics of facies B and C. and their origins as explained by deposition from tidal currents.

characteristic	origin
• decreasing thickness of graded beds from facies B to C	• current velocities decrease landward • lower suspended sediment concentration • shallower water
• increasing mud content of the graded beds from facies B to C	• current velocities decrease landward • settling lag model • scour lag model
• higher velocity currents in facies B	• current velocities decrease landward across tidal environment
• lower velocity currents in facies C	• current velocities decrease landward across tidal environment
• higher frequency of deposition from current x than from average storm-generated currents	• 2 tides per day verses 1 storm per week
• lamina-cycles in microlaminated graded beds	• neap-spring tidal cycles induced by orbital mechanics
• alternating high-low sandstone/ mudstone ratios in microlaminated graded beds	• semi-diurnal tidal inequality induced by orbital mechanics

"The ubiquity of [tidal] channels in modern tidal environments indicates to me that tidal flow forms

channels, just like fiver flow does, and that the formation of channels is an intergral part of tidal flow. . ."

(D. Winston,1995, writen communication). D. Winston (1995, writen communication) feels that the

absence of recognizable channels means that I can not apply the other tidal processes to the deposits in the

Helena and Wallace formations.

STORM DEPOSITION. As shown in Chapters VI.G and VI.H, the rare lenticular graded beds

reflect deposition from less frequent average storm generated currents, and the anomalous graded beds

reflect deposition from very rare extreme storm generated currents. Storms in tidal environments are

common and many of the features common in tidal environments were produced by storm generated

currents. For instance, Reineck and Singh (1980, Figs. 193, 194 and 195, p. 117) show lenticular bedding

from North Sea tidal flats. Many of the ripple lenses in the photographs are symmetrical ripple forms, with

either concordant or discordant internal laminae and clearly record deposition from pure oscillatory

currents or oscillatory current dominated combined currents.

The relatively low number of oscillatory current events interbedded with the very high number of

current x events also suggests current x was driven by tidal mechanics. Tidal systems experience from 1 to

2 high waters in a 24 hour period (Archer et al., 1991), but winter storms commonly only occur once every

3 to 4 days. Thus, tidal currents have the potential to produce many more graded beds than typical winter

storms.

FACIES B. The background graded beds in facies B have greater thickness, higher sandstone/

mudstone ratios and coarser grain sizes than those in facies C. All these features indicate deposition of

facies B in a higher energy environment, and in deeper water than facies C. The total lack of desiccation

cracks in facies B suggests the sediments were never exposed. Thus, I place facies B in the subtidal zone of

the tidal environment.

FACIES C. Conversely. facies C was deposited in shallower water. from lower velocity currents

than facies B. At the very minimum these features are permissive of a tidal environment. The lamina-

cycles and the alternating high-low sandstone/ mudstone ratios in the microlaminated graded beds implicate

tidal mechanics in their formation. Given the occurrence of very rare desiccation cracks in facies C

(Winston and Lang,1977), I infer the facies experienced only infrequent or very short periods of exposure

(Amos et al.. 1988). Thus, I place facies C in the deepest part of the intertidal zone of the tidal

environment.

DISCUSSION

INTRODUCTION

In the previous chapters. I have shown that facies A and D were deposited in a wave dominated environment. Facies A was a very high energy environment, where erosion was common. Facies D was deposited in a low energy wave environment that acted as a sediment sink. I also showed that facies B and C were deposited in an environment dominated by a very frequent unidirectional or combined current events, current x, but oscillatory current events were rare. Very rare centimeter scale thick sequences of even microlaminated graded beds that display lamina cycles or alternating high-low sandstone/ mudstone ratios in facies C. The changes in sandstone/ mudstone ratio suggest neap-spring and semi-diurnal tidal mechanics may have been responsible for current x. Based on similarities in morphology and internal structures, I then inferred that thicker even and shallowly scoured graded beds in facies B and C were also deposited from tidal currents.

Arguments for a tidal environment for facies B and C hinge on the origin of the microlaminated graded beds and the driving mechanism for current x. In this chapter I discuss some of the previous interpretations for the origin of current x and the origin of the microlaminated graded beds.

In the second part of this chapter. I present a hypothetical environmental systems track that describes the processes operating in each environment. The systems tract model places facies D and A in an offshore, storm dominated environment, and facies B and C in a tidal environment. The problem with this systems tract model is that it juxtaposes a storm dominated shelf with a tidal environment, without an intervening beach or barrier island environment.

- 154

INTERPRETATION OF MICROLAMINATED GRADED BEDS

The microlaminated graded beds form some of the most distinctive sequences in the Helena and Wallace formations (Winston 1986 a; 1986 b; Grotzinger, 1981). Microlaminated graded beds also occur in the St. Regis, Empire , Snowslip and Shepard formations (Winston, 1986 b; 1989; Winston and Link, 1993; Woods, 1986; Ackman, 1988; Lemoine, 1979). Interpreting the origin of the microlaminated graded beds is critical to interpreting the depositional environment of facies B and C.

Recall that the microlaminated graded beds are composed of very common even graded beds and common shallowly scoured graded beds, interbedded with rare lenticular graded beds. But, the microlaminated graded beds are less than 0.3 mm thick. The even and shallowly scoured varieties of microlaminated graded beds where deposited by current x, which was either a unidirectional or combined current. The lenticular variety records deposition from average storm generated currents in shallow water.

The even and shallowly scoured varieties of the microlaminated graded beds have also been interpreted as the deposits of turbidity currents operating in a lake, and as oil shale deposits. Suggested water depths range from deep, in the center of the lake, to shallow and periodically exposed. The previous interpretations of the water depths, sediment transport mechanisms, and depositional environments for the microlaminated graded beds and their authors are shown on Table IX.1.

Winston (1986 b, p. 100) identified three varieties of microlamina sediment type. (1) Millimeter scale graded beds composed of siltstone laminae, overlain by carbon-poor, hematite rich or hematite poor claystone laminae which form red (hematitic) or greenish gray (hematite absent) very thinly laminated intervals. (2) Carbonate rich graded beds composed of tan or yellowish gray weathering dolomitic siltstone layers overlain by calcareous claystone layers; and (3) Carbonaceous graded beds composed of siliciclastic siltstone layers overlain by carbonaceous claystone layers that forms thinly laminated black outcrops. The microlaminated graded beds in the Helena and Wallace formations are approximately equivalent to

Table IX.1. *Water depths, sediment transport mechanisms, and depositional environments for the microlaminated graded beds proposed in previous studies. The microlaminated graded beds of this report equal "black siltite-argillite rock type" of Lemoine (1979); "microlaminated rock subtype" of Grotzinger, 1981; "dolomite laminated subfacies" and "dolomite blob subfacies" of O'Connor, 1967; "microlamina sediment type" Winston (1986 b; 1989;1991) and Winston and Link (1993).*

water depth	depositional mechanism/ environment	reference
deep	suspension settleout-turbidity currents implied	Grotzinger (1981, p. 18)
deep	suspension settleout-turbidity currents	Lemoine (1979. p. 42)
deep	analogous to oil shale formation in lakes	Winston et al. (1984)
deep	analogous to oil shale formation in lakes	Winston (1986 b, p. 118)
shallow	suspension settleout in intratidal to supratidal zone	O'Connor (1967, p. 149)
shallow	analogous to oil shale formation in lakes	Woods (1986)
shallow	distal interflows, underflows and turbidity currents in lakes	Winston (1989, p. 61)
shallow	analogous to oil shale formation in lakes	Winston (1991, p. 551)
shallow	no transport mechanism-suspension settleout in lakes	Winston (1993)
shallow	analogous to oil shale formation in lakes	Winston and Link (1993)Table

Winston's carbonate rich microlamina sediment type and the carbonaceous microlamina sediment types. Greenish gray microlaminated graded beds are very rare, and the red variety does not occur in the Helena and Wallace formations.

SHALLOW VERSES DEEP WATER DEPOSITION. Based on the lack of oscillation ripples, Grotzinger (1981) and Lemoine (1979) suggested that the microlaminated rock subtype was deposited in deep water, below wave base. Winston, Woods and Byer (1984, p. 110) and Winston (1986 b, p. 118) also suggest that the microlamina sediment type was deposited in deep water. by pelagic settling of siliciclastic material and algal growth.

Other authors favor shallow water deposition. Based on the scour surfaces that separate microlamina cosets. Woods (1986, p. 48), Winston (1991) and Winston and Link (1993) suggested microlamina sediment type deposition took place in water shallower than storm wave base. Also. O'Connor (1967). Winston (1989: 1993) and Winston and Link (1993) used stratigraphic relationships to place deposition of the microlaminated graded beds in shallow water.

I agree with the shallow water interpretation. The thickness of the other types of graded beds in facies C, the interbedded scour surfaces, and the rare lenticular graded beds, indicate the microlaminated graded beds were probably deposited in the shallowest water environment preserved the Helena and Wallace formations. But, the near absence of desiccation cracks imply little or no exposure. Green and red microlaminated graded beds in the overlying Snowslip formation contain common desiccation cracks that imply exposure (Ackman, 1988).

OTHER ARGUMENTS FOR A TIDAL ENVIRONMENT

Other authors, using analogy with tidal depositional environment models, interpreted the Helena

and Wallace formations as tidal deposits. Their arguments are based on: (1) similarities in sedimentary structures, (2) similarities in bedding style, or (3) similarities in stratigraphy.

EVIDENCE FROM SEDIMENTARY STRUCTURES. Horodyski (1983; 1976 a) interpreted the Siyeh [Helena] Formation in Glacier National Park as tidal deposits. Horodyski based his interpretation on the occurrence of coarse oolitic beds containing herringbone cross-stratification, the presence of wavy bedding and reactivation surfaces. Whipple and Johnson (1988) also interpreted the Helena Formation in Glacier National Park as tidal deposits based on the presence of oolite beds with herringbone cross-stratification. However, Winston and Lyons (1993) interpreted these deposits to be beaches and shoals with foreshore and washover crossbeds.

Herringbone cross-stratification is a process produced structure that record high velocity currents, that transported medium to coarse-grained sand and produced large scale bedforms (Klein, 1977). Foreset laminae on the bedforms in adjacent beds dip in opposite directions, recording reversing transport directions due to flood and ebb tides (Klein, 1977).

EVIDENCE FROM BEDDING STYLE. O'Connor (1967) used the thinness and morphology of the microlaminated graded beds to interpret the Helena depositional environment as tidal deposits. O'Connor (1967, p. 149) concluded the dolomite laminated subfacies, equivalent to the microlaminated graded beds in facies C, was deposited in a supratidal environment based on an analogy with Andros Island tide flats.

STRATIGRAPHIC EVIDENCE. The stratigraphy of the transition of Helena Formation to the Snowslip Formation indicates increasing exposure across the contact (O'Connor, 1967). Increasing exposure is consistent with a transition from very low in the intertidal zone (Helena and Wallace formations) to moderately high intertidal zone (Snowslip Formation). The gray, uncracked microlaminated

graded beds near the top of the Helena and Wallace formations grade upward into green, mudcracked

microlaminated graded beds and interbedded green mudchip conglomerate beds of the Snowslip formations

(O'Connor, 1967; Ackman, 1988; Lemoine, 1979). O'Connor used this as evidence for a tidal environment.

The color change and the increase in desiccation cracks indicates increased exposure, and the

microlaminated graded beds indicates continued deposition from current x. The gray color and lack of

mudcracks in the Helena and Wallace formations suggests that the uncracked gray microlaminated beds

were deposited in the deep intertidal zone, where evaporation from the mud flats is minimal (Amos et al.,

1988) and oxidation of organic material is low (Potter et al., 1980).

The green mudcracked microlaminated graded beds in the overlying Snowslip formation are

consistent with deposition in a more exposed, higher intertidal environment. The green color is induced by

the clays in the absence of carbonaceous material and hematite (Potter et al., 1980). Oxidation apparently

was sufficient to remove the carbonaceous material but not sufficient to form hematite.

DEPOSITIONAL ENVIRONMENT SYSTEMS TRACT

The thickness of the graded beds and the sedimentary structures in the graded beds suggest the

facies were deposited in different depths of water, shown on Figure VIII.1. The water depths of the facies

imply the position of each facies, relative to the others. Thus, combining the water depths, types of currents

and the current velocities produces a theoretical depositional environment systems tract. Figure IX.1

displays the basin margin showing the theoretical depositional environment systems tract and the locations

of the facies. The processes and products of the systems tract are listed in Table IX.2.

The environmental systems tract places facies B and C in a tide dominated environment, based on

the inconclusive evidence that current x was a tidal current. But, the data strongly support my conclusion

that facies A and D deposition occurred in wave dominated environments. The theoretical systems tract and

Figure IX.1
Diagrammatic cross-basin profile showing the locations of the facies and subfacies, and the hypothetical depositional environment systems tract.

increasing velocity

maximum tidal current velocity

large storm surf zone

extreme storm surf zone

principal zones of longshore sediment transport

E1   E2   E3   Bg   Ab   E4   E5   Aw   E6   B   C

D

depositional environment

facies

stationary suspensions formed by tidal currents

stationary suspensions formed by large storms

stationary suspensions formed by extreme storms
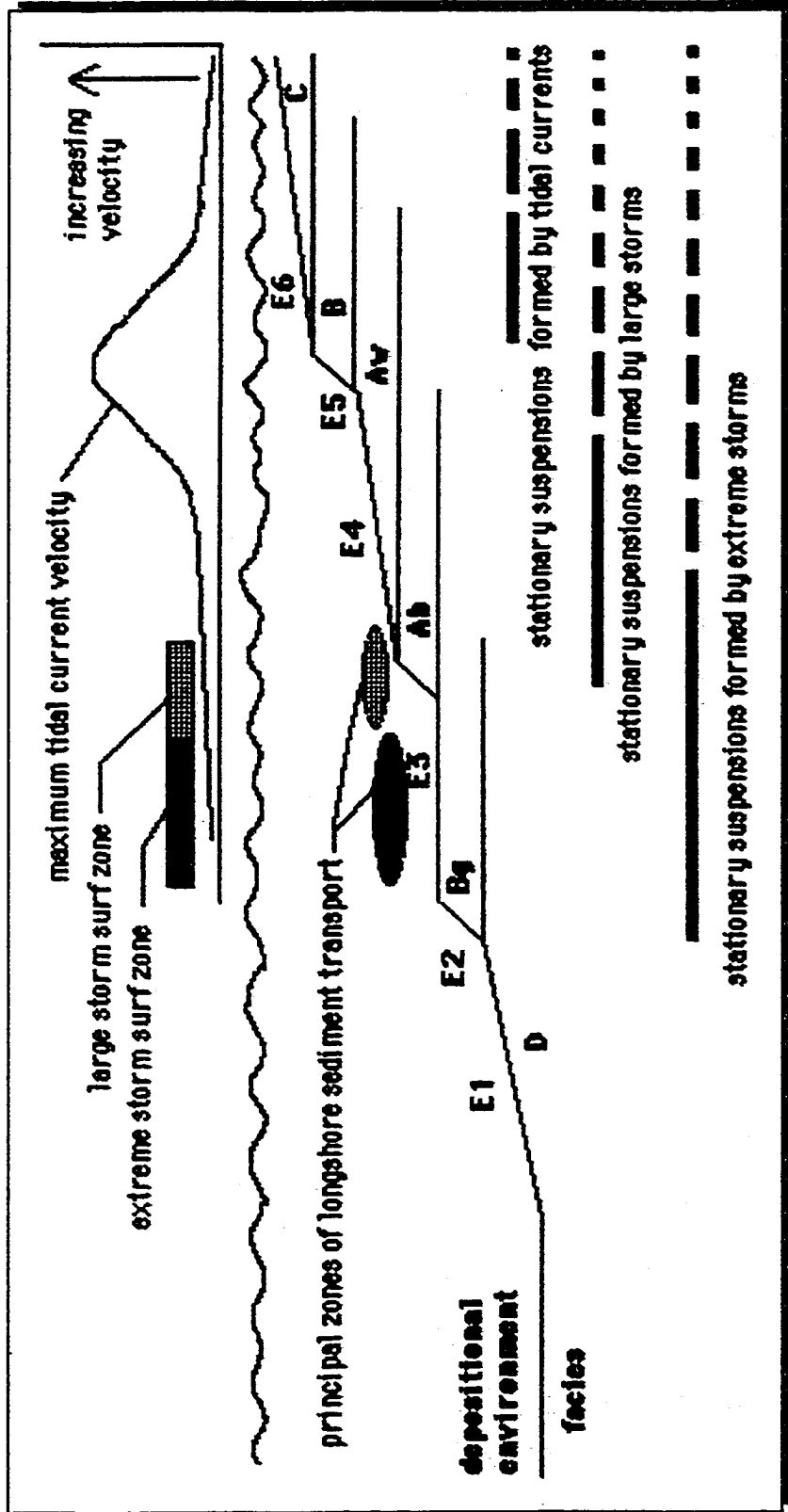
the processes are model driven; they represent what I would expect if the facies were deposited in storm

dominated and tidal environments.

However, the widely accepted model for the marine-to-tidal transition places a beach-barrier

island environment between the marine environment and the tidal environment (Johnson and Baldwin,

1986; McCubbin, 1982; Weimer et al., 1982). Winston, Woods and Byer (1984) cited the missing barrier

island environment as evidence that the Helena and Wallace formations were not deposited in a tidal

environment. The absence of a barrier island environment in the Helena and Wallace formations means I

have either misinterpreted the origin of current x, or the widely accepted marine-to-tidal facies model norm

does not capture all the variability in open marine-to-tidal systems.

SYSTEMS TRACT PROCESSES

The systems track model incorporates both storm generated currents and tidal currents. To obtain

the juxtaposition of the tidal and shelf environments requires a complex interplay of (1) the supply of

muddy sediment. (2) tidal activity, (3) the action of storm waves and (4) the presence of stationary and

mobile suspensions that form mud banks.

ASSUMPTIONS. The environmental systems tract model, Figure IX.1, is based on 3

assumptions. (1) Current x was a tidal current, where flood tidal currents transported sediment onshore, and

ebb tidal currents transported sediment offshore. (2) There was an extreme storm surf zone that acted as the

principal zone of longshore sediment transport. (3) Average and small storm waves, and fair-weather

waves, were dampened out by stationary and mobile suspensions.

TIDAL CURRENTS. Because of its great depth, environment E1 was not effected by tidal

currents. But, net sediment transport and deposition in the other environments were probably effected by

tidal currents. Tidal currents reach their highest velocities in moderately deep water (G. P. Allen, 1991), and

Table IX.2. Processes operating in the environments comprising the depositional systems tract. Environments are listed from the deepest to the shallowest.

ENVIRONMENT E1- facies D

DEEP, STORM-DOMINATED SHELF, DEEP WATER MUDS
    DEPTH 40-200 m
    BACKGROUND EVENTS-average storms with coastal setup
        moderate occurrence frequency
        low velocity, oscillatory currents
        low suspended sediment concentrations
        little or no erosion
        little or no sediment bypass-sediment sink
    ANOMALOUS EVENTS-extreme storms with coastal setup
        very low occurrence frequency
        very high velocity oscillatory currents
        very high suspended sediment concentrations
        little or no erosion
        little or no sediment bypass-sediment sink

ENVIRONMENT E2- subfacies Bg

MODERATELY DEEP STORM-DOMINATED SHELF; DEEP WATER MUDS
    DEPTH 35-45 m
    BACKGROUND EVENTS-average storms with coastal setup + ebb tide currents
        moderate occurrence frequency
        high velocity combined currents
        high suspended sediment concentrations
        little or no erosion
        high sediment bypass-offshore transport
    ANOMALOUS EVENTS-extreme storms with coastal setup
        very low occurrence frequency
        very high velocity combined currents
        very high suspended sediment concentrations
        deep erosion, truncation surfaces
        very high sediment bypass-offshore transport

ENVIRONMENT E3- subfacies Ab

A) STORM-DOMINATED SHELF, SURF ZONE DURING EXTREME STORMS
B) DEEP SUBTIDAL + LARGE STORMS, SAND FLATS
    DEPTH 25-40 m
    BACKGROUND EVENTS-??, no background graded beds preserved
    ANOMALOUS EVENTS-extreme storm events-very low occurrence frequency
      preservation of rare tabular and wedge anomalous graded beds extreme erosion
    BEDS- amalgamation of the bases of anomalous graded beds?

NOTES   *Stokes, cnoidal and breaking waves produced combined currents, deep erosion and deposit upper plane bed and quasi-planar laminae

        * acts as a source area for offshore or onshore sediment transport by combined small storm and tidal currents by reworking stationary suspensions

Table IX.2. continued.

ENVIRONMENT E4- subfacies Aw

A) LARGE STORM DOMINATED, SANDY SHELF- TO-

B) STATIONARY SUSPENSION INFLUENCED, DEEP SUBTIDAL, MUD FLATS

    DEPTH 15-30 m

    BACKGROUND EVENTS-average storm events

        moderate occurrence frequency

        moderate velocity oscillatory currents, offshore of surf zone

        high suspended sediment concentrations

        moderate erosion

        minor or no sediment bypass

    ANOMALOUS EVENTS-extreme storms

        low occurrence frequency

        very high velocity combined currents-high velocity oscillatory currents

        very high suspended sediment concentrations

        deep erosion, truncation surfaces

        high sediment bypass-evolving to no sediment bypass

NOTES * acts as source area for onshore or offshore sediment transport by combined small

ENVIRONMENT E5- facies B

STATIONARY SUSPENSION DOMINATED, MOD. DEEP SUBTIDAL, MUD FLATS DEPTH 5-20 m

    BACKGROUND EVENTS-flood tide currents + average or sm. storms with coastal setdown

        very high occurrence frequency

        high velocity unidirectional or combined currents

        moderate suspended sediment concentrations

        moderate erosion

        moderate sediment bypass

    BACKGROUND EVENTS-average storms with coastal setdown

        moderate occurrence frequency

        moderate velocity oscillatory currents

        moderate suspended sediment concentrations

        moderate erosion

        little or no sediment bypass

    ANOMALOUS EVENTS-extreme storms

        very low occurrence frequency

        high velocity combined currents

        very high suspended sediment concentrations

        little or no erosion

        moderate sediment bypass

NOTES   * extreme, average and small storm waves dampened out by high suspended sediment
           concentrations induced by shoaling waves
        *with storm waves dampened out the tidal processes dominate

Table IX.2. continued.

ENVIRONMENT E6- facies C
STATIONARY SUSPENSION DOMINATED, SHALLOW SUBTIDAL
TO DEEP INTERTIDAL, MUD FLATS

DEPTH 1-10 m

BACKGROUND EVENTS-flood tide currents + average or small storms with coastal setdown
    very high occurrence frequency
    moderate to low velocity unidirectional or combined currents
    moderate to low suspended sediment concentrations
    little or no erosion
    no sediment bypass

BACKGROUND EVENTS-average storms with coastal setdown
    moderate occurrence frequency
    moderate velocity oscillatory currents
    moderate suspended sediment concentrations
    moderate erosion
    little or no sediment bypass

ANOMALOUS EVENTS-extreme storms with coastal setdown
    very low occurrence frequency
    high velocity combined currents
    low suspended sediment concentrations-sediment starved currents
    deep erosion, truncation surfaces
    very high sediment bypass

NOTES   * environment acts as a sediment sink during background events and a source during
             anomalous events

I speculate that this coincides with environment E5, and environments E4 and E6 experience

lower velocity currents.

STATIONARY AND MOBILE SUSPENSIONS. The high mud content in the graded beds in

facies B and C suggests the presence of stationary and mobile suspensions. Chapter IV.C. Stationary and

mobile suspensions, also called fluid mud deposits (Wells and Coleman, 1981) form offshore of some

exposed coast lines and as well as within some tidal environments (Wells, 1983; Kirby and Parker, 1983).

Rine (1980), Kirby and Parker (1983) and Kemp (1986) have linked centimeter to decimeter scale, very

fine-grained sand-to-mud graded beds to deposition from mobile suspensions.

Stationary and mobile suspensions extend up to 20 km offshore along the coast of Surinam, into

water 10-20 m deep (Wells and Coleman, 1981 a). The mud banks offshore of Kerala, India, extend about 6

km offshore, into water 7-10 m deep Nair (1976). Wells (1983, p. 138) states that the most important

process of the stationary and mobile suspensions is their dampening effect on waves, and the protection

from wave attack this offers to the shoreline.

THE EFFECT OF THE SUBSTRATE ON WAVES. Stationary and mobile suspensions

offshore of Surinam dampen fair-weather waves (Wells and Coleman, 1981), and they dampen storm and

fair-weather waves offshore of Kerala, India (Nair, 1976). Waves go un-dampened offshore of the Kerala

stationary and mobile suspensions, where the bottom is composed of hard, well consolidated mud

(Gopinathan and Qasim, 1974).

As shown in Figure VIII.1, 10 year typhoons in the Yellow Sea are capable of producing a surf

zone in water about 10 m deep. However, if the bottom was composed of weakly consolidated 50-50 sand/

mud graded beds of facies B, then the wave action would suspend large amounts of muddy sediment,

expending their energy keeping the mud in suspension and dampening out the waves.

Thus, wave dampening is a function of the wave height, period, water depth and the sand/ mud ratio of the bottom sediments. Since E3 and E4 are underlain by very sandy graded beds, 100 year storm waves would not have been dampened out, and a surf zone could form. The surf zone was the location of very high velocity combined currents that deposited the common planar, quasi-planar and long low angle laminae in the sandstone beds in subfacies Ab. Waves produced by 10 year storms would produce Airy waves in E3 and E4, but suspend large amounts of mud in E5, where they would be dampened out before they break. Thus, the very abundant small hummocky ripples in the wavy graded beds in facies Aw were probably produced by Airy waves produced by 10 year storms.

Therefore, I suggest that a combination of deep water wave breaking and wave dampening by stationary and mobile suspensions takes the place of the barrier island environment that should separate the tidal environment from the shelf environment. Extreme storm waves broke in water 20-40 m deep in E3, and large storm waves produced airy waves in E4. Large, average and small storm waves were damped out by suspended sediment in E5.

FAIR-WEATHER SURF ZONE. The stationary-mobile suspension model also predicts that no fair-weather surf zone existed. The model suggests all the energy in the fair-weather waves was absorbed in the stationary and mobile suspensions in the deep to shallow subtidal environment (Wells and Coleman, 1981 a).

EXTREME STORM SURF ZONE. The highest sediment transport in wave dominated environments occurs within and is parallel to the surf zone (Komar, 1976). High amplitude, long period waves break in deeper water (Komar, 1976), thereby moving the surf zone offshore. Wave calculations show that 10 year typhoons in the Yellow Sea produce waves that break in 10-11 m deep water, and a 100 year typhoons produce waves that break in water about 25 m deep. The largest theoretical wave with a period of 20 s and height of 34 m would create a surf zone in water about 40 m deep. Large storm waves

break and form a surf zone offshore of the Kerala mud banks during large storms (Nair, 1976). Assuming E5 extended to a depth of 20 m, then 50 year and larger storm events probably produced surf zones in E3 and E4. Furthermore, the model requires the presence of a surf zone to supply sediment to the prograding system systems tract.

CROSS-SHELF STORM INDUCED CURRENTS. Studies on modern shelves show that storms with offshore winds cause coastal setdown. Coastal setdown produces upwelling currents and these induce near-bed, onshore transport of coarse wash load sediment. At the same time, wind friction induces an offshore current in the top of the water column, which induces offshore transport of fine wash load sediment (Swift et al., 1986 a; Vincent, 1986). On the other hand, storms that cause coastal setup induce onshore currents in the upper water column and the onshore transport of fine wash load. At the same time, coastal setup also causes downwelling, and induce offshore transport of coarse wash load (Swift et al., 1986 a; Vincent, 1986).

Thus, water movement in the upper part of the water column tends to preserve stationary and mobile suspensions under conditions of coastal setup. But stationary and mobile suspensions tend to be destroyed under conditions of coastal setdown.

COMBINED SMALL STORM AND TIDAL CURRENTS. I speculate that extreme storms probably created short lived stationary suspensions in environments E4 and E3. I further speculate that combined small storm and tidal currents re-mobilized these short lived stationary suspensions.

A possible analogous situation was reported by Shinn et al. (1993) on the oolite shoals in the Bahamas. They found a mud layer covering the troughs of megaripples on the oolite shoals after Hurricane Andrew. They also observed the oolite megaripples migrating across the mud layer, thereby locally preserving it.

Shinn et al. (1993) believe the mud layer was deposited across the tops of oolite megaripples as well as in the troughs. either during or immediately after the passage of Hurricane Andrew. Deposition of mud in such a high energy environment probably requires the formation of stationary and mobile suspensions. The water over the oolite shoals remained turbid for weeks. showing that much of the original mud layer was continuously re-suspended and transported off of the oolite shoals. Thus, the Hurricane Andrew mud layer probably acted as a stationary suspension source for the subsequent formation and transport of mobile suspensions before it was covered by migrating megaripples.

Re-suspension and transport of the mud layer probably resulted from the activity of tidal currents combined with currents generated by average storms. Since the currents generated by Andrew itself did not transport the original mud off of the shoals. it must have been the tidal currents that produced the required net transport of re-suspended sediment. Certainly if Andrew could not transport the original mud off the shoals. then subsequent smaller storms, by themselves. should not have been able to transport the re-suspended mud off the shoals either.

By analogy, stationary suspensions, produced by extreme storms and deposited in E3 and E4, could have been re-suspended by currents generated by smaller than average storms combined with a tidal current. Ebb tides combined with small storms would then transport sediment from E3 or E4 and deposit it in E1 or E2 during the slack water periods. Flood tides combined with small storms would transport sediment from E3 or E4 and deposit it in E5 or E6 during the slack water periods. Re-suspension continued until some the material in the initial stationary suspension formed a very thin settled bed in E4, or was completely removed from E4. Thus, net progradation of the systems tract probably occurred in the years after an extreme storm event.

WATER DEPTHS. The water depth of the individual environments is a complex function of the rate of sediment supply, the activity of extreme storms, the presence of coastal setup or setdown, and the

subsidence rate. If the supply of sediment is cut off, then the stationary-mobile suspensions would become depleted and waves would be able to attack the entire system, except E1. Wave attack would erode the facies, possibly producing short lived stationary suspensions. But, sediment in these would only be deposited in E1 and possibly E2.

Continued subsidence would preserve sequentially shallower environments by placing them out of reach of the waves, so that environments E1 and E2 would become transgressive. If the sediment supply returned, then the mobile-stationary suspensions would reform and the system would prograde again.

CONCLUSIONS

The hydrodynamic approach to interpreting sedimentary deposits leads to the theory that facies D and A of the Helena and Wallace formations were deposited in a storm dominated environment. Less compelling evidence suggests facies B and C were deposited in a tide dominated environment, punctuated by infrequent storms.

Juxtaposition of these two environments, without an intervening beach or barrier island environment, is not covered by existing tidal environment models. Thus, either the existing tidal depositional models do not cover all the possible variability in the geologic record, or the tidal origin for current x presented in this dissertation is incorrect. However, these interpretations represent valid theories because they are testable.

PLATES

PLATE 1 Common features of facies A

PLATE 1. Common features of facies A, the sandstone facies. Facies A is in part equivalent to Winston's (1986 b) and Winston and Link's (1993) pinch-and-swell couple sediment type.

A. Facies A (subfacies Aw) comprised mainly of very sandy wavy background graded beds. A deeply scoured anomalous graded bed displaying gutters and a planar sandstone-mudstone contact is visible near the top of the photo. A wedge anomalous graded bed occurs in the lower one-third of the photo. Note, the wavy, very thin mud drapes characteristic of facies A. Oregon Gulch, 684 m.

B. Facies A (subfacies Aw) comprised of very sandy wavy background graded beds. Note that most mudstone layers maintain the same thickness across the exposure. Some mudstone layers (top center of photo, and just below the right end of the scale) have folded sand filled dikelets projecting downward into them from the overlying sandstone layer. Most sandstone layers display either planar or quasi-planar laminae and low amplitude rounded ripple forms at the sandstone-mudstone transition. Also, note the general upward thinning of the sandstone layers and the thickening of the mudstone layers. Oregon Gulch, 246.4 m.

C. Facies A (subfacies Ab and Aw) comprised of anomalous and background graded beds and interbedded sandstone beds. The whole interval is composed of fine sand sized particles; the white strata are composed of very fine-grained quartz sandstone; the gray strata are composed of very fine sand sized calcitic intraclasts. A major truncation surface cuts out (gray) wavy background graded beds in the middle of the photo, about 60 cm above the Jacob's staff. The wavy truncation surface is overlain by a wavy white sandstone bed that pinches out to the right. The white sandstone bed is overlain by (gray) wavy background graded beds. The large number of truncation surfaces and wavy sandstone beds implies frequent very high velocity currents. Libby Dam, east side of river, 69-71 m.

D. Facies A (subfacies Aw) comprised of sandy wavy background graded beds. Two wedge anomalous graded beds occur near the top of the photo, and a wedge anomalous graded bed ends near the center of the photo. Oregon Gulch, 859 m.
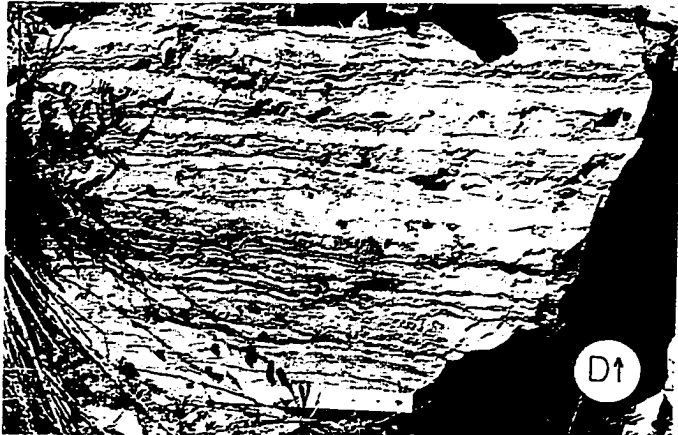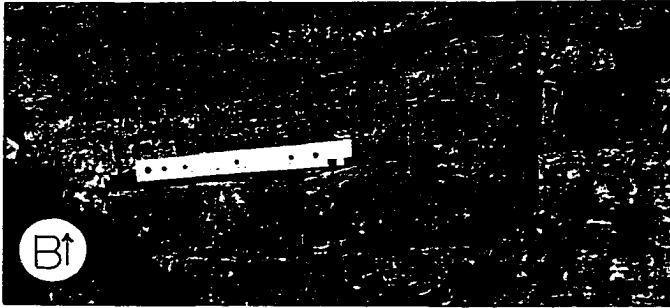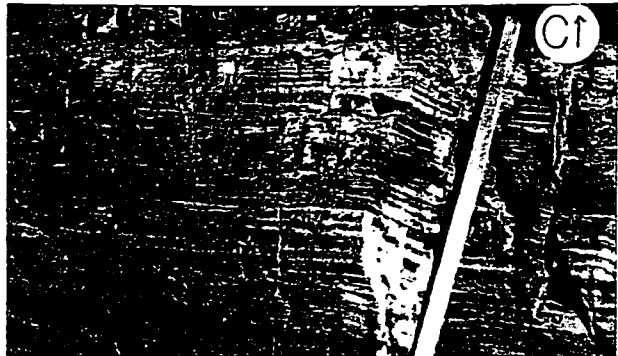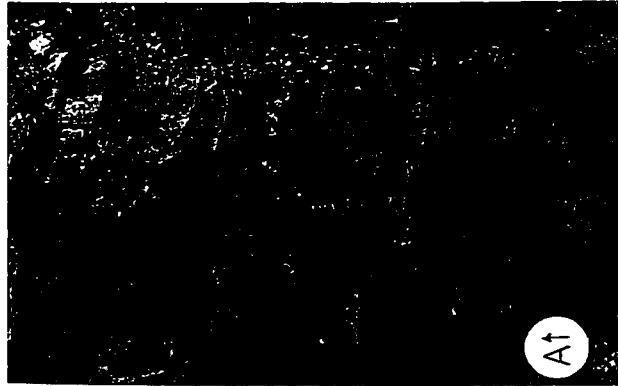
PLATE 2. Common features of facies B

PLATE 2. Common features of facies B, the 50/50 sandstone-mudstone facies. Facies B is in part equivalent to Winston's (1986 b) and Winston and Link's (1993) pinch-and-swell couple and couplet sediment types, and in part equivalent to the uncracked even couplet sediment type.

A. Facies B, (subfacies Bl) loaded, shallowly scoured and lenticular background graded beds, interbedded with long lens and wedge anomalous graded beds. The bases of some anomalous graded beds are loaded and some have folded sand dikelets projecting downward into the underlying mudstone layer. Note that the loading produces graded beds that look like they have guttered bases. However, close examination shows that they do not cut through the underlying graded beds. The bases of some anomalous graded beds (just above the hammer handle) truncate the underlying graded beds at a low angle, indicating very high current velocities and low suspended sediment loads during the accelerating part of the event. The sandstone layers of both the background and anomalous graded beds appear massive, indicating rapid deposition from rapidly decelerating flow events. Note the great difference in the thicknesses between the background and anomalous graded beds, recording very different magnitude events. Weeksville Road, 492.8 m.

B. Facies B (subfacies Besl) composed of equal to sandy even and shallowly scoured background graded beds. Even and shallowly scoured graded beds display massive sandstone layers but some display faint planar laminae. Two wedge anomalous graded beds overlie one deeply scoured (short lens?) anomalous graded bed in the upper half of the photo. The hammer head rests on a tabular graded bed with large hummocky-cross stratification. Subfacies Besl is overlain by subfacies Bl in upper most part of the photo. Weeksville Road, 550.2 m.

C. Facies B, (subfacies Bss) comprised of thinning-upward, equal, even and shallowly scoured background graded beds. Note the lack of interbedded anomalous graded beds. Hungry Horse Dam, upper road, 2.4 m.

D. Facies B composed of equal lenticular and wavy graded beds. Some graded beds contain folded sand filled dikelets. These graded beds are composed of quartz sandstone layers overlain with intarclastic dolomitic mudstone. The lenticular graded beds contain trochoidal ripples with concordant internal laminae at their sandstone-mudstone transitions. The wavy graded beds contain rounded trochoidal ripple forms. This sequence is transitional between facies A and facies B, it is too muddy to be facies A but the wavy graded beds are not common in facies B. Morrell Falls, 27.0 m.

PLATE 3. Common fractures of subfacies Bg

PLATE 3. Common features of subfacies Bg, the guttered 50/50 sandstone-mudstone facies.

A. This photos shows a deeply scoured anomalous graded bed containing rare matrix supported mud chips at the base of the gutter. The lower one-third of the gutter contains planar laminae, indicating sand deposition from high velocity currents. The planar laminae are overlain by massive sandstone, which records deposition rates too high for sorting to take place. Note that the gutter cuts through several shallowly scoured and lenticular background graded beds and at least one other anomalous graded bed (arrow). Weeksville Road, 525.5 m

B. Photo showing three tabular anomalous graded beds overlain by a sequence of equal even and shallowly scoured background graded beds. The sequence of background graded beds also contain two deeply scoured and three long lens anomalous graded beds. Howard Creek, 9.9 m.

C. Photo showing two anomalous graded beds overlain by two background graded beds in subfacies Bg. The lower anomalous graded bed is a deeply scoured graded bed that clearly truncates underlying background graded beds. The lower two-thirds of the deeply scoured graded bed contains planar or quasi-planar laminae, overlain by massive sandstone. The massive sandstone is continuously graded (shown by the darkening of the sandstone) into the mudstone layer across a planar boundary. The deeply scoured graded bed is overlain by a wedge graded bed that rests on a low angle truncation surface which has scalloped the underlying mudstone layer. A sand filled dikelet projects downward from the base of the sandstone layer into the underlying mudstone layer. Note, the dikelet is not ptygmaticly folded, indicating the mud was highly compacted before deposition of the long lens graded bed. Long low angle laminae occur in the bottom of the bed (arrow) indicating deposition under combined currents with orbital velocities between 38 and 65 cm/s. The sandstone-mudstone transition is abrupt and displays symmetrical 3D ripple forms. The mudstone layer is only 1 cm or so thick suggesting possible re-suspension by current x. It is overlain by equal shallowly scoured background graded beds. Howard Creek, 14.1 m.

D. Subfacies Bg displaying several deeply scoured anomalous graded beds, one sandstone bed (a), one wedge anomalous graded bed (arrow), interbedded with even, shallowly scoured, and lenticular background graded beds. The wedge anomalous graded bed pinches out just to the left of the arrow in a series of trochoidal ripples with discordant internal laminae indicating the forms were migrating to the right. The 2D ripple forms clearly record different current conditions than the massive bedding in the deeply scoured and shallowly scoured graded beds. The beds are overturned, but photo shows them right size up. Cyr Tunnel 163.4 m.
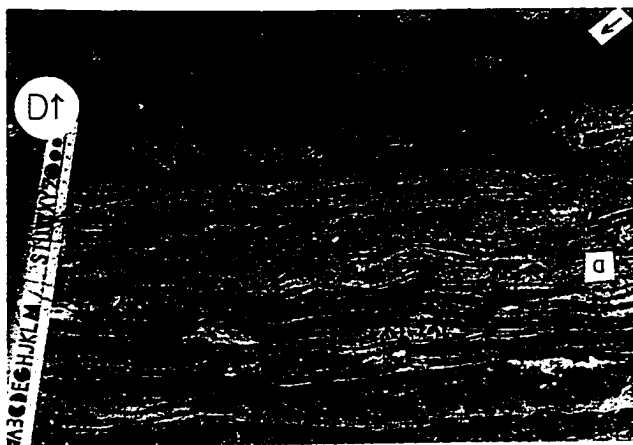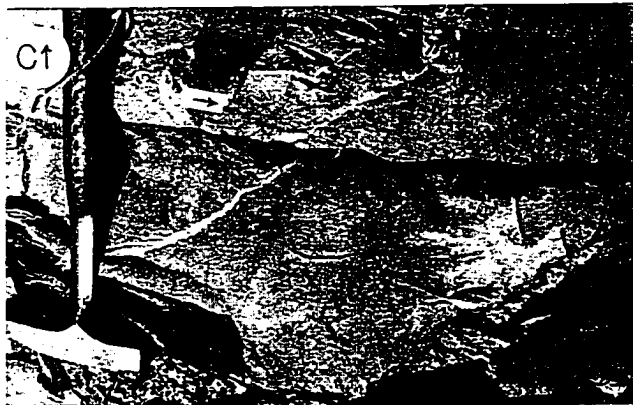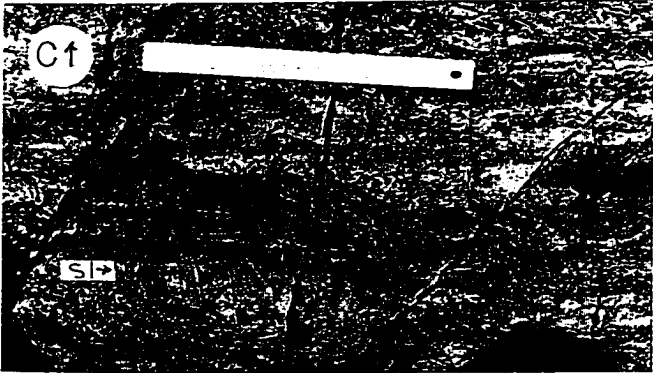
PLATE 4. Common features of facies C.

PLATE 4. Common features of facies C, the thinly graded bedded mudstone facies. Facies C is in part
equivalent to Winston's (1986 b) and Winston and Link's (1993) microlaminae sediment type, and in
part equivalent to the uncracked even couplet sediment type.

A. Facies C (subfacies Cs) composed of centimeter scale even graded bed cosets separated by individual
shallowly scoured graded beds. Oregon Gulch, 707.5 m.

B. Facies C (subfacies Cc) comprised of interbedded cryptalgalimanite beds (c), molar-tooth intraclast
conglomerate beds (i), and microsparic mudstone beds (m). Rogers Pass, section B, 274.9 m.

C. Facies C (subfacies Cs) composed of centimeter scale even and shallowly scoured background graded
beds, interbedded with long lens (with numbers) and short lens (sl) anomalous graded beds. Both
anomalous graded beds have guttered bases. Storm Lake Pass, 205.5 m.

D. Facies C (subfacies Cs) composed of centimeter scale even and shallowly scoured background graded
beds, interbedded with one short lens graded bed. Note, the wedge shaped package between the "1
m" mark on the Jacob's staff and 20 cm below the mark. This package of background graded beds
rests on a scour surface cut into background graded beds. The complete package (not shown) is
about 3 m long and forms a flat toped channel-like lens, 30 cm thick. Channel-like lenses at this
scale are fairly common in facies C, but are very difficult to see. Storm Lake Pass, 367 m.

PLATE 5. Common features of the microlaminated graded beds in facies C
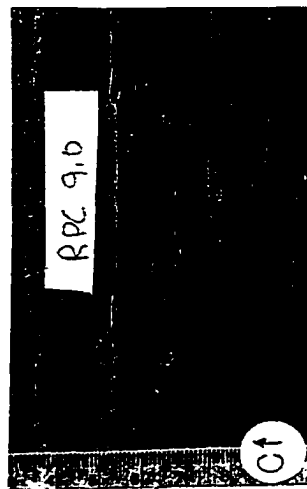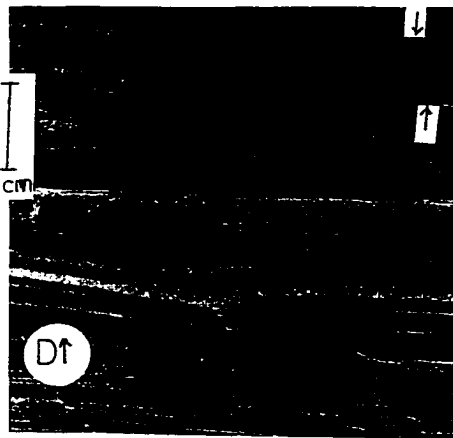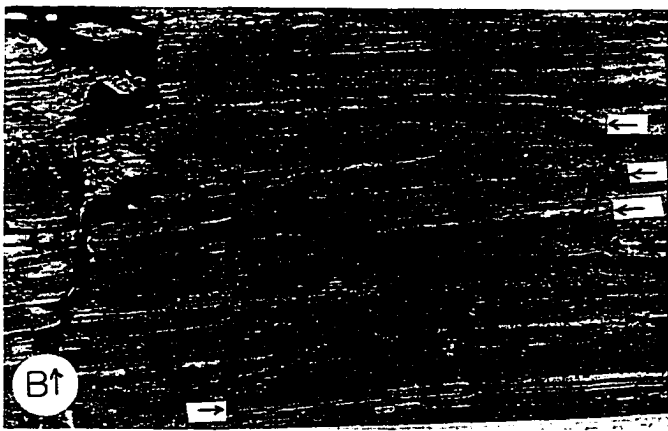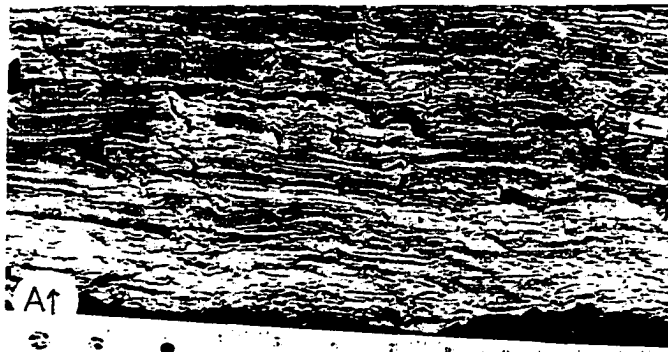
PLATE 5. Common features of the microlaminated graded beds in facies C.

A. A sequence of microlaminated graded bed cosets. Cosets are separated by erosional surfaces 3 to 5 cm apart. The erosional surface at the arrow truncates vertical ribbon molar-tooth structures. The molar-tooth ribbons at this location contain authogenetic quartz, hence they stand in relief on weathered surfaces. The photo also displays sandy- (yellowish weathering)muddy (grayish weathering) lamina-cycles (Williams, 1989 a;1989 b). Oregon Gulch, 782 m.

B. Sequence of greenish-gray microlaminated and even graded bed cosets. The cosets are separated by erosional surfaces (some are marked by arrows) about 2 to 5 cm apart. This interval lacks lamina-cycles and molar-tooth ribbons. Several thin even graded beds in the lower right of the photo contain mudcracks. This photo is about 8 m below the Snowslip Formation which does contains common mudcracks. The greenish color is due to the color of the clays and the absence of hematite and carbon. Rogers Pass, C section, 7.6 m.

C. Slab showing possible lamina-cycles in very dark gray microlaminated graded beds. The interval contains no mudcracks but contains molar-tooth ribbons. The gray color is due to carbon that masks the green color of the clays. Rogers Pass, C section, 9.0 m.

D. Close-up of polished slab of microlaminated graded beds. The arrows point to erosion surfaces. The interval between the two arrows contain alternating thick-thin microlaminated graded beds that may record semi-diurnal tidal inequality. The middle of the photo contains a sequence of possible lamina-cycles that may record neap-spring, synodic month or tropical month one-half cycles (two neap and two spring intervals record one synodic month or tropical month). Howard Creek area.

E. Sequence of microlaminated graded beds showing possible lamina-cycles. Two long lens anomalous graded beds occur in the center of the photo (LL). The lower long lens graded bed rests on a truncation surface and pinches out to the right in a series of symmetrical ripple lenses. Erosion on the surface appears to have removed at least 2 to 3 cm of microlaminated graded beds. The lower third of the photo shows several possible lamina-cycles (L-C). Oregon Gulch 799 m.

PLATE 6. Common features of facies D.
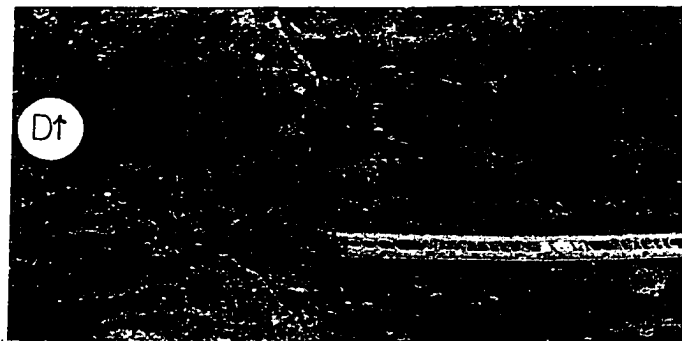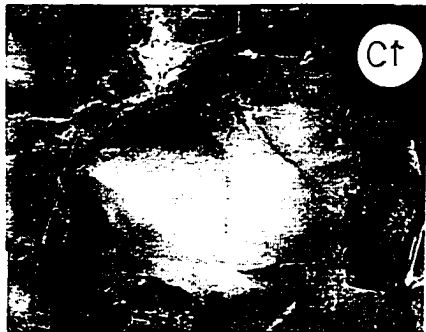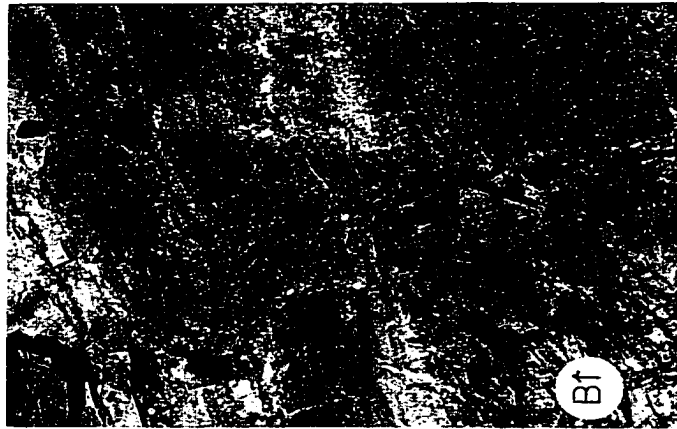
PLATE 6. *Common features of facies D, the thickly graded bedded mudstone facies. Facies D is in part equivalent to Winston's (1986 b) and Winston and Link's (1993) carbonate mud sediment type. Previous workers in the Helena and Wallace formations did not recognize the differences between the laminated mudstones and the thickly graded bedded mudstones.*

A. *Facies D (subfacies Desl,m) consisting of very muddy even and shallowly scoured background graded beds. The pencil lies on a massive mudstone bed with a guttered base and vertical ribbon molar-tooth structures. The guttered base of the mudstone bed records high velocity undersaturated currents. The massive mudstone bed may record deposition of a stationary suspension. The massive mudstone bed is overlain by muddy lenticular and even graded beds. Weeksville Road, 256.5 m.*

B. *Facies D (subfacies Desl,a) containing very muddy even, shallowly scoured and lenticular background graded beds, best seen in the lower right corner of the photo. The interval also contains two long lens and two wedge anomalous graded beds, spaced about 30 cm apart. The lowest long lens graded bed is opposite the "b". The paint spot is on a gutter at the base of the uppermost wedge graded bed. The long lens graded bed about 30 cm below the paint spot contains rounded trochoidal ripples at the sandstone-mudstone transition. The wedge graded bed just below the center of the photo contains long low angle laminae and rounded trochoidal ripples at the sandstone-mudstone transition. Libby Dam, 390 m.*

C. *Facies D (subfacies Desl) containing very muddy even, shallowly scoured and lenticular background graded beds. This exposure of facies D does not contain any anomalous graded beds, compare with Plate 6 b which contains anomalous graded beds. The exposure is moderately weathered. This photo clearly shows the difference between facies C mudstone and facies D mudstones. Hungry Horse Dam upper road, 26.1 m.*

D. *Facies D (subfacies Dl) composed of very muddy loaded, lenticular and shallowly scoured background graded beds. The lenticular graded bed near top of photo displays folded sandstone dikelets projecting downward from its base. Note the sandstone psuedonodules in the thick mudstone layer in the center of the photograph. These formed when ripple lenses sank completely into the underlying graded bed's mud layer. The dominance of loading suggests this location experienced no strong erosive currents and the transporting currents were saturated with sediment when they reached this location. Subfacies Dl is similar to subfacies Desl, but subfacies Dl is dominated by loaded anomalous and background graded beds. Trout Creek road, between mile markers 15 and 16.*

PLATE 7. Common features of facies D.
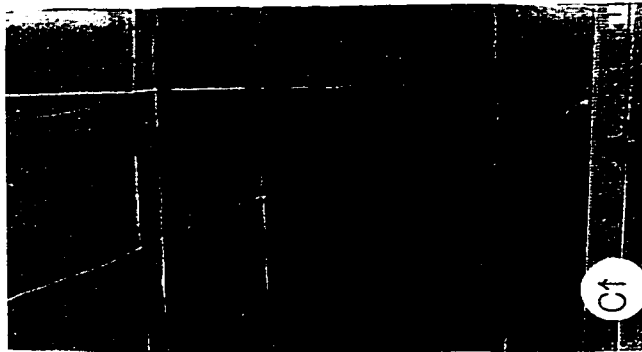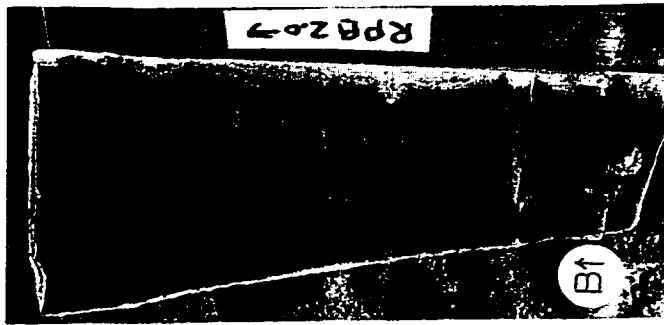
PLATE 7. *Common features of facies D, the thickly graded bedded mudstone facies.*

A. *Facies D (subfacies D1) slowing even, shallowly scoured and loaded background graded beds, with psuedonodules just below the scale. The upper part of the photo shows a tabular anomalous graded bed containing large hummocky ripples (only about one third of one bedform is shown), overlain by trochoidal ripples. The tabular graded bed also displays two types of loading: (a) loading by sinking of individual sand grains into the underlying mud; and (b) by formation of psuedonodules. The loading means that the current that transported the sediment in the anomalous graded bed site was saturated with sediment, and thus not able to erode even very soft mud. Trout Creek road, between mile markers 15 and 16.*

B. *Polished slab of facies D (subfacies Des1) showing very muddy shallowly scoured graded beds. Most scours are filled with massive lower very fine-grained sand, but near the bottom of the slab one scour is filled with planar laminated very fine-grained sand. Note that some of the erosion surfaces are angular but others are rounded. The graded beds also display mature grading, i.e., grading is continuous throughout the graded beds This proves that all the sediment in the graded bed was transported to the site of deposition during one sedimentation event. Sediment could not have been continuously transported to the site or be due to long term pelagic suspension deposition. Rogers Pass, section B, 2.0 m.*

C. *Polished slab of facies D (subfacies Des1) composed of even and lenticular background graded beds. The second graded bed from the bottom a trochoidal ripple with discordant internal laminae, showing the ripple migrated to the left. The graded beds also display mature grading rippled very fine-grained sand to massive siltstone to streaky mudstone. Vertical white lines are calcite filled tectonic fractures. Hungry Horse, upper dam road, 26.5 m.*

D. *Facies D (subfacies Des1,m) displaying a guttered surface in very muddy loaded and shallowly scoured background graded beds (loads only show up on polished slabs). Two gutters about 20 cm deep are shown, one to either side of the "RPB 50.0". Matrix supported mud clast conglomerate, in coarse silt matrix, fill about one-half of the gutters. The rest of the gutters are filled by very muddy shallowly scoured background graded beds. Eby (1977, p. 84) interpreted the gutters as subaerial "solution collapse structures", and used them as evidence for now missing evaporites. But, note the complete lack of evidence for exposure and desiccation on the guttered surface. The carbonate rich mudstone clasts in the gutter are composed of the same material that the gutter is cut into. Also, the mudstone clasts display no weathering rinds and no desiccation. Rogers Pass, section B, 50.0 m.*

REFERENCES

Ackman, B. C., 1988, The stratigraghy and sedimentology of the Middle Proterozoic Snowslip Formation in the Lewis, Whitefish and Flathead Ranges, Northwest Montana (M. S. thesis): University of Montana, Missoula, 89 p.

Adshead, J. D., 1963, Petrrology of the carbonate rocks of the Siyeh Formation, S. W. Alberta (M. S. thesis): University of Alberta.

Allen, G. P., 1991, Sedimentary processes and facies in the Gironde estuary: a recent model for macrotidal estuarine systems, in, Smith, D. G., Reinson, G. E., Zaitlin, B. A., and Rahmani, R. A., Clastic Tidal Sedimentology Canadian Society of Petroleum Geologists, Memoir 16, p. 20-40.

Allen, J. R. L., 1966, On bed forms and paleocurrents: Sedimentology v. 6. p, 153-190.

Allen, J. R. L., 1973, Physical Processes of Sedimentation: George Allen and Unwin Ltd., London, 248 p.

Allen, J. R. L., 1984 a, Sedimentary Structures, their Character and Physical Basis, Volume I: Elsevier, 593 p.

Allen, J. R. L., 1984 b, Sedimentary Structures, their Character and Physical Basis, Volume II: Elsevier, 663 p.

Allen, J. R. L., 1985 a, Loose-boundary hydraulics and fluid mechanics: selected advances since 1961, in Brenchley, P. J., and Williams. B. P. J., (editors), Sedimentology:L Recent Developments and Applied Aspects: Oxford, Blackwell Scientific Publications, p.7-28.

Allen, J. R. L., 1985 b, Physical Sedimentology: George Allen and Unwin, London, 272 p.

Allen, J. R. L., 1991, The Bouma division A and the possible duration of turbidity currents: Journal of Sedimentary Petrology, v. 61, p. 291-295.

Anderton, R., 1985, Clastic facies models and fadies analysis. in, Brenchley, P. J., and Williams, B. J. P., (editors), Sedimentology: recent developments and applied aspects: Oxford, Blackwell Scientific Publications, p. 31-47.

Anderson, J. B., and Smith, M. J., 1989, Formation of modern sand-rich facies by marine currents on the Antarctic continental shelf, in, Morton, R. A., and Nummedal, D., (editors.), Shelf sedimentation, shelf sequences and related hydrocarbon accumulation: Proceedings of the Seventh Annual Research Conference, Gulf Coast Section Society of Economic Paleontologists and Mineralogists Foundation, p. 41-52.

Archer, A. W., Kvale, E. P., and Johnson, H. R., 1991, Analysis of modern equitorial tidal periodicities as a test of information encoded in ancient tidal rhythmites: in, Smith, D. G., Reinson, G. E., Zaitlin, B. A., and Rahmani, R. A., (eds.). Clastic Tidal Sedimentology: Canadian Society of Petroleum Geologists, Memior 16, p. 189-196.

Arnott, R. W. C., and Hand, B. M., 1989, Bedforms, primary structures and grain fabric in the presence of suspended sediment rain: Journal of Sedimentary Petrology, v. 59, p. 1062 - 1069.

185

Arnott, R. W., and Southard, J. B., 1990. Exploratory flow-duct experiments on combined-flow bed configurations. and some implications for interpreting storm-event stratification: Journal of Sedimentary Petrology. v. 60, p. 211-219.

Arnott, R. W. C., 1993. Quasi-planar-laminated sandstone beds of the lower Cretaceous Bootlegger Member, north-central Montana: Evicence of combined-flow sedimentation: Journal of Sedimentary Petrology. v. 63. p. 488-494.

Ashley, G. M., Symposium Chairperson, 1990, Classification of large-scale subaqueous bedforms: A new look at an old problem: Journal of Sedimentary Petrology, v. 60, p. 160-172.

Aspler, L. B.. Chiarenzelli, J. R., and Bursey, T. L.. 1994, Ripple marks in quartz arenites of the Hurwitz Group, Northwest Territories. Canada: evidence for sedimentation in a vast, early Proterozoic. shallow. fresh-water lake: Journal of Sedimentary Research, v. A64, p. 282- 298.

Bagnold. R. A.. 1946, Motion of waves in shallow water: Royal Society London, Proceedings, Series A, v. 187, p. 1-16.

Bagnold, R. A.. 1966, An approach to the sediment transport problem from general physics: U. S. Geological Survey Professional Paper 422-I.

Bagnold. R. A.. 1973, The nature of saltation and of "bed-load" transport in Water: Proceedings of the Royal Society of London, Series A, v. 332, p. 473-504.

Bates, R. L.. and Jackson, J. A., (editors), 1980, Glossary of Geology, Second Edition: Falls Church. Virginia, American Geological Institute.

Bell, R. T.. 1966, Precambrian rocks of the Tuchodi Lakes Map Area, northwestern British Columbia, Canada, PhD. dissertation, Princeton University, Princeton, N. J.

Black, M., 1933, The algal sediments of Andros Island, Bahamas: Philosophical Transactions
Royal Society, London, series B, v. 122, p. 165-192.

Blatt, H., Middleton, G. V., and Murray, R. C., 1980, Origin of Sedimentary Rocks. 2nd. ed.: New Jersey, Prentice-Hall, 782 p.
Boggs, S., Jr., 1987, Principles of sedimentology and stratigraphy: Columbus, Ohio, Merrill Publishing Company, 784 p.

Boothroyd, J. C., and Ashley, G. M., 1975, Processes, bar morphology, and sedimentary structures on braided outwash fans, northeastern Gulf of Alaska, in, Jopling, A. V.. and McDonald B. C., (eds.). Glaciofluvial and Glaciolacustrine Sedimentation: Society of Economic Paleontologists and Mineralogists, Special Publication No. 23, p. 193-222.

Brenchley, P. J., and Newall, G., 1982, Storm-influenced inner-shelf sand lobes in the Caradoc (Ordovician) of Shropshire, England: Journal of Sedimentary Petrology, v. 52, p. 1257- 1269.

Bryant, R., James, A. E., and Williams, D. J. A., 1980, Rheology of cohesive suspensions, in, Industrialized embayments and their environmental problems: a case study of Swansea Bay: Proceedings of an interdisciplinary symposium: Oxford, Pergamon Press, p. 279- 287.

Bryant, R., and Williams, D. J. A., 1983, Characteristics of suspended cohesive sediment of the Severn Estuary, U. K.: Canadian Journal of Fisheries and Aquatic Science, v. 40 (Suppliment 1), p. 96-101.

Calkins, F. C., and Emmons, W. H., 1915, Description of the Phillipsburg quadrangle. Montana: U. S. Geological Survey, Geologic Atlas, Folio 196, 25 p.

Carstens, M. R., Neilson, F. M., and Altingilek, H. D., 1969, Bed forms generated in the laboratory under an oscillatory flow: analytical and experimental study: U. S. Army corps of Engineers. Coastal Engineering Research Center. Technical Memorandum No. 28, 39 p., Appendix A, Appendix B.

Childers, M. O., 1963, Structure and stratigraphy of the south west Marias Pass area. Flathead County, Montana: Geological Society of America Bulletin, v. 74, no. 2, p. 141-164.

Clapp, C. H., and Deiss, C. F., 1931, Correlation of Montana Algonkian formations: Geological Society of America Bulletin v. 42, p. 673-696.

Clifton, H. E., and Dingler, J. R., 1984, Wave-formed structures and paleoenvironmental reconstruction: Marine Geology, v. 60, p. 165-198.

Clifton, H. E., Hunter, R. E., and Phillips, R. L., 1971, Depositional structures and processes in the non-barred high-energy nearshore: Journal of Sedimentary Petrology, v. 41, p. 651- 670.

Collinson, J. D., and Thompson, D. B., 1989, Sedimentary Structures, second edition: London, Unwin Hyman, 207 p.

Dalrymple R. W., 1992, Tidal depositional systems, in, Walker, R. G., and James. N. P., (eds.), Facies Models: Response to Sea Level Change: Geological Association of Canada, p. 195- 218.

Dalrymple, R. W., and Makino, Y., 1989, Description and genesis of tidal bedding in the Cobequid Bay-Salmon River estuary, Bay of Fundy, Canada, in, Taria, A., and Masuda, F., (eds.), Sedimentary Facies in the Active Plate Margin: Tokyo, Terra Scientific Publishing Co., p. 151-177.

Daly, R. A., 1912, Geology of the North American Cordillera at the 49th parallel: Canada Geological Survey Memoir 38, pts 1, 2, and 3, 857 p.

Dott, R. H., Jr., 1983, Episodic sedimentation- how normal is average? How rare is rare? Does it matter?: Journal of Sedimentary Petrology, v. 53, p. 5-23.

Dott, R. H., Jr., 1988, An episodic view of shallow marine clastic sedimentation, in, De Boer, P. L., van Gelder, A., and Nio, S. D., Tide-influenced sedimentary environments and facies: D. Reidel Publishing Company, Dordrecht, Holland, p. 3-12.

Eby, D. E., 1977, Sedimentation and early diagenesis within eastern portions of the "middle Belt carbonate interval" (Helena Formation), Belt Supergroup (Precambrian Y), western Montana (Ph.D. thesis): State Univ. of New York at Stony Brook, 504 p.

Einstein, H. A., and Krone, R. B., 1962, Experiments to determine modes of cohesive sediment transport in salt water: Journal of Geophysical Research, v. 67, p. 1451-1461.

Elder, D. McG., and Sills, G. C., 1984, Time and stress dependent compression in soft sediments, in, Yong, R. N., and Townsend, R. C., (editors), Sediment consolidation models: New York. American Society of Civil Engineers, p. 425-444.

Elliott, T., 1986, Siliciclastic shorelines, in, Reading, H. G., ed., Sedimentary Environments and Facies, 2nd edition: Oxford. Blackwell Scientific Publications, p. 155-188.

Fenton, C. L., and Fenton, M. A., 1937, Belt series of the north: stratigraphy, sedimentation, paleontology: Geological Society of America Bulletin, v. 48, p. 1873-1970.

Fritz, W. J., 1991, Theoretical wave modeling of large wave ripples in volcaniclastic sediments. Ordovician Llewelyn Volcanic Group, North Wales: Sedimentary Geology, v. 74, p. 241- 250.

Gilbert, G. K., 1914. The transportation of debris by running water: U. S. Geolgoical Survey Professional Paper 86, 263 p.

Godlewski, D. W., 1980, Origin and classification of the middle Wallace breccias (Ms. thesis): University of Montana, Missoula, 74 p.

Gopinathan, C. K., and Qasim, S. Z., 1974, Mud bands of Kerala- Their formation and characteristics: Indian Journal of Marine Sciences. v. 3, p. 105-114.

Grant, W. D., and Madsen, O. S.,1979, Combined wave and current interaction with a rough bottom: Journal of Geophysical Research, v. 84, p. 1797-1808.

Grotzinger, J. P., 1981, The stratigraphy and sedimentation of the Wallace Formation, northwest Montana and norhtern Idaho (M. S. thesis): University of Montana, Missoula, 153 p.

Grotzinger, J. P., 1986. Shallowing-upward cycles of the Wallace Formation. Belt Supergroup, northwestern Montana and northern Idaho, in S. M. Roberts, editor, Belt Supergroup: A guide to Proterozoic rocks of western Montana and adjacent areas: Montana Bureau of Mines and Geology Spedial Publication 94, p. 143-160.

Hampton, M. A., 1975, Competence of fine-grained debris flows: Journal of Sedimentary Pertology, v. 45, p. 834-844.

Harms, J. C., 1969, Hydraulic significance of some sand ripples: Geological Society of America Bulletin, v. 80, p. 363-396.

Harms, J. C., 1975. Brushy Canyon Formation, Texas: A deep-water density current deposit: Geological Society of America Bulletin, v. 85, p. 1763-1784.

Harms, J. C., Southard, J. B., and Walker, R. G., 1982, Structures and sequences in clastic rocks: Society of Economic Paleontologists and Minertalogists Short Course No. 9.

Harrison, J. E., 1972, Precambrian Belt basin of northwestern United States: Its geometry, sedimentation, and copper occurrences: Geological Society of Aamerica Bulletin, v. 83, p. 1215-1240.

Harrison, J. E., 1984, Stratigraphy and lithocorrelation of the Wallace Formation, in The belt, Abstracts with Summaries, Belt Symposium II, 1983: Montana Bureau of Mines and Geology Special Publication 90, p. 24-26.

Harrison,J. E. and A. B. Campbell, 1963, Correlations and problems in Belt Series stratigraphy. northern Idaho and western Montana: Geological Society of America Bulletin, v. 74, p. 1413-1428.

Harrison, J. E., and Grimes, D. J., 1970, Mineralogy and geochemistry of some Belt rocks, Montana and Idaho: U. S. Geological Survey Bulletin 1312-O, p. O1-O49.

Harrison, J. E. and Jobin, D. A., 1963, Geology of the Clark Fork quadrangle, Idaho-Montana: U. S. Geological Survey Bulletin 1141-K, p. K1-K38.

Hawley, N., 1981 a, Mud consolidation during a short time interval: Geo-Marine Letters, v. 1, p. 7-10.

Hawley, N., 1981 b, Flume experiments on the origin of flaser bedding: Sedimentology v. 28, p. 699-712.

Hesse, R., and Chough, S. K., 1980, The norhtwest Atlantic mid-ocean channel of the Labrador Sea: II. Deposition of parallel laminated levee-muds from the viscous sublayer of low density turbidty currents: Sedimentology, v. 27, p. 697-711.

Hiscott, R. N., 1994, Loss of capacity, not competence, as the fundamental process governing deposition form turbidity currents: Journal of Sedimentary Research, v. A64, p. 209- 214.

Howard, C. D. D., 1965, Discussion of "Hyperconcentrations of suspended sediment": Journal Hydraulics Division American Society Civil Engineers, v. 91, p. 386-388.

Hjulstrom, F., 1935, Studies of the morphological activities of rivers as illustrated by the River Fyris: Geological Institute Bulletin, University of Uppsala, v. 25, p. 221-527.

Horodyski, R. J., 1976 a, Stromatolites of the upper Siyeh Limestone (Middle Proterozoic), Belt Supergroup, Glacier National Park, Montana: Precambrian Research, v. 3, p. 517-536.

Horodyski, R. J., 1983, Sedimentary geology and stromatolites of the Middle Proterozoic Belt Supergroup, Glacier National Park, Montana: Precambrian Research, v. 20, p. 391-425.

Horodyski, R. J., 1989, Stromatolites of the Belt Supergroup, Glacier national Park, Montana, in, Winston, D., Horodyski, R. J., and Whipple, J. W., eds., Middle Proterozoic Belt Supergroup, Western Montana, 28th International Geological Congress, Field Trip Guidebook T334, p. 27-42.

Hunter, R. E., and Clifton, H. E., 1982, Cyclic deposits and hummocky cross-stratification of probable storm origin in Upper Cretaceous rocks of the Cape Sebastian area, southwestern Oregon: Journal of Sedimentary Petrology, v. 52, p. 127-143.

Hurberger, D., 1986, Sedimentation and mineralization of a sandstone lead-zinc occurrence in the Helena Formation, Belt Supergroup, Lewis and Clark County, Montana (Ms. thesis): University of Montana, Missoula, 74 p.

Johnson, H. D., and Baldwin, C. T., 1986, Shallow siliciclastic seas, in, Reading, H. G., ed., Sedimentary Environments and Facies, second edition: Oxford, Blackwell Scientific Publications, p. 229-282.

Kemp, G. P., 1986, Mud deposition at the shoreface: Wave and dediment dynamics on the cheinier plain of Louisiana, Ph. D. dissertation, Louisiana State University.

Kirby, R., and Parker, W. R., 1983, Distribution and behavior of fine sediment in the Severn Estuary and Inner Bristol Chanel, U. K.: Canadian Journal of Fish and Aquatic Science, v. 40, (Suppliment 1), p. 83-95.

Klein, G. deV., 1975, Paleotidal range sequences, Middle Member, Wood Canyon Formation (Late Precambrian), eastern California and western Nevada, in, Ginsburg, R. N., (ed.), Tidal deposits: New York, Springer-Verlag, p. 171-178.

Klein, G. deV., 1977, Clastic tidal facies: Champaign, Il., Continuing Education Publication Co., 149 p.

Knight, R. J., and Dalrymple, R. W., 1975, Intertidal sediments from the south shore of Cobequid Bay. Bay of Fundy, Nova Scotia, Canada, in, Ginsburg, R. N., (ed.), Tidal deposits: New York, Springer-Verlag, p. 47-56.

Komar, P. D., 1976, Beach processes and sedimentation: Englewood Cliffs, N. J., Prentice-Hall, Inc.

Komar, P. D., 1985, The hydraulic interpretation of turbidites from their grain sizes and sedimentary structures: Sedimentology, v. 32, p. 395-407.

Komar, P. D., Neudeck, R. H., and Kulm, L. D., 1972, Observations and significance of deep-water oscillatory ripple marks on the Oregon Continental Shelf, in, Swift, D. J. P., Duane, D. B., and Pilkey, O. H., (editors), Shelf Sediment Transport Processes and Pattern: Stropudsbourg, Pa., Dowden, Hutchinson and Ross, p. 601-619.

Krone, R. B., 1962, Flume studies of the transport of sediment in estuarial shoaling processes. Hydraulic Engineering Research Labratoryand Sanitary Engineering Labratory, University of California, Berkeley, 110 p.

Krone, R. B., 1986, The significance of aggregate properties to transport processes, in, Metha, A. J., (editor), Esturine cohesive sediment dynamics: Berlin, Springer, p. 66-84.

Kvale, E. P., and Archer, A. W., 1991, Characteristics of two, Pennsylvanian-age, semidiurnal tidal deposits in the Illinois Basin, U.S. A.: in, Smith, D. G., Reinson, G. E., Zaitlin, B. A., and Rahmani, R. A., (editors.). Clastic Tidal Sedimentology: Canadian Society of Petroleum Geologists, Memior 16, p. 179-188.

Kvale, E. P., Archer, A. W. and Johnson, H. R., 1989, Daily, monthly, and yearly tidal cycles within laminated siltstones of the Mansfield Formation (Pennsylvanian) of Indiana: Geology, v. 17, p. 365-368.

Lane, E. W., 1940, Notes on limit of sediment concentration: Journal of Sedimentary Petrology, v. 10, p. 95-96.

Larsonneur, C., 1975, Tidal deposits. Mont Saint-Michel Bay, France, in, Ginsburg, R. N., (editor), Tidal deposits: New York, Springer-Verlag, p. 21-30.

Lemoine, S. R., 1979, Correlation of the upper Wallace with the lower Missoula Group and resulting facies interpretations, Cabinet and Coeur d'Alene mountains, Montana (M.S. thesis): University of Montana, Missoula, 162 p.

Lemoine, S. R., and Winston, D., 1986, Correlation of the Snowslip and Shepard formations of the Cabnet Mountains with upper Wallace rocks of the Coeur d'Alene Mountains, western Montana, in, Roberts. S. M. (ed.), Belt Supergroup: A guide to Proterozoic rocks of western Montana and adjacent areas: Montana Bureau of Mines and Geology Spedial Publication 94, p. 161-168.

Little-Gadow, S., and Reineck, H. -E., 1974, Diskontinuierliche Sedimentation von Sand und Schlick in Wattensedimenten: Senckenbergiana maritina, v. 6, p. 149-159

Maxwell, D. T., 1973, Layer silicate mineralogy of the Precambrian Belt Series: in Belt Symposium 1973, Volume II: IBMG, p. 113-138.

Maxwell, D. T., and Hower, J., 1967, High-grade diagenesis and low-grade, metamorphism of illite in the Precambrian Belt Series: American Mineralogist, v. 52, p. 843-857.

McCave, I. N., 1984, Erosion, transport and deposition of fine-grained marine sediments, in Stow. O. A. V., and Piper, D. J. W., (editors) Fine-grained Sediments: Deep Water Processes and Facies: Geological Society of London, Special Publication no. 15, p. 35-69.

McCave, I. N., and Swift, S. A., 1976, A physical model for the rate of deposition of fine-grained sediments in the deep sea: Geological Society of America Bulletin, v. 87, p. 541-546.

McCubbin, D. G., 1982, Barrier-island and strand plain facies, in, Scholle, P. A., and Spearing, D., (eds.), Sandstone depositional environments: American Association of Petroleum Geologists, Memoir 31, p. 247-280.

Middleton, G. V., 1966 b, Experiments on density and turbidity currents II. Uniform flow of density curmets: Canadian Journal of Earth Sciences, v. 3, p. 627-637.

Miller, M. C., and Komar, P. D., 1980, Oscillation sand ripples generated by laboratory apparatus: Journal of Sedimentary Petrology. v. 50, p. 173-182.

Miller, M. C., and Komar, P. D., 1980, A field investigation of the relationship between oscillation ripple spacing and the near-bottom water orbital motions: Journal of Sedimentary Petrology, v. 50, p. 183-191.

Morton, R. A., 1988, Nearshore responses to great storms, in, Clifton H. E., (editor) Sedimentologic consequences of convulsive geologic events: Geological Society of America Special Paper 229, p. 7-22.

Myrow, P. M., and Southard, J. B., 1991, Combined-flow model for vertical stratification sequences in shallow marine storm-deposited beds: Journal of Sedimentary Petrology, V. 61, p. 202-210.

Nair, R. R., 1976, Unique mud banks, Kerala, Southwest India: American Association of Petroleum Geologists Bulletin, v. 3, p. 616-621.

Nio, S. D., and Yang, C., 1991, Diagnostic attributes of clastic tidal deposits: a review, in, Smith, D. G., Reinson, G. E., Zaitlin, B. A., and Rahmani, R. A., (eds.). Clastic Tidal Sedimentology: Canadian Society of Petroleum Geologists, Memior 16, p. 3-28

Nordin, C. F., and Perez-Hernandez, , 1988, The waters and sediments of the Rio Orinoco and its major tributaries, Venezuela and Columbia: U. S. Geological Survey Water Supply Paper 2326 A.

O'Connor, M. P., 1967, Stratigraphy and peterology across the Precambrian Piegan Group-Missoula Group boundary, southern Mission Range, Swan Range, Montana (Ph.D. dissertation): Missoula, Montana, University of Montana, 269 p.

O'Conner, M. P., 1972, Classification and environmental interpretation of cryptalgal organosedimentary "molor-tooth" structure from the late Precambrian Belt-Purcell Supergroup: Journal of Geology, v. 80, p. 592-610.

Partheniades, E., 1986, A fundamental framework for cohesive sediment dynamics, in, Metha, A. J., (editor), Esturine cohesive sediment dynamics: Berlin, Springer, p. 219-250.

Pierson, T. C., and Scott, K. M., 1985, Downstream dilution of a lahar: Transition from debris flow to hyperconcentrated streamflow: Water Resources Research, v. 21, p. 1511-1524.

Postma, H., 1967, Sediment transport and sedimentation in the estuarine environmont, in, Lauff, G. H., (ed.), Estuaries: American Association for the Adavancement of Science Publication 83, p. 158-179.

Potter, P. E., Maynard, J. B., and Pryor, W. A., 1980, Sedimentology of shale: New York, Springer-Verlag, 307 p.

Price, R. A., 1964, The precambrian Purcell System in the Rocky Mountains of southern Alberta and British Columbia: Bulletin of Canadian Petroleum Geology, v. 12, Field Conference Guide Book Issue, p. 399-426.

Qian, Y., Yang, W., Zhao, X., Zhang, L., and Xu, W., 1980, Basic characteristics of flow with hyperconcentration of sediment, in, Proceedings of the International Symposium on River Sedimentation, p. 175-184.

Raaf, de, J. F. M., Boersma, J. R., and Gelder, van, A., 1977, Wave- generated structures and sequences from a shallow marine succession, Lower Carboniferous, County Cork, Ireland: Sedimentology, v. 24, p. 451-483.

Ransome, F. L., 1905, Ore deposits of the Coeur d'Alene district, Idaho: U. S. Geological Survey Bulletin 260, p. 274-303.

Reineck, H.-E., 1967, Layered sediments of tidal flats, beach, and shelf bottoms of the North Sea, in, Lauff, G. H., (editor), Estuaries: American Association for the Adavancement of Science Publication No. 83, p. 191-206.

Reineck, H-E., and Singh, I. B., 1980, Depositional Sedimentary Environments with Reference to Terrigenous Clastics, 2nd edition: New York, Springer-Verlag, 549 p.

Reineck, H-E., and Wunderlich, F., 1968, Classification and origin of flaser and lenticular bedding: Sedimentology, v. 11, p. 99-104.

Reynolds, R. C., 1963, Potassium-rubidium ratios and polymorphism in illites and microclines from the clay size fractions of Proterozoic carbonate rocks: Geocheimia et Cosmochimica Acta, v. 27, p. 1097-1112.

Rickets,B. D., and Donaldson, J. A.,Stone rosettes as indicators of ancient shorelines: examples from the Precambrian Belcher Group, Northwest Territories: Canadian Journal of Earth Science, V. 16, p. 188-218.

Rijn, L. C., van,1984, Sediment transport. Part II: Suspended load transport: Journal of Hydraulic Engineering, v. 110, p. 1613-1641.

Rine, J. M., 1980. Depositional environments and Holocene reconstruction of an argillaceous mud belt—Suriname, South America, Ph. D dissertation, University of Miami, Coral Gables. Fl., 204 p.

Rine, J. M., and Ginsburg, R. N., 1985, Depositional facies of a mud shoreface in Suriname, South America- a mud analogue to sandy, shallow-marine deposits: Journal of Sedimentary Petrology. v. 55, p. 633-652.

Rodine, J. D., 1974. Analysius of mobilization of debris flows, Ph. D. thesis, Stanfod University, Stanford, California, 226 p.

Rouse, H., 1937, Modern conceptions of the mechanics of turbulence: Transactions American Society of Civil Engineers, v. 102.

Rubin, D. M., 1987, Cross-bedding, bedforms, and paleocurrents: Society of Economic Paleontologists and Mineralogists, Concepts in Sedimentology and Paleontology, V. 1, 187 p.

Shinn, E. A., Steinen, R. P., Dill, R. F., and Major, R., 1993, Lime-mud layers in high-energy tidal channels: A record of hurricane deposition: Geology, v. 21, p. 603-606.

Sills, G. C., and Elder, D. McG., 1986. The transition from sediment suspension to settling bed, in, Metha. A. J., (editor), Esturine cohesive sediment dynamics: Berlin, Springer, p. 192- 205.

Smoot, J. P., 1983. Depositional subenvironments in an arid closed basin; the Wilkins Peak Member of the Green River Formation (Eocene), Wyoming, U.S.A.: Sedimentology, v. 30, p. 801-827.

Sneeden, J. W., and Nummedal D., 1989, Sand transport kinematics on the Texas continental shelf during hurricane Carla, September 1961, in, Morton, R. A., and Nummedal, D. (editors) Shelf sedimentation. shelf sequences and related hydrocarbon accumulation: Proceedings of the Seventh Annual Research Conference, Guof Coast Section of Society of Economic Paleontologists and Mineralogists foundation, p. 63-76.

Snedden, J. W., and Nummedal, D., 1990, Coherence of surf zone and shelf current flow on the Texas (U. S. A.) coastal margin: implications for interpretation of paleo-current measurments in ancient coastal sequences: Sedimentary Geology, v. 67, p. 221-236.

Stickney, A. J., 1991. Stratigraphy and dedimentology of Baicalia-Conophyton cycles, Helena Formation. (Middle Proterozoic Belt Supergroup) northwest Montana (M. S. thesis): University of Montana, Missoula, MT.

Stow, D. A., and Bowen, A., 1980, A physical model for the transport and sorting of fine-grained sediment by turbidity currents: Sedimentology, v. 27, p. 31-46.

Swift, D. J. P., Han, G., and Vincent, C. E., 1986 a, Fluid processes and sea-floor response on a modern storm-dominated shelf: Middle Atlantic Shelf of Norht America. Part I: The storm-current regime, in, Knight, R. J., and McLean, J. R., (editors), Shelf Sands and Sandstones: Canadian Society of Petroleum Geologists, Memoir 11, p. 99-119.

Swift, D. J. P., Thorne, J. A., and Oertel, G. F., 1986 b, Fluid processes and sea-floor response on a modern storm-dominated shelf: Middle Atlantic Shelf on North America. Part II: Response of the shelf floor, in, Knight, R. J., and McLean, J. R., (editors), Shelf Sandstones: Canadian Society of Petroleum Geologists, Memoir 11, p. 191-211.

Thompson, R. W., 1968, Tidal flat sedimentation on the Colorado River Delta, northwestern Gulf of California: Geological Society of America Memoir 107, 133 p.

Van Andel, T. H., and Komar, P. D., 1969, Ponded sediments on the Mid-Atlantic Ridge between 22° and 23° north latitude: Bulletin Geological Society of America, v. 80, p. 1163-1190.

Van Straaten, L. M. J. U., and Kuenen, Ph. H., 1958, Tidal action as a cause for clay accumulation: Journal of Sedimentary Petrology, v. 28, p. 406-413.

Vincent, C. E., 1986, Processes affecting sand transport on a storm- dominated shelf, in Knight, R. J., and McLean, J. R., (Eds.), Shelf Sands and Sandstones: Canadian Society of Petroleum Geologists, Memoir 11, p. 121-132.

Vincent, C. E., Young, R. A., and Swift, D. J. P., 1982, On the relationship between bedload and suspended sand transport on the inner shelf, Long Island, New York: Journal of Geophysical Research, v. 87, p. 4163-4170.

Walcott, C. D., 1899, Pre-Cambrian fossiliferous formations: Geological Society of America Bulletin, v. 10, p. 199-244.

Walcott, C. D., 1914, Abrupt appearance of the Cambrian fauna on the North American continent, in, Cambrian geology and paleontology, II: Smithsonian Miscelaneous Collection, v. 7, p. 1- 16.

Walker, R. G., (ed.), 1979, Facies Models: Geoscience Canada, Reprint Series 1, 211 p.

Walker, R. G., (ed.), 1984, Facies Models, Second Edition: Geoscience Canada, Reprint Series 1, 317 p.

Walker, R. G., 1992 , Facies, facies models and modern stratigraphic concepts, in, Walker, R. G., and James. N. P., (eds.), Facies Models: Response to Sea Level Change: Geological Association of Canada, p. 1-14.

Walker, R. G., and James. N. P., (eds.), 1992, Facies Models: Response to Sea Level Change: Geological Association of Canada, 409 p.

Wallace, C. A., Harrison, J. E., Lidke, D. J., and Whipple, J. W., 1989, Time equivalence of lithofacies in parts of the Middle Belt Carbonate (Belt Supergroup, Middle Proterozoic), Montana and Idaho. (abs.): Program, Geological Society of America, Cordilleran Section and Rocky Mountain Section Meeting, Spokane, Washington, 1989, p. 155.

Weimer. R. J., Howard. J. D., and Lindsay. D. R., 1982, Tidal flats, in, Scholle, P. A., and Spearing, D., (eds.), Sandstone depositional environments: American Association of Petroleum Geologists, Memoir 31, p. 191-246.

Wells, J. T., 1983, Dynamics of coastal fluid muds in low-,moderate-, and high -tide-range environments: Canadian Journal of Fish and Aquatic Science, v. 40, (Supplement 1), p. 130-142.

Wells, J. T., and Coleman, J. M., 1981 a, Physical processes and fine- grained sediment dynamics, coast of Suriman, South Amerca: Journal of Sedimentary Petrology, v. 51, p. 1053-1068.

Whipple, J. W., and Johnson, S. N., 1988. Stratigraphy and lithocorrelation of the Snowslip Formation (Middle Proterozoic Belt Supergroup), Glacier National Park, Montana: U. S. Geological Survey Bulletin 1833, 30 p.

Williams, G. E., 1981, Sunspot periods in the late Precambrian gracial climate and solar- planetary relations: Nature, v. 291, p. 624-628.

Williams, G. E., 1985, Solar affinity of sedimentary cycles in the late Precambrian Elatina Formation: Australian Journal of Physics, v. 38, p. 1027-1043.

Williams, G. E., 1989 a, Late Precambrian tidal rhythmites in South Australia and the history of the Earth's rotation: Journal of the Geological Society. London, v. 146, p. 97-111.

Williams, G. E., 1989 b, Precambrian tidal sedimentary cycles and Earth's paleorotation: Eos. v. 70, no. 3, p. 33, 40-41.

Willis, Bailey, 1902. Stratigraphy and structure. Lewis and Livingston ranges. Montana: Geological Society of America Bulletin, v. 13, p. 305-352.

Winston, D., 1986 a, Stratigraphic correlation and nomenclature of the Middle Proterozoic Belt Supergroup, Montana, Idaho, and Washington, in, Roberts, S. M. (ed.), Belt Supergroup: A guide to Proterozoic rocks of western Montana and adjacent areas: Montana Bureau of Mines and Geology Spedial Publication 94, p. 69-84.

Winston, D., 1986 b, Sedimentology of the Ravalli Group, Middle Belt Carbonate and Missoula Group, Middle Proterozoic Belt Supergroup, Montana, Idaho, and Washington, in, Roberts, S. M., (ed.), Belt Supergroup: A guide to Proterozoic rocks of western Montana and adjacent areas: Montana Bureau of Mines and Geology Spedial Publication 94, p. 85-124.

Winston, D., 1989, A sedimentologic and tectonic interpretation of the Belt, in, Winston, D., Horodyski, R. J., and Whipple, J. W., eds., Middle Proterozoic Belt Supergroup, Western Montana, 28th International Geological Congress, Field Trip Guidebook T334, p. 47-70.

Winston, D., 1991, Evidence for intracratonic, fluvial and lacistrine settings of Middle to Late Proterozoic basins of western U. S. A., in Gower, C. F., Rivers, T., and Ryan, B., (eds.), Mid-Proterozoic Laurentia-Baltica: Geological Association of Canada, Special Paper 38, p. 535-564.

Winston, D., 1993, Cycles of the upper Helena Formation, Middle Proterozoic Belt Supergroup, Montana, in, Belt Symposium, III: Belt Association, Inc., P.O. Box 1816, Spokane, Wa., 99210.

Winston, D. and Link, P. K., 1993, Middle Proterozoic rocks of Montana, Idaho and Eastern Washington: The Belt Supergroup, in, Reed, J. C., Jr., Bickford, M. E., Houston, R. S., Link, P. K., Rankin, D. W., Sims, P. K., and Van Schmus, W. R., Precambrian: Conterminous U. S.: Geological Society of America, The Geology of North America Volume C- 2, p. 487-517.

Winston, D., and Lyons, T., 1993, Sedimentary cycles in the St. Regis, Empire and Helena formations of the Middle Proterozoic Belt Supergroup, northwestern Montana, in, Link, P. K. (editor) Geologic guidebook to the Belt-Purcell Supergroup, Glacier National Park and vicinity, Montana and adjacent Canada: Belt Association, Inc., Spokane, Washington, p. 21- 50.

Winston, D., Woods, M. O., and Byer, G. B., 1984, The case for an intracratonic Belt-Purcell basin: Tectonic, stratigraphic and stable isotopic considerations, in Northwest Montana and adjacent Canada, J. D. McBane and P. B. Garrison, (eds,) Montana Geological Society Guidebook, 1984 Field Conference and Symposium, p. 103-118.

Woods, M. O., 1986, Depositional subenvironments in a closed basin: The Shepard Formation (Middle proterozoic Belt Supergroup), Southern Mission, Sawn, and Lewis and Clark Ranges, Montana (M. S. Thesis): University of Montana, Missoula, 111 p.

A Revised Oscillatory and Combined Current Bed Phase Diagram

ABSTRACT

Symmetrical ripple forms are produced by oscillatory currents. Flume studies show that the shape, spacing and heights of symmetrical bedforms in very fine-grained sand systematicly change with increasing near bed orbital velocities. Symmetrical bedforms in the Helena and Wallace formations display the same shapes, spacings and heights as the bedforms produced in wave tunnel and wave tank experiments. Thus, the ancient bedforms show that the experimental bedforms have physical meaning, and bed phase diagrams based on experiments probably reflect real world flow conditions.

However, original oscillatory-combined current bed phase diagram (Arnott and Southard, 1990) did not recognize the differences between symmetrical and asymmetrical ripple forms. The accepted bed phase diagram for oscillatory and combined flow currents (Duke et al., 1991) only recognizes the difference between hummocky ripples, formed by purely oscillatory currents, and bed configurations produced by combined flow currents. The Duke et al. (1991) diagram does not differentiate between small symmetrical and asymmetrical forms.

I herein present a modified oscillatory-combined current bed phase diagram that includes a symmetrical ripple field, encompassing all symmetrical ripple forms. I also subdivide the symmetrical ripple field into seven subfields, based on the bedform's shape, spacing and height.

INTRODUCTION

Arnott and Southard (1990) presented the first combined unidirectional and oscillatory current bed

197

phase diagram, reproduced on Figure A.1. This diagram suffers from the fact that Arnott and Southard

(1990) did not differentiate between asymmetric bedforms and symmetric bedforms. Thus, they failed to

differentiate between purely oscillatory current bedforms and combined current bedforms, and thereby

missed a lot of valuable hydrodynamic information. However, large body of experimental and field

evidence (Turner, 1967; Harms, 1969) shows that symmetrical ripples only form under symmetrical

currents, and that asymmetrical ripples form under combined currents (Harms, 1969).

HUMMOCKY RIPPLE FIELD. Duke et al. (1991) recognized this flaw in the Arnott and

Southard (1990) bed phase diagram, and subdivided the large, low angle, 3D ripple field, creating a field of

hummocky ripples parallel to oscillatory current axis, Figure A.2. Hummocky ripples are symmetrical,

dome-shaped, 3D bedforms, Chapter III.B. Thus, Duke et al. (1991), sought to differentiate between

symmetrical 3D bedforms produced by purely oscillatory, or purely oscillatory currents combined with a

very weak unidirectional current, from asymmetric bedforms produced under combined oscillatory and

unidirectional currents.

THE SYMMETRICAL RIPPLE FIELD. However, Duke et al. (1991) did not make the same

distinction between small symmetrical 2D ripples and small asymmetrical 2D ripples, or between small

symmetrical 3D and small asymmetrical 3D ripples. Therefore, in order to differentiate between all the

symmetric bedforms and all asymmetric bedforms, I herein extend the line for the hummocky ripple field

(Duke et al., 1991) to the no movement line, defining a symmetrical ripple field, Figure A.3.

HUMMOCKY RIPPLES VERSES HUMMOCKY CROSS-STRATIFICATION. I define

hummocky ripples as symmetrical, rounded, dome-shaped bedforms, no matter what their spacing, to

differentiate the bedforms from the term "hummocky cross-stratification" (Harms et al., 1982). Hummocky

cross-stratification actually refers to the laminae produced by vertically climbing, dome-shaped ripples with

a spacing greater than about 100 cm. Furthermore, observations in modern environments (Greenwood and
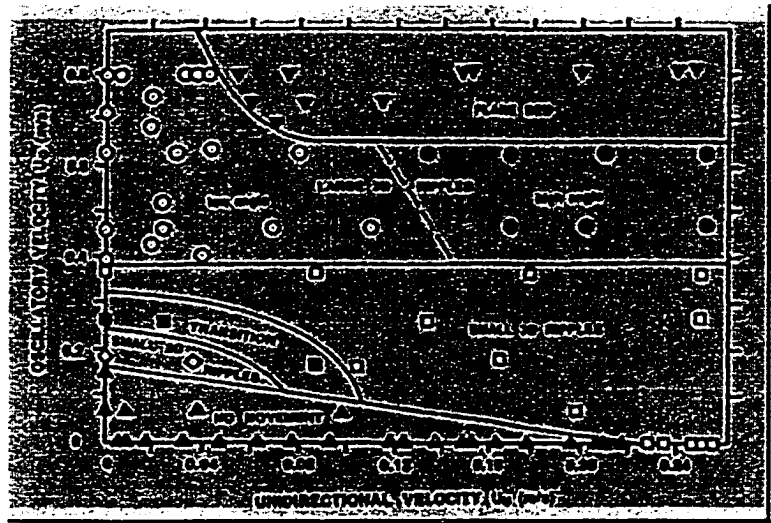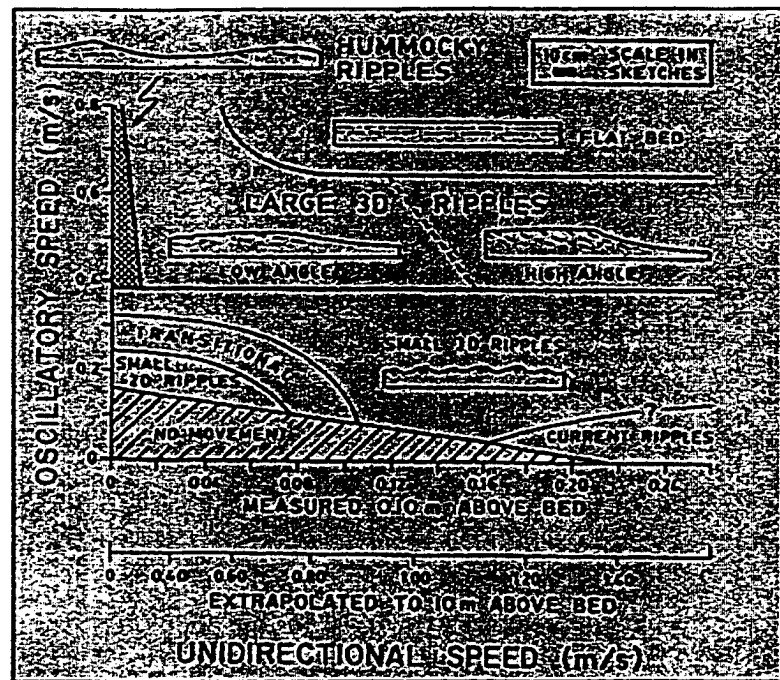
Figure A.1.
Experimental results of oscilliatory velocity Uo vs.
unidirectional velocity Uu; from Arnott and Southard
(1990) Figure 3.

Figure A.2.
Bed phase diagram showing the region of hummocky ripples
and the unidirectional velocity extrapolated to 10 m above
the bed; from Duke. et al (1991) Figure 3.
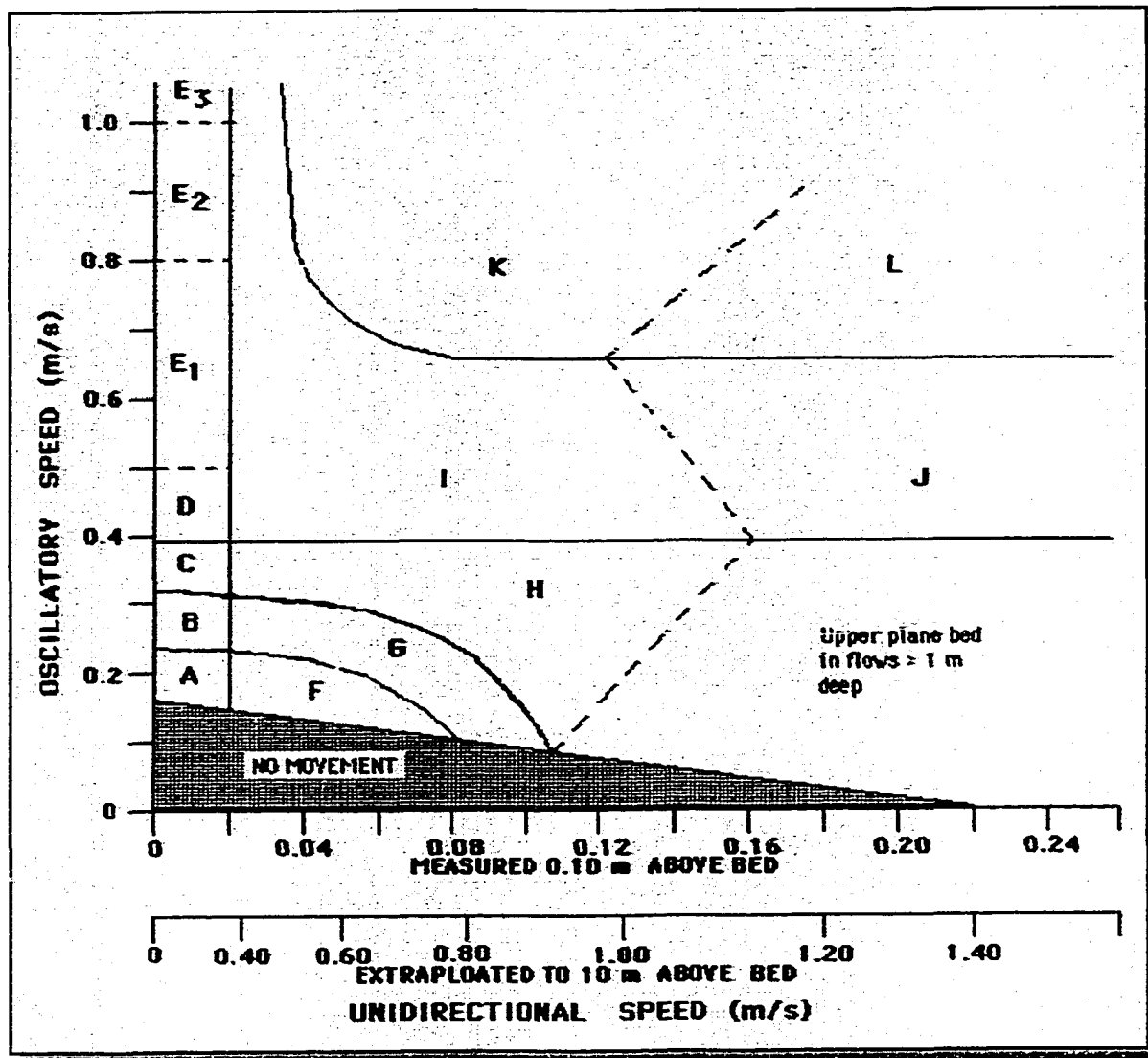
Figure A.3.
Bed phase diagram showing the symmetrical ripple field.

Sherman, 1985) and wave tunnel experiments (Carstens et al., 1969; Southard et al., 1990) show that dome-shaped ripples with spacings under 100 cm also exist. Thus, I use the term "hummocky ripples" to describe all dome-shaped bedforms, no matter what there spacing.

HUMMOCKY RIPPLES IN THE HELENA AND WALLACE FORMATIONS

Based on observations in the Helena and Wallace formations, hummocky ripples fall into three size classes. Small hummocky ripples display spacings less than 21 cm apart, and commonly about 10 to 15 cm, medium hummocky ripples display spacings between 30 and 70 cm apart, and large hummocky ripples are spaced greater than 100 cm apart.

Bedding plane exposures are very rare in the Helena and Wallace formations, but at one location where a hummocky rippled bed is exposed, the ripples are more-or-less symmetrical domes, about 5-7 cm high and spaced about 80-100 cm apart. Some domes display a slight amount of asymmetry, being slightly steeper on one side of the dome. But, the steep side occurs at different locations around domes, thus, showing no preferred direction of bedform asymmetry.

On vertical exposures, the internal laminae are commonly concordant to the bedform's outline, and dip symmetrically about the ripple crest. Ripple expression occurs by thickening of the laminae over the ripple's crest, and by thinning into the troughs. Internal truncation surfaces are common, but the truncation surfaces, traced along the exposure, commonly merge into a normal lamina, indicating contemporaneous erosion and deposition. These features are the same as those observed by Southard et al. (1990, Fig. 15, 16 and 17) in wave tunnel experiments and on vertical exposures of ancient sedimentary rocks. Southard et al. (1990, p. 15) described this style of stratification as "aggradational-bed-configuration" hummocky cross-stratification.

Small, medium and large hummocky ripples are very common throughout the Helena and Wallace formations. But, small and medium hummocky ripples have not been described from other formations in

the Belt Supergroup, or from formations around the world. However, in some studies. small and medium hummocky ripples may have been incorrectly lumped in with the hummocky cross-stratification. Hummocky cross-stratification, outlining large hummocky ripples. has been described from a large number of formations around the world.

Three features link the small. medium and large hummocky ripples. and suggest they formed under the same general current conditions. (1) All three types display symmetrical outlines and they commonly contain concordant, symmetrical internal laminae. (2) Flume and wave tunnel experiments show that small. medium and large hummocky ripples are part of a continuum of forms, and (3) Rarely, large and medium, or medium and small hummocky ripples occur above the one another, within a fining-upward graded bed.

The largest grains in the Helena and Wallace formations, about 100 μm, primary current laminae and the grading in the graded beds document suspension transport and deposition as a result of decreasing current capacity. Also, the locations where hummocky ripples were deposited were aggrading, which means that sediment must have been carried to the site of deposition from elsewhere. Thus. the graded beds in the Helena and Wallace formations strongly suggest that hummocky ripples were deposited from slowly moving, wave dominated suspensions; where at least some, if not all of the sediment was transported to the depositional site by a weak unidirectional current.

THE ORIGIN OF HUMMOCKY RIPPLES

In spite of contrary conclusions (P. A. Allen and Underhill, 1989; Nottvedt and Kreisa, 1987; P. A. Allen, 1985; Swift et al., 1983), data from wave tunnel experiments (Carstens et al., 1969; Southard et al., 1990; Arnott and Southard, 1990) and hydraulic interpretations of ancient hummocky ripples (Hunter and Clifton, 1982; Dott and Bourgeois, 1982) provide compelling evidence that hummocky ripples form under high velocity, pure, or nearly pure, oscillatory currents. That is, hummocky ripples record deposition under

conditions of little or no wave asymmetry, or where the oscillatory currents were combined with, at most, very weak unidirectional currents (Duke et al., 1991).

PERMISSABLE WAVE TYPES. Wave tunnel and wave tank experiments (Carstens et al., 1969; Komar and Miller, 1975; Southard et al., 1990; Arnott and Southard, 1990) suggest symmetrical ripples only form under waves that have near bed fore-stroke velocities equal to the near bed back-stroke velocities. Symmetric fore-stroke and back-strokes are produced only under Airy waves. Stokes, cnoidal and solitary waves produce asymmetric forestroke and backstroke velocities (Komar, 1976; Shore Protection Manual, 1977), and thus produce more sediment transport in the direction of wave propagation than in the reverse direction. This produces asymmetry in sediment transport which must result in bedform migration (Komar, 1976; Clifton et al., 1971; Reineck and Singh, 1980), and commonly in bedform asymmetry also. The amount of the velocity difference needed to produce asymmetry and migration in the bedforms is not known (Clifton and Dingler, 1984, p. 183). But, Clifton and Dingler (1984) suggest a difference of one to a few centimeters per second between the forestroke and backstroke is enough to produce asymmetry in the bedforms. Migration of symmetrical ripples, producing uniformly dipping cross-laminae (Newton, 1968), may occur under slightly asymmetric Airy waves.

VELOCITIES OF UNIDIRECTIONAL CURRENTS. The same arguments as above show that symmetrical ripples with concordant laminae can not form under combined currents with a strong unidirectional component (Allen, 1979, p. 678). The symmetrical ripple form, symmetrical laminae thicknesses, and symmetrical dip of the laminae about the ripple crests show that the ripple forms aggraded vertically. Southard et al. (1990, p. 13) and Newton (1968) suggest that the presence of more than a negligible unidirectional current cause the bedforms to migrate and migrating symmetrical bedforms produce internal laminae that dip uniformly in one direction (Newton, 1968).

However, Swift et al. (1983) and Hunter and Clifton (1982) also present compelling argument for the presence of a weak unidirectional component, combined with the strong oscillatory component. Their arguments revolve around the fact that the area of deposition was aggrading. Thus, sediment must have been transported to the site of deposition, and that could only be accomplished by a unidirectional current. So the question arises, just how strong of a unidirectional current can combine with the oscillatory current and still produce a symmetric bedform?

The data in Arnott and Southard (1990) suggest that asymmetric bedforms are produced when near bed unidirectional velocities reach about 3 cm/s. Their data also imply that symmetric bedforms persist in currents with up to near bed unidirectional velocities of 2 cm/s. This agrees with Duke et al. (1991) who suggested that hummocky ripples form under combined flow currents with unidirectional core flow velocities up to about 30 cm/s measured at 10 m above the bed, or unidirectional velocities of about 2 cm/s near the bed. Therefore, based on Duke et al. (1991), I place the upper limit of symmetrical ripple field at 2 cm/s near bed unidirectional velocity, or about 30 cm/s extrapolated to 10 m above the bed. Boundary layer theory suggests that symmetrical forms could occur at even higher unidirectional current velocities in deeper water.

Unidirectional current velocities of 2 cm/s near the bed or 30 cm/s measured 10 m above the bed are supported by the structures found in ancient formations. Hunter and Clifton (1982) suggested the deposition 2 to 4 m spaced hummocky ripples occurred under combined flow currents with orbital velocities of about 200 cm/s. The hummocky ripples grade upward into planar laminae, which grade upward into symmetric to slightly asymmetric, low angle climbing ripple bedding. Both the slightly asymmetric ripples and the low angles of climb suggest the presence of unidirectional currents. Swift et al. (1983) measured shore-parallel Ekman currents, with velocities up to 30 to 40 cm/s, across the entire width of the Atlantic shelf. Given sufficient oscillatory current velocities, hummocky ripples should form under these currents in water greater than about 10 m deep (Duke et al., 1991).

WATER DEPTHS. The presence of mudstone layers capping the graded beds containing hummocky ripples in the Helena and Wallace formations, indicate mud deposition out of reach of fair-weather waves. Otherwise the mud would have been re-suspended and transported away during fair weather conditions. Leithold and Bourgeois (1984), Dott and Bourgeois (1982) and Hunter and Clifton (1982) also suggest that large scale hummocky ripples were deposited below fair-weather wave base. However, some medium and large hummocky ripples found in amalgamated sandstone beds in the Helena and Wallace formations may record deposition within fair-weather wave base. The structures may have been preserved because the beds were thicker than could be re-suspended under fair-weather conditions.

BED AGGRADATION RATES. The conformable vertically climbing internal laminae in the hummocky ripple forms also record little or no lateral migration of the bedforms during deposition. As shown, symmetrical forms probably can form in unidirectional currents up to 30 cm/s velocity currents measured at 10 m above the bed. If the bed aggradation rate is low, then the unidirectional current causes the symmetrical bedform to migrate during deposition (Allen, 1991). Bedform migration produces either an angle of climb or uniformly dipping internal laminae, or both. On the other hand, if bed aggradation rate is high, corresponding to a rapid decline in current capacity, then the bedform can grow vertically, producing concordant internal laminae. Thus, if a low velocity unidirectional current is present, then vertically climbing bedforms indicate the bed aggradation rate was high.

OFFSHORE, STORM DEPOSITION. The bedform's characteristics restrict the location at which small, medium and large hummocky ripples can occur. Deposition must have occurred offshore of the wave build-up zone and surf zone (Clifton et al. 1971). Hummocky ripples probably form more than 3 to 5 km offshore of the shore line, because high velocity offshore directed jets are formed near the shore line during storms (Swift et al., 1983).

Storm transport of sediment and deposition of the hummocky ripples is also supported by: (1) The absence of hummocky ripples forming under fair weather conditions in modern wave environments. (2) The observation that large hummocky ripples commonly underlie medium hummocky ripples, and medium hummocky ripples underlie small hummocky ripples suggests the activity of decelerating, symmetrical oscillatory currents throughout deposition. (3) Greenwood and Sherman (1986) collected box cores of small hummocky ripples immediately after a storm, and linked them to deposition under the wave recorded during the storm. (4) The high orbital velocities indicated by the flume experiments could have only been produced by large amplitude, long period waves.

SUMMATION. The preferred model for the formation of hummocky ripples includes the following points. (1) Symmetrical ripples must form under Airy waves, or possibly Airy waves combined with very weak unidirectional currents. (2) The thicknesses of graded beds containing large hummocky ripples (10 to 45 cm thick) implies currents and current generating events with enough energy to maintain very large amounts of sediment in suspension. (3) Since the ripples climb vertically, the migration rate of the ripples (if any) was very low relative to the rate at which sediment was deposited on the bed. (4) Unidirectional current velocities were less than 30 cm/s, measured at 10 m above the bed. (5) Deposition of symmetrical hummocky ripples probably occurred offshore of the wave build-up zone and definitely offshore of the surf zone.

JUSTIFICATION FOR SUBDIVIDING OF THE SYMMETRICAL RIPPLE FIELD

The Helena and Wallace formations contain a wide variety of symmetrical ripple forms, shown on Figure III.3, a-e. The presence of symmetrical, 2D ripple forms and the wide range of sizes of symmetrical, 3D ripple forms in the Helena and Wallace formations suggests the possibility of subdividing of symmetrical ripple field, Figure A.3.

The symmetrical bedforms in the Helena and Wallace formations display roundness, shape,

spacing and heights that duplicates those observed in wave tunnel experiments of Carstens et al. (1969) and

Southard et al. (1990). The similarity of bedforms in the ancient sediments to those made in the

experiments suggest the bedform roundness, shapes, spacings and heights observed in experiments are real,

and are not artifacts of the experiments. This provides the justification for dividing the symmetrical ripple

field, Figure A.3, into 7 different symmetrical forms based on the bedform's roundness, shape, spacing and

height shown on Figure V.2.

The subdivisions the symmetrical ripple field are based on the observed progression of different

symmetrical ripple shapes and spacings under progressive higher maximum near bed oscillatory current

velocities in wave tunnel experiments (Carstens et al., 1969; Southard et al., 1990).

Symmetrical ripples in the Helena and Wallace formations can be divided into 2D (trochoidal)

forms and 3D (hummocky) forms. The 2D forms are spaced under 20 cm apart, and are divided into

trochoidal ripples and rounded trochoidal ripples; both display straight, continuous ripple crest-lines.

Hummocky ripples in the Helena and Wallace formations are dome-shaped and appear to fall into three

basic sizes. The smallest hummocky ripples commonly range from about 7 to 15 cm spaced. The medium

sized hummocky ripples commonly range from about 30 to 70 cm spaced, and the large hummocky ripples

are spaced at about 100 cm, or more. Thus, there appears to be: (1) a natural division between 2D and 3D

forms, and (2) natural gaps in the spacing of the hummocky ripples in the Helena and Wallace formations.

The shapes, spacing and heights of symmetric ripple forms observed in the Helena and Wallace

formations have been reproduced in the wave tunnel experiments described in Carstens et al. (1969),

Komar and Miller (1975), Southard et al. (1990), and Arnott and Southard (1990). Data presented in

Southard et al. (1990, Fig. 13) suggest the gap in sizes between the small and medium hummocky ripples is

real, but their data do not support the apparent gap between the medium and large hummocky ripples.

The experiments by Carstens et al. (1969) clearly link increasing orbital velocity under short period waves to the progressive change from sharp straight-crested (trochoidal) ripples to rounded straight-crested (rounded trochoidal) ripples. Southard et al. (1990) and Arnott and Southard (1990) show that, under medium period waves, the spacing of the hummocky bedforms increases with increasing orbital velocity. Table A.1 gives the progression of bed configurations observed in wave tunnel and wave tank experiments.

The natural gap between the small and medium in the hummocky ripples in the bedforms in the Helena and Wallace formations appear to match the natural gap between 20 and 50 cm observed in the wave tunnel data (Southard et al., 1990, Fig. 13). Since the ripples in the wave tunnel experiments appear to shift back and forth (Southard et al., 1990, Fig. 15), the preserved bedforms should have a smaller spacing.

DIFFERENCES IN THE EXPERIMENTAL BEDFORMS. The bedforms described in Southard et al. (1990) differ from those in Carstens et al. (1969). Southard et al. (1990) describe ripples with straight, continuous and sharp-crests (Runs 2-5 and 2-6), that evolve into sinuous, sharp-crested forms that vary greatly in height along the crest (Runs 2-1 and 2-8). The change in ripple shape correlates with increasing maximum orbital velocity. At higher velocities (34 cm/s, Run 2-7), fully 3D forms appear, but these bedforms exhibit sharp crests, and areas of local and temporary scour in the ripple troughs.

On the other hand, Carstens et al. (1969) described straight, sharp crested forms that evolved into rounded, straight crested forms and then become discontinuous forms with increasing orbital velocities. The ripple crests in the Carstens et al. (1969, Fig. 9) experiments break into shorter segments without the crests becoming sinuous, as in Southard's et al. (1990) experiments. Thus, descriptions in Carstens et al. (1969) suggest the rounding of the forms occurs before the ripple crests begin to breakup. Rarely, in the Helena and Wallace formations, rounded 2D ripple forms are overlain by sharp-crested, 2D ripple forms,

but I have never observed the reverse. Thus, the field data suggest that Carstens et al. (1969) sequence, not the Southard et al. (1990) sequence is the sequence that occurs in nature.

It is probable that the differences between bedforms observed in the Carstens et al. (1969) and Southard et al. (1990) experiments are due to differences in experimental conditions. Carstens' et al. (1969) experiments were conducted under waves with periods of about 3.6 s. in 190 μm sand. Southard's et al. (1990) experiments were conducted with wave periods ranging from 6.7 to 9.6 s, in 90 μm sand.

This may mean that the trochoidal and rounded trochoidal ripples in the Helena and Wallace formations record deposition under short period waves, whereas the small, medium and large hummocky ripples record deposition under intermediate to long period waves. This is consistent with the wave conditions calculations. Figure V.7 shows that longer period waves are required to produce the high orbital velocities required for the deposition medium and large hummocky ripples.

Also, the threshold of movement under purely oscillatory currents is a function of maximum orbital velocity and wave period. Shorter period waves induce movement at lower orbital velocities than do long period waves (Clifton and Dingler, 1984). The short period waves in the Carstens' et al. (1969) experiments may induce earlier rounding of the ripple forms.

The high orbital velocity experiments described in Southard et al. (1990, Appendix) show that all the larger hummocky ripple forms also display small superimposed asymmetric bedforms. These asymmetric forms may reflect local flow asymmetry induced by the larger symmetrical form. Arnott and Southard's (1990) descriptions to not include superimposed bed forms, and the lack of small scale bedforms on the bed configuration tracings in Southard et al. (1990, Fig. 15) suggest that small, asymmetric superimposed bedforms, if present, are ephemeral features, and leave no record in the deposits.

SUPERPOSITION OF BEDFORMS. Single sandstone beds in the Helena and Wallace

formations commonly contain two and rarely three successive symmetrical ripple forms. In all instances,

lower velocity forms overlie higher velocity forms. Large hummocky ripples are commonly overlain by

medium hummocky ripples, or by trochoidal ripples. Rarely rounded trochoidal ripples are overlain by

trochoidal ripples. The superpositioning of lower velocity bedforms above higher velocity bedforms in the

sandstone beds supports the inference that the bedform's shape and spacing are a function of the current's

velocity.

DISCUSSION

Assuming the hummocky ripples in the Helena and Wallace formations formed at the same orbital

velocities as those formed equivalent bedforms in the wave tunnel experiments run several risks. (1) The

walls of the wave tunnel may have induced secondary turbulence that effected the bed configurations

(Arnott and Southard, 1990). (2) There exists the possibility that high clay content in the suspended load

may change the bed configurations or the orbital velocities needed to produce a given bedform, and (3)

High suspended sediment fallout rates may effect the current velocities for the various bed configurations

(Lowe, 1988).

Furthermore, Figure V.2 bed phase diagram is only valid for about 90 μm quartz sand. It is not

known how, or if, the bed phase boundaries shift with larger or smaller diameter grains. However, 90 μm

quartz is so close to the dominant 100 μm sand size in the sandstones in the Helena and Wallace formations

that it is unlikely that this introduces any error for the interpretation of the bedforms in Helena and Wallace

formations.

The progression of bed phases is based on experiments with short period waves (Carstens et al.,

1969) and moderate period waves (Southard et al., 1990). Without a series of systematic experiments with

long period waves, I must assume that changes in wave periods only effect the threshold of movement line.

That is, I assume the other bed phase fields occur at the same velocities in Figure V.2 , regardless of the wave's period.

Experiments have shown that short period waves are more efficient at moving sand than long period waves (Clifton and Dingler, 1984). For instance, the threshold of movement of 100 μm quartz sand is about 16 cm/s under waves with a period of 3 s, and about 24 cm/s under 20 second waves. But, the latter velocity is above the existence field of trochoidal ripples. This limits the formation of trochoidal ripples to waves with periods less than 20 seconds.

REFERENCES

Allen, J. R. L., 1979, A model for the interpretation of wave ripple- marks using their wavelength, textural composition, and shape: Journal Geological Society of London, v. 136, p. 673-682.

Allen, P. A., 1985, Hummocky cross-stratification is not produced purely under progressive gravity waves: Nature, v. 313, p. 562-564.

Allen, P. A., and Underhill, J. R., 1989, Swaley cross-stratification produced by unidirectional flows, Bencliff Gritt (Upper Jurassic), Dorset, UK: Journal of the Geological Society, London, v. 146, p. 241-252.

Arnott, R. W. C., and Southard, J. B., 1990, Exploratory flow-duct experiments on combined-flow bed configurations, and some implications for interpreting storm-event stratification: Journal of Sedimentary Petrology, v. 60, p. 211-219.

Bagnold, R. A., 1946, Motion of waves in shallow water. Interaction between waves and sand bottoms: Proceedings Royal Society of London, v. A187, p. 1-16.

Carstens, M. R., Neilson, F. M., and Altingilek, H. D., 1969, Bed forms generated in the laboratory under an oscillatory flow: analytical and experimental study: U. S. Army corps of Engineers, Coastal Engineering Research Center, Technical Memorandum No. 28, 39 p., Appendix A, Appendix B.

Clifton, H. E., and Dingler, J. R., 1984, Wave-formed structures and paleoenvironmental reconstruction: Marine Geology, v. 60, p. 165-198.

Clifton, H. E., Hunter, R. E., and Phillips, R. L., 1971, Depositional structures and processes in the non-barred high-energy nearshore: Journal of Sedimentary Petrology, v. 41, p. 651-670, and in Davis, R. A., Jr., compiler, Beach and Nearshore Sediments and Processes: Society of Economic Paleontologists and Mineralogists, Reprint Series Number 12, p. 51-70.

Duke, W. L., Arnott, R. W. C., and Cheel, R. J., 1991, Shelf sandstones and hummocky cross-stratification: New insights on a stormy debate: Geology, v. 19, p. 625-628.

Greenwood, B., and Sherman, D. J., 1986, Hummocky cross-stratification in the surf zone: flow parameters and bedding genesis: Sedimentology, v. 33, p. 33-45.

Dott, R. H. Jr., and Bourgeois, J., 1982, Hummocky stratification: Significance of its variable bedding sequences: Geological Society of America Bulletin, v. 93, p. 663-680.

Harms, J. C., 1969, Hydraulic significance of some sand ripples: Geological Society of America Bulletin, v. 80, p. 363-396.

Harms, J. C., Southard, J. B., and Walker, R. G., 1982, Structures and sequences in clastic rocks: Society of Economic Paleontologists and Mineralogists Short Course No. 9.

Hunter, R. E., and Clifton, H. E., 1982, Cyclic deposits and hummocky cross-stratification of probable storm origin in Upper Cretaceous rocks of the Cape Sebastian area, southwestern Oregon: Journal of Sedimentary Petrology, v. 52, p. 127-143.

Komar, P. D., 1976, Beach processes and sedimentation: Englewood Cliffs, N. J., Prentice-Hall, Inc.

Komar, P. D., and Miller, M. C., 1975, The initiation of oscillatory ripple marks and the development of plane-bed at high shear stresses under waves: Journal of Sedimentary Petrology, v. 45, p. 697-703.

Leithold, E. L., and Bourgeois, J., 1984, Characteristics of coarse- grained sequences deposited in nearshore, wave-dominated environments-examples from the Miocene of south-west Oregon: Sedimentology, v. 31, p. 749-775.

Lowe, D. R., 1988, Suspended-load fallout rate as an independent variable in the analysis of current structures: Sedimentology, v. 35, p. 765-776.

Miller, M. C., and Komar, P. D., 1980 a, Oscillation sand ripples generated by laboratory apparatus: Journal of Sedimentary Petrology, v. 50, p. 173-182.

Miller, M. C., and Komar, P. D., 1980 b, A field investigation of the relationship between oscillation ripple spacing and the near-bottom water orbital motions: Journal of Sedimentary Petrology, v. 50, p. 173-182.

Nottvedt, A., and Kreisa, R. D., 1987, Model for the combined-flow origin of hummocky cross-stratification: Geology, v. 15, p. 357-361.

Newton, R. S., 1968, Internal structure of wave-formed ripple marks in the nearshore zone: Sedimentology, v. 11, p. 275-292.

Reineck, H-E., and Singh, I. B., 1980, Depositional Sedimentary Environments with Reference to Terrigenous Clastics, second edition, Springer-Verlag, New York, 549 p.

Shore Protection Manual, 1977: U. S. Army Coastal Engineering Research Center.

Southard, J. B., Lambie, J. M., Federico, D. C., Pile, H. T., and Weidman, C. R., 1990, Experiments on bed configurations in fine sands under bidirectional purely oscillatory flow, and the origin of hummocky cross-stratification: Journal of Sedimentary Petrology, v. 60, p. 1-17.

Swift, D. J. P., Figueiredo, J. G., Jr., Reeland, G. L., and Oertel, G. F., 1983, Hummocky cross-stratification and megaripples: a geological double standard?: Journal of Sedimentary Petrology, v. 53, p. 1295-1317.

Tanner, W. F., 1967, Ripple mark indices and their uses: Sedimentology, v. 9, p. 89-104.